UNIVERSITÉ DE MONTRÉAL

EARTHQUAKE RESPONSE ANALYSIS AND RESISTANT DESIGN OF MODERATELY DUCTILE REINFORCED CONCRETE SHEAR WALLS CONSIDERING HIGHER MODE EFFECTS

QUANG HIEU LUU

DÉPARTEMENT DES GÉNIES CIVIL, GÉOLOGIQUE ET DES MINES

ÉCOLE POLYTECHNIQUE DE MONTRÉAL

THÈSE PRÉSENTÉE EN VUE DE L'OBTENTION

DU DIPLÔME DE PHILOSOPHIAE DOCTOR

(GÉNIE CIVIL)

AVRIL 2014

UNIVERSITÉ DE MONTRÉAL

ÉCOLE POLYTECHNIQUE DE MONTRÉAL

Cette thèse intitulée:

EARTHQUAKE RESPONSE ANALYSIS AND RESISTANT DESIGN OF MODERATELY DUCTILE REINFORCED CONCRETE SHEAR WALLS CONSIDERING HIGHER MODE EFFECTS

présentée par: LUU Quang Hieu

en vue de l'obtention du diplôme de : Philosophiae Doctor

a été dûment acceptée par le jury d'examen constitué de :

M. BOUAANANI Najib, Ph.D., président

M. LÉGER Pierre, Ph.D., membre et directeur de recherche

Mme KOBOEVIC Sanda, Ph.D., membre

M. SAATCIOGLU Murat, Ph.D., membre

DEDICATION

To my mother, Tam Thi Minh Nguyen, my father, Binh Truong Luu, and my brother, Trung Tien Luu. Thanks for being always willing to listen and for helping me keep focusing. Your supports help me more than you know.

Con cám ơn bố mẹ, anh Trung, và gia đình mình. Sự giúp đỡ và động viên của cả nhà đã giúp con rất nhiều để hoàn thành luận văn này.

To my wife, Anh Thi Mai Tran. Thanks for your love, patience, and understanding for me.

To my daughter, Adelina Mai Linh Luu. You are my all.

ACKNOWLEDGEMENTS

I would like to express my deepest gratitude to my advisor, Prof. Léger, for his guidance and support during my time at Ecole Polytechnique of Montreal, Montreal, Quebec, Canada. Thank you, Prof. Léger, for your patience guiding me throughout this research. It's you who has helped me understand the essential work of a researcher, which will help me through the path of my scientific career.

I would like to present my special thanks to Prof. Tremblay for his critical reviews and scientific supports for my research. Thank you, Prof. Tremblay, your comments are truly valuable and essentially help to improve my research quality.

I would also like to thank my committee members, Prof. Saatcioglu from University of Ottawa, and Prof. Bouaanani and Prof. Koboevic from Ecole Polytechnique of Montreal, who have read and evaluated this Ph.D thesis.

I also want to extend my gratitude to Dr. Ghorbanirenani for making a great experimental report that helped me so much in this research. I thank my friends, colleagues, and the department faculty and staff for making my time at Ecole Polytechnique of Montreal a great experience.

Thanks to the financial support provided by the Quebec Fund for Research on Nature and Technology (FQRNT) and the Natural Science and Engineering Research Council of Canada (NSERC).

Finally, thanks to my wife, for her love, patience and warm encouragement and thanks my family in Vietnam who always support me despite of thousands of miles between us. Thank God for helping my whole family stay healthy and strong.

RÉSUMÉ

Des études numériques récentes ont démontré que les exigences des codes actuels peuvent sous-estimer les efforts de cisaillement sismique à la base et les sollicitations des forces de flexion sur toute la hauteur des murs de refend en béton armé. Cette situation peut conduire à des ruptures par cisaillement à la base et à la formation de rotules plastiques involontaires dans la partie supérieure des murs. Les sous-estimations des sollicitations sont attribuées à des imprécisions en considérant l'effet des modes supérieurs de vibration (HMEs - higher mode effect) lorsque les éléments structuraux réagissent dans le domaine non linéaire. Des chercheurs ont proposé des méthodes pour prendre en compte les HMEs. Cependant, la plupart des méthodes proposées étaient fondées sur des études numériques utilisant des logiciels d'analyse des structures par éléments finis simples avec des éléments de poutre avec rotules plastiques concentrées aux extrémités, ou des modèles d'éléments finis avec des hypothèses qui n'ont pas été validées à l'aide de l'expérimentation dynamique. En outre, la plupart de ces propositions ont été limitées aux murs de refend situés dans l'ouest de l' Amérique du nord avec des sollicitations sismiques essentiellement de basses fréquences d'environ 2 Hz par opposition aux secousses sismiques de 10 Hz dans l'est de l' Amérique du nord est (ENA). Par conséquent, une étude des HMEs utilisant des modèles constitutifs de murs de refend validés expérimentalement, en considérant des secousses sismiques de hautes fréquences typiques de l'ENA est nécessaire.

Un projet de recherche sur les murs de refend est en cours à l'École Polytechnique de Montréal (Québec, Canada). La recherche consiste à proposer une méthode pratique pour la conception des murs de refend en béton armé situés dans l'ENA en considérant les HMEs. Le projet est limité à des murs de refend de ductilité modérée avec un coefficient de réduction de la force sismique $R_d = 2.0$ soumis à des tremblements de terre de l'ENA. Dans la première phase du projet, des essais sur simulateur sismique de deux spécimens de mur de 9 m de hauteur mis à l'échelle pour représenter un mur d'un bâtiment de 8 étages modérément ductile (MD) en béton armé ont été réalisés par Ghorbanirenani (2012). Les murs ont été conçus en conformité avec le Code national du bâtiment du Canada (CNB) 2005 et de la norme de béton CSA A23.3 -04 et ont été soumis à des secousses sismiques typiques de l'est de l'Amérique du Nord. Les résultats obtenus indiquent que les demandes en cisaillement et en flexion du Code ont été sous-estimées. Un comportement inélastique a été observé à la base des murs.

Cette thèse est la deuxième étape du projet sur les murs de refend, et elle met l'accent sur les

modélisations numériques des HMEs sur les réponses structurales des murs. La thèse se compose de trois parties principales, et chaque partie correspond à un article de revue scientifique. Les deux premières parties ont été limitées à des modèles de murs de refends isolés et bidimensionnels sans tenir compte de l'effet des interactions entre les différentes murs qui peuvent être présent dans un bâtiment et les effets de torsion des sections transversales. En revanche, la dernière partie aborde la conception et l'évaluation de la performance sismique en trois dimensions des murs de refend en béton armé dans le contexte d'un bâtiment existant.

La première partie était de développer de nouveaux modèles de comportement de mur de refend en utilisant à la fois la technique des éléments finis (Vector 2 - VT2) et des éléments fibres (OpenSees - OS). Le logiciel VT2 est basé sur la théorie des éléments finis en contraintes planes et permet la représentation de la plupart des phénomènes présents dans le comportement couplé des actions axiales, flexionnelles et de cisaillement des structures en béton armé. OS est un logiciel d'éléments finis comprenant des éléments poutres-colonnes fibres dont la formulation repose sur la théorie d'Euler- Bernoulli. OS représente une alternative intéressante pour la modélisation par rapport aux éléments finis "classiques" (VT2), car il peut reproduire la réponse à la flexion inélastique dominant le comportement prévu dans les murs de refend avec un temps très court de calcul. Les modèles ont été validés par les essais de gros spécimens en se servant des résultats des essais de la table vibrante de l'étape 1 du projet sur les murs de refend.

Dans la deuxième phase de cette thèse, les modélisations proposées (et expérimentalement validées) via les logiciels OS et VT2 de la phase 1 ont été utilisés comme modèles constitutifs représentatifs des murs de refend afin d'étudier les HMEs. Des études paramétriques impliquant des analyses transitoires non linéaires (NTHA) ont été réalisées pour étudier l'influence des paramètres de conception sur l'augmentation des effets d'amplification des modes supérieurs et sur la demande des efforts sismique internes (moments de flexion, efforts tranchants). Les résultats ont été utilisés pour proposer une nouvelle méthode de conception de capacité plus élevée compte tenu des effets d'amplification pour les murs de refend de type MD en béton armés situés dans l'ENA. La méthode conception propose des enveloppes de capacité pour les demandes en flexion et la résistance au cisaillement pPour obtenir une réponse sismique où la rotule plastique est située uniquement à la base des murs.

La dernière phase de cette thèse est de valider l'approche de conception proposée dans la phase 2, pour des murs plans, dans le contexte tridimensionnel comprenant des murs en forme de U dans un véritable bâtiment avec des propriétés structurales irrégulières. Les efforts tranchants locaux dans les

ailes induits par la torsion dans les murs en U et les interactions entre les différents murs de refend qui agissent ensemble dans un bâtiment ont été pris en compte. La validation a été mis en œuvre par l'évaluation de la performance attendue des configurations des murs de refend par l'approche de conception proposée en phase 2 pour un bâtiment de 9 étages situé dans l'ENA. L'évaluation de la performance sismique du bâtiment a été réalisée selon les lignes directrices ASCE/SEI 41-13 (« évaluation sismique et réhabilitation des bâtiments existants »). Les résultats ont montré que la procédure de conception proposée dans la phase 2 pourrait limiter la déformation plastique à la base des murs et de prédire avec précision la demande des forces de cisaillement pour les murs de refend avec des sections transversales planes (rectangulaires). Cependant, la prédiction des efforts tranchants est sous-estimée d'environ 70% à la base pour des murs de refend avec des sections transversales en U. En outre, l'enveloppe des efforts tranchants dans la partie supérieure des murs a été affectée par la répartition des masses irrégulières le long des murs, mais pas par l'effet des interactions entre tous les murs.

ABSTRACT

Recent numerical studies have demonstrated that current code requirements may underestimate the seismic shear at the base and the flexural strength demands along the height of reinforced concrete (RC) shear walls. These may lead to shear failure at base and unintended plastic hinge formation in the upper part of walls. The underestimations of the demands in codes are attributed to inaccuracies in considering higher mode effects (HMEs) when structural walls behave in the nonlinear range. Researchers have proposed methods to consider HMEs. However, most of the proposed methods were based on numerical studies using simple finite element structural analysis program with lumped plasticity beam elements or finite element models with assumptions that have not been validated by using experimental dynamic tests. In addition, most of these proposals were restricted to shear walls located in western North America (WNA) with low dominant frequency around 2 Hz as opposed to 10 Hz for eastern North America (ENA) earthquakes. Therefore, an investigation of HMEs using experimentally verified constitutive shear wall models considering high frequency ENA ground motions is necessary.

A shear wall research project is being conducted on this topic at Ecole Polytechnique of Montreal, Montreal, Quebec, Canada. The research is to propose a practicable method for RC shear wall designs located in ENA considering HMEs. The project is restricted to moderately ductile (MD) shear wall with a ductility-related force modification R_d = 2.0 subjected to ENA ground motion records. In the first stage of the project, shake table tests on two 9 m high scale specimens of slender 9-storey moderately ductile RC shear walls were performed by Ghorbanirenani (2012). The walls had been designed in accordance with the National Building Code of Canada (NBCC) 2005 and the CSA A23.3-04 standard and were subjected to ENA earthquake ground motions in the tests. The obtained results indicated that shear and flexural demands from the code were underestimated. Inelastic behaviour was observed at the base and in the sixth storey of the specimens.

This thesis is the second stage of the shear wall project, and it focuses on numerical investigations of HMEs on structural wall responses. The thesis consists of three main phases, and each phase corresponds to one (available online or submitted) journal paper. The first two phases were restricted to isolated and two-dimensional RC shear wall models without considering cross-sectional torsional effect and interactions between different shear walls. On the other hand, the last phase investigated three-dimensional RC shear walls in the context of an existing building.

The first phase was to develop new constitutive shear wall models using both finite (Vector 2-VT2) and fibre (OpenSees-OS) programs. VT2 is based on two-dimensional plane stress finite element theory and includes most of the phenomenological features present in RC members. OS is a multi-fibre beam element program based on the Euler-Bernoulli theory. OS represents an attractive alternative to finite element modelling (VT2), because it can reproduce the dominant inelastic flexural response anticipated in shear walls. The models were validated by large specimen shaking table test results of stage 1 of the shear wall project.

In the second phase, the proposed experimental validated OS and VT2 modelling procedures in phase 1 were used as representative constitutive shear wall models to investigate HMEs. Parametric studies involving nonlinear time history analyses (NTHA) were performed to investigate the influence of design parameters on higher mode amplification effects and related seismic force demand. The results were used to propose a new capacity design method considering higher mode amplification effects for MD type RC shear wall located in ENA. The method determined capacity design envelops for flexural and shear strength demands to achieve a single plastic hinge response at the wall base.

The last phase of this thesis is to validate the proposed design approach in phase 2 for three-dimensional RC shear walls in the context of a real building with structural irregular properties. Wall cross-sectional torsional effects and interactions between different shear walls while acting together in a building were considered. The validation was implemented by assessing the expected performance of the RC shear wall configurations designed by proposed design approach in phase 2 for an 8-storey RC shear wall building located in ENA. The assessment of the seismic performance of the building was conducted according to ASCE/SEI 41-13 guidelines ("Seismic Evaluation and Retrofit of Existing Buildings"). The results showed that the proposed design procedure in phase 2 could constrain plastic deformation at the base of the walls and predict accurately base shear force demand for planar (rectangular cross section) shear walls. However, the related prediction underestimated approximately by 70% base shear force demand for U shape shear walls. Moreover, shear force envelop in the upper part of the wall was significantly affected by irregular mass distribution, but not by the effect of interactions with other walls.

TABLE OF CONTENTS

LIST OF TABLES

LIST OF FIGURES

LIST OF SYMBOLS

A	The horizontal design ground acceleration
A_g	Gross concrete section area
A_s	Area of longitudinal steel bar
a_M	Mass-proportional damping coefficient
b_K	Stiffness-proportional damping coefficient
$[C]_{com}$	Damping matrix with committed stiffness matrix
$[C]_{ini}$	Damping matrix with initial stiffness matrix
$[C]_{tan}$	Damping matrix with tangent stiffness matrix
D & D_s	The dimension of lateral force-resisting system in a directional parallel to applied forces
E_c	Modulus of elasticity of concrete
E_s	Modulus of elasticity of steel
F	Foundation factor
f'_c	Compressive strength of concrete
f_t	Tensile strength of concrete
F_t	Portion of lateral force located at the top of the structure to consider higher mode effects
f_u	Ultimate tensile strength of steel
f_y	Yield tensile strength of steel
g	Gravity acceleration
h_n and h	Height of structure
h_{inel}	Distance from force resultant position from nonlinear time history analyses to the base
h_{el}	Distance from force resultant position from linear analyses to the base

h_w	Height of wall
I	Importance factor
J	Factor considering higher mode effects for bending moment according to NBCC 2010
$[K]_{com}$	Stiffness matrix with committed stiffness
$[K]_{ini}$	Stiffness matrix with initial stiffness
$[K]_{tan}$	Stiffness matrix with tangent stiffness
K	Numerical coefficient that reflects that material and type of construction, damping, ductility and/or energy-absorptive capacity of the structure
l_w	Length of the wall
[M]	Mass matrix
M_b	Flexural demand at base
M_c^*	Design moment at the mid-height of the wall
$M_{E,C}$	Moment at the mid-height of the wall obtained by elastic analysis
M_u	Moment capacity of the wall and moment obtained by elastic analysis
M_f	Factored moment
M_n	Nominal moment resistance
M_p	Probable moment resistance
M_r	Factored moment resistance
M_{uc}	Moment multiplied by the specified ultimate load factor
M_v	Factor considering higher mode effects for base shear according to NBCC 2010
n	Number of storey
V_d	Base shear force obtained from linear analyses
V_{inel} & V_{NL}	Base shear force obtained from nonlinear time history analyses.

P	Axial load at base
q	Behaviour factor according to Eurocode 8
R_d	Force reduction factor
R_o & f_o	Flexural overstrength factor
S_a	Spectral acceleration (g)
$S_e(T_c)$	The ordinate of the constant spectral acceleration region of the spectrum in short periods
T_a	Empirical fundamental period
T, T_1	Cracked section fundamental period
T_{uncr}	Uncracked section fundamental period
V_b	Shear force demand at base
V_d	Base shear force determined by elastic analysis
V_f	Factored shear demand
V_n	Nominal shear resistance
V_r	Factored shear resistance
V_y	Yield lateral load
W	Seismic weight of the structure
δ	Storey drift
Γ_θ	Normalized demand capacity ratio based on rotation
Γ_δ	Normalized demand capacity ratio based on drift
γ_w & γ_{Rd}	Wall base overstrength factor defined by ratio of nominal moment resistance and factor moment
ν_c	Poisson ratio of concrete
μ_θ	Storey rotation ductility
θ	Storey rotation demand

θ_{ic}	Plastic rotation capacity
θ_{id}	Inelastic rotation demand
θ_p	Plastic rotation
ω_n	Natural frequency
Ω_v	Base shear factor
ϕ_c	Resistance factor of concrete
ϕ_s	Resistance factor of steel
ε_o	Strain corresponding to compressive strength of concrete
ω_v & ε	Shear dynamic amplification factor
ξ	Damping ratio
ψ_v	Base shear ratio
α	Factor to construct tri-linear shear design envelop
ξ	Factor to construct tri-linear shear design envelop
β	Factor to construct tri-linear shear design envelop
μ_Δ	Displacement ductility
Δ_f & Δ_{top}	Wall top lateral deflection
Δ_y	Wall top lateral yield deflection

LIST OF ACRONYMS AND ABREVIATIONS

1D	One-Dimensional
3D	Three-Dimensional
ACI	American Concrete Institute
ASCE	American Society of Civil Engineering
COV	Coefficient of Variation
CP	Collapse Prevention
CSA	Canadian Standard Association
DCH	Ductility Class High
DCM	Ductility Class Medium
DCR	Demand Capacity Ratio
DSFM	Disturbed Stress Field Model
DPH	Dual Plastic Hinge
EC	Eurocode 8
ENA	Eastern North America
ESFP	Equivalent Static Force Procedure
EXP	Experiment
Fbk	Feedback
FE	Finite Element
FQRNT	Quebec Fund for Research on Nature and Technology
HME	Higher Mode Effect
IO	Immediate Occupancy
LS	Life Safety
MCFT	Modified Compression Field Theory
MD	Moderately Ductile

MMS	Modified Modal Superposition
NBCC	National Building Code of Canada
NTHA	Nonlinear Time History Analysis
NZS	New Zealand Standard
NSERC	Natural Science and Engineering Research Council of Canada
RC	Reinforced Concrete
OS	OpenSees
SC	Soil Class
SD	Standard Deviation
SPH	Single Plastic Hinge
SRSS	Square Root of the Sum of the Squares
SW	Shear Wall
TSE	Tension Stiffening Effect
UHS	Uniform Hazard Spectra
VT2	VecTor2
W1 and W2	Wall 1 and Wall 2
WNA	Western North America

INTRODUCTION

Buildings braced by reinforced concrete (RC) shear walls are invariably stiffer than framed structures, reducing the possibility of excessive deformations under earthquakes (Paulay & Priestley, 1992). The use of RC shear walls in buildings is becoming a very popular scheme in the design of multi-storey buildings to resist lateral loads such as earthquake and wind in Europe and North America. Thus, it is very important to understand the behaviour of RC shear walls and evaluate their response appropriately.

Most seismic design codes, including National building Code of Canada (NBCC) 2010 (NRCC, 2010), Eurocode 8 (CEN, 2004) and New Zealand codes (NZS, 2006) are based on capacity design principles. Seismic design procedures for walls are required to ensure that: i) inelasticity is restricted in ductile response mechanisms in predefined locations; ii) there is no shear failure during seismic events; iii) the capacity of ductile mechanisms has adequate ductility to sustained expected inelastic deformations.

Recent numerical studies (Boivin & Paultre, 2012a; Rutenberg & Nsieri, 2006) have investigated the importance of higher mode effects (HMEs) in structural wall response. These studies demonstrated that the current code requirements may underestimate the seismic shear at the wall base and flexural strength demands in the wall middle height; and may thus lead to shear failure at the wall base and unintended plastic hinge formation in the upper part of the wall.

The reasons of these deficiencies in both shear and flexure demands could be explained as follows. Current building codes (NRCC, 2010; NZS, 2006; CEN, 2004) recommend using modal response spectrum analysis (MRSA) for seismic design. This technique is based on mode superposition method (Figure i-1a), which is restricted to linear elastic analysis. To account for nonlinear behaviour in design, the computed force demand from an elastic analysis is simply reduced by applying inelastic response modification coefficients (R_dR_0 in NBCC 2010; behaviour factor, q, in EC8) (Figure i-1b). However, at the time of base plastic hinge formation, the shear wall responds like a pinned-base structure after base hinging (Figure i-1c), with relatively greater importance of HMEs. The force distribution from base to the top of the structure is redistributed and the position of the resultant force is lowered down, $h_{inel}<h_{el}$, (Figure i-1c) as the structure becomes inelastic. The factor R_dR_o in NBCC 2010 or q in EC8 does not account for this redistribution of force. This anticipated behaviour causes inaccuracies in seismic shear wall response predictions, especially underestimation

of base shear force prediction ($V_{inel}>V_d$) (Figure 1c) and nonlinearity formation in the upper part of the wall.

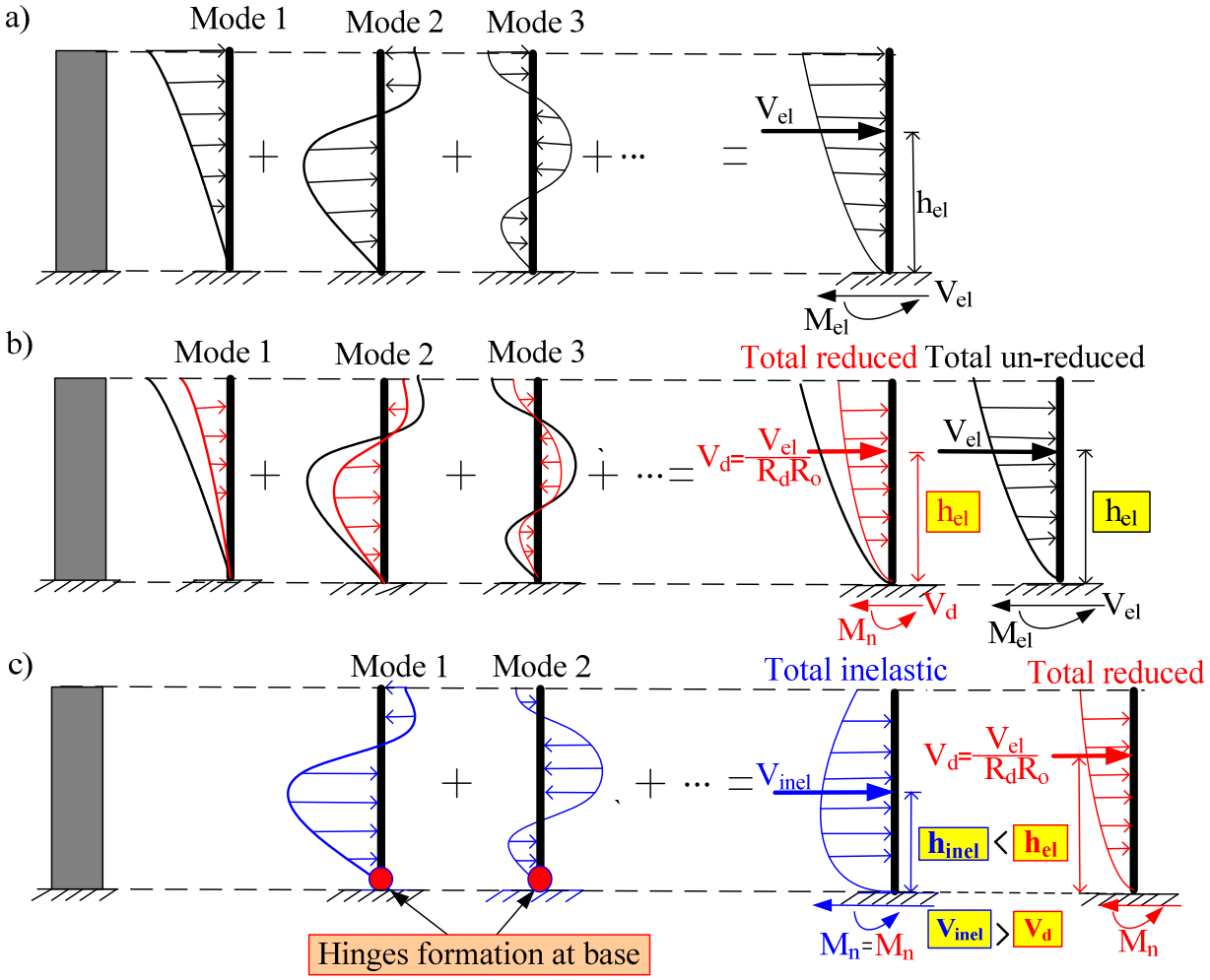

Figure i-1: Analysis considering higher mode effects on structural wall responses: a) linear modal response spectrum analysis; b) linear modal response spectrum analysis considering nonlinearity; and c) real nonlinear behaviours.

Seismic design provisions (NRCC, 2010; NZS, 2006; CEN, 2004) and researchers (Boivin & Paultre, 2012b; Rejec et al., 2012; Velev, 2007; Ruttenberg & Nsieri, 2006) have proposed methods to consider HMEs. However, most of the proposed methods were based on numerical studies using simple finite element structural analysis programs with lumped plasticity beam elements (Rejec et al., 2012; Velev, 2007; Ruttenberg & Nsieri, 2006) or finite element models with assumptions that have not been validated using dynamic tests (Boivin & Paultre, 2012b). Modelling assumptions may affect

HME predictions in numerical analysis results (Wallace, 2007). Therefore, an investigation of HMEs using experimentally verified constitutive shear wall models is necessary.

In eastern North America (ENA), moderately ductile (MD), with a ductility-related force modification $R_d = 2.0$, is the most commonly used RC shear wall category because of moderate and low seismic demand in the region. The earthquakes herein are inherently rich in high frequencies ground motions, of the order of 10 Hz, which are coinciding with the frequencies of high vibration modes of RC shear walls. Therefore, the HMEs might be especially critical for ENA (Ghorbanirenani et al., 2009; Panneton et al., 2006).

Shaking table tests were conducted on 0.43 scaled, 9m high wall models of an 8-storey MD shear walls designed according to Canadian codes under high-frequency-content ENA earthquakes (Ghorbanirenani et al., 2012). The tests indicated that shear and flexural demands from the code were underestimated. Inelastic behaviour was observed at the base and in the sixth storey of the specimens.

Using the experimental data of the shaking table tests as a starting point (Ghorbanirenani et al., 2012), the research presented in this thesis addresses the analysis and design of MD RC shear walls located in ENA considering HMEs.

Objectives

This research project is aimed to address analysis and design of slender MD RC shear walls. It studies typical RC shear wall behaviours considering high frequency ENA ground motions with dominant frequency around 10Hz as opposed to 2Hz for western North America (WNA), where most previous earthquake resistant researches were done. Constitutive shear wall models validated by large specimen shaking table tests are proposed. This research develops, validate, and advance a new seismic design procedure in the context of Canadian building code for MD RC shear wall buildings to ensure that slender MD RC shear walls only develop the desired inelastic flexural response mechanism at the base of the wall during seismic events.

The objectives of this study are summarized as follows:

a. To develop modelling recommendations that provide accurate seismic simulations of RC shear walls located in ENA considering HMEs. The recommendations are validated by large specimen shaking table tests.

b. To evaluate Canadian seismic design procedures for walls by conducting nonlinear time history analysis (NTHA) using the above modelling recommendations.
c. To develop simplified methods to determine the shear and bending moment magnitudes at base of walls and distributions over wall heights considering HMEs.
d. To investigate seismic performance assessment of 3D RC shear walls in the context of an existing building considering the interactions between different shear walls while acting together.
e. To formulate practical recommendations for the design of RC shear walls located in ENA considering HMEs.

Methodology

The research focuses on the development of a method for accurately simulating dynamic response of RC shear wall and the application of this method to evaluate and advance current design procedures for shear wall buildings in the context of Canadian code.

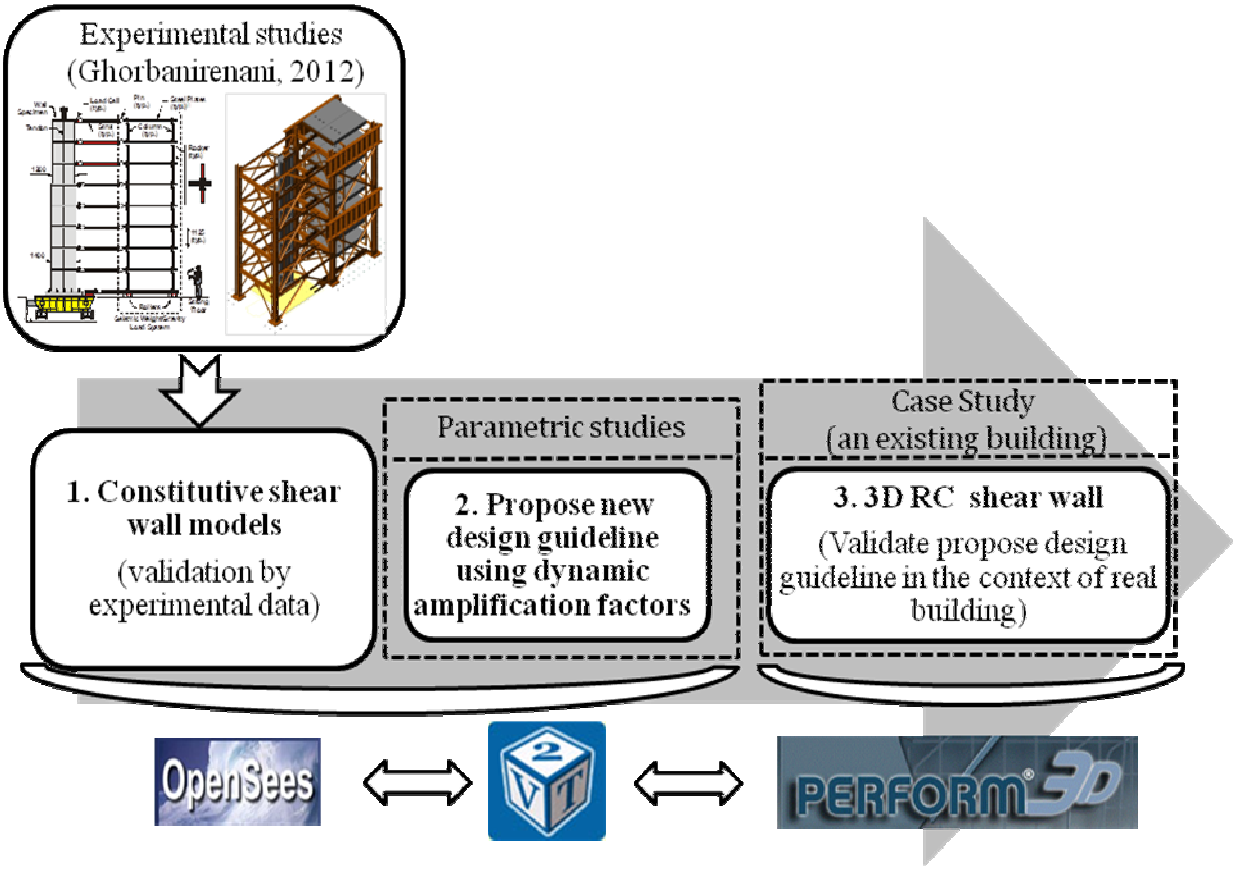

Figure i-2: Three research stages presented in the thesis.

The overview of the research approach is shown in Figure i-2, and the main tasks were performed as follows:

a. Literature review on HMEs on structural responses of RC shear wall.
b. Literature review on numerical simulations of slender RC shear wall using conventional modelling approaches.
c. Literature review on experimental studies of RC shear walls (large specimen cyclic and shaking table tests).
d. The development of constitutive shear wall model by using both finite (Vector 2, VT2) and fibre (OpenSees, OS) models.
e. The validation of the proposed models through comparisons of simulated and measured responses of large specimen shaking table tests.
f. Conducting NTHA using the developed OS and VT2 modelling procedures to propose new code-type procedures to determine the seismic demand on structural walls under high-frequency-content ENA earthquakes (a new shear force magnification factor, Ω_v has been developed).
g. The development 3D shear wall models using fiber element method (Perform 3D).
h. The validation 3D shear wall modelling using measured response of large scale cyclic U shape shear wall test available from the literature.
i. Conducting NTHA as a key step of ASCE 41-13 guidelines to investigate seismic performance assessment of complex cross section (U shape) RC shear walls in the context of an existing building considering the interactions between different shear walls.
j. The investigation of the efficiency of the proposed shear force magnification factor, Ω_v, considering higher mode effects for complex cross section (U shape) RC shear walls.
k. Proposing recommendations for shear wall designs considering the interaction between shear walls in a context of real building.

Original contributions

The main scientific contributions of this research are as follows:

a. Demonstrating that finite element models are capable of reproducing most of the nonlinear dynamic responses of large specimen shaking table tests of reinforced concrete shear walls, and especially predicting the HMEs on the tested wall responses.

b. Demonstrating that the fibre element model is capable of reproducing most of the nonlinear dynamic responses of large specimen shaking table tests of reinforced concrete shear walls if the shear stiffness is adequately modelled as proposed herein, and especially predicting the HMEs on the tested wall responses.
c. Demonstrating that the tension stiffening effect (TSE) should not be considered in developing seismic numerical models of slender RC shear walls. Consideration of the TSE may result in inaccurate estimations of the structural responses of the walls.
d. The development of a new simplified method to determine the shear and bending moment magnitude at base and distributions over wall height of isolated 2D planar RC shear walls considering higher mode effects in the context of high frequency ground motions of ENA.
e. A case study using ASCE-41-13 guidelines as a basis for seismic performance assessment of two alternative designs using an existing ENA reinforced concrete shear wall building initially braced by two cores considering the interaction between shear walls in the building.
f. The development of a simplified method to simulate accurately seismic response of a shear wall building located in ENA with a commercial computer program (Perform 3D).

CHAPTER 1 REVIEW OF LITERATURE

This chapter presents a literature review on the matters which form the basis of developments of the research project. This chapter is divided into 3 sections. The first section presents different approaches for finite element modelling tools. These approaches are currently in widespread use by both the design and research structural engineering communities to simulate the response of shear walls and HMEs. In the second section, we discuss current and recent proposed methods to consider HMEs on structural wall responses for building codes. We terminate this chapter by the section considering experimental studies, large specimen cyclic and shaking table tests of structural walls, conducted recently.

1.1 Numerical modelling approaches for nonlinear analysis of RC shear wall buildings

Inelastic flexural shear wall models can be differentiated by the way that plasticity is distributed through the member cross sections and along its length. Figure 1-1 shows three commonly used modelling techniques for RC shear walls with varied sophistication levels. The simplest model is elastic frame elements with hysteretic lumped plastic hinges concentrated at their ends (Figure 1-1a). The behaviour of the plastic hinge is based on either the moment-curvature hysteretic rule or multi-linear moment-rotation backbone curve. The moment curvature relationship for each wall is developed considering actual steel reinforcement and factored axial load. The multi-linear moment-rotation backbone curve is selected using ASCE/SEI 41-13 guidelines ("Seismic Evaluation and Retrofit of Existing Buildings") (ASCE, 2013). This curve was developed using data from laboratory tests of walls with varying design characteristics. For shear walls, the curve is dependent on the nominal flexural resistance, the axial load level at base, and shear demands developed. A hinge length of half the length of the wall is implicitly assumed. The models concentrating nonlinearity on lumped plasticity sections are computationally efficient and numerically robust, and have been used in researches addressing earthquake design and response of walls (Rejec et al., 2012; Calugaru & Panagiotou, 2012; Boivin & Paultre, 2010; Panneton et al., 2006;). However, the moment-curvature (or rotation) response of the hinge following lumped plasticity model is defined prior to the analysis, so the model cannot account for the effect on the response of variations in axial or shear load. In addition, beyond the simplified representation of the response, because nonlinear behaviour is concentrated on the location of the lumped-plastic hinge, multiple analyses may be required in which

additional hinges are introduced or hinges are moved to accurately simulate the distributed nonlinearity within the wall (Pugh, 2012).

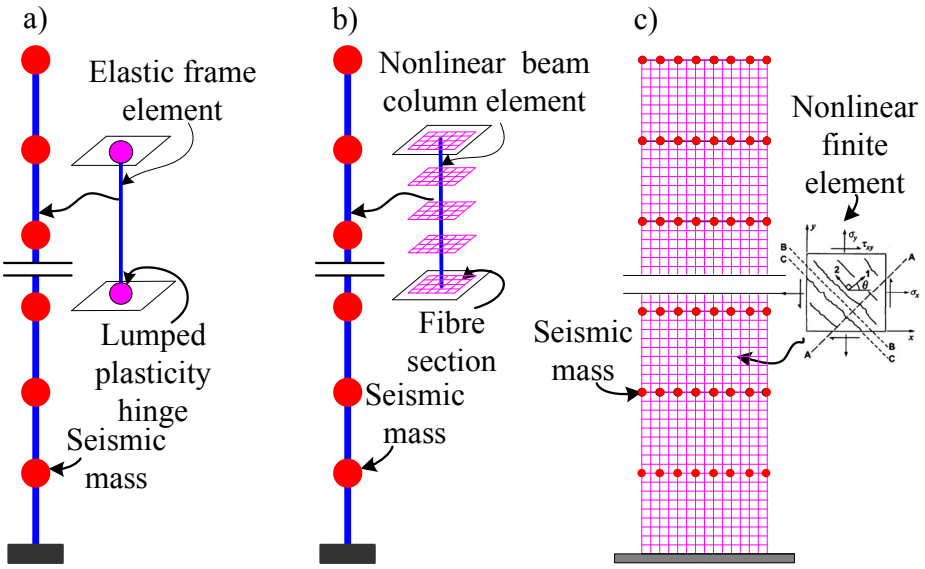

Figure 1-1: Idealized nonlinear models of RC shear wall buildings : a) elastic frame based lumped plasticity; b) fibre element based distributed plasticity; and c) finite element based distributed plasticity.

A more sophisticated approach to represent nonlinear response of RC shear walls is the fibre element distributed plasticity model (Figure 1-1b). The model distributes plasticity by numerical integrations through the member cross sections and along the member length. The fibre-type discretization of the section comprises concrete and steel fibres for which uniaxial material models are defined to capture the nonlinear hysteretic behaviour. The uniaxial material "fibres" are numerically integrated over the cross section to compute moment and axial load and incremental moment-curvature and axial force-strain relations, so these models enable simulation of the effect of axial load on flexural response. A fibre element based distributed plasticity model does not require prior moment curvature analysis as in lumped plasticity models. There is also no need to define the RC element hysteretic response because it is defined by the material models. The post-peak strength reduction factor resulting from material strain-softening or failure can be directly modeled. The fibre based distributed plasticity model has been employed within finite element programs, for example OpenSees (OS) (Mazzoni et al., 2006) and Perform 3D (CSI, 2013), to predict the nonlinear response of RC shear walls (Ghorbanirenani et al, 2009; Boivin & Paultre, 2012a).

The main disadvantage of fibre element based distributed plasticity model is the assumption of sections remaining plane during analyses. This causes errors for simulation of fibre strains and thus inaccurate simulate of the strength and/or deformation capacity, and de-coupling of the responses between shear and flexure. In addition, there is strain localization problem in using fibre element based distributed plasticity model (Coleman & Spacone, 2001). This might cause fibre model to produce an inaccurate prediction for loss of lateral load carrying capacity.

This type of model was used to reproduce the results of a RC shear wall large scale shaking table tests subjected to WNA earthquakes (Schotanus & Maffei, 2008; Martinelli & Filippou, 2009) and a RC shear wall large scale cyclic tests (Pugh, 2012). Good agreements with experiments were obtained except the shear prediction in Martinelli & Filippou (2009). Noting that Pugh (2012) employed an effective shear stiffness equal to 10% of the initial elastic shear stiffness used in Martinelli & Filippou (2009).

The most sophisticated models (Figure 1-1c) discretize the continuum along the shear wall length and through the cross sections into finite elements with nonlinear hysteretic properties. This type of model has the greatest potential to simulate accurately the nonlinear response of RC shear walls including nonlinear axial, flexure and shear interactions. However, the model usually asks for numerous input parameters, which presents the most challenge in terms of model parameter calibration analysis (Loh et al., 2002; Krawinkler, 2006). In addition, nonlinear analyses using finite element models are extremely computationally demanding, and typically analyses are done using implicit solution algorithms, which are often plagued by convergence issues, especially when solutions are sought beyond the point at which strength loss initiates (Powel, 2010; Pugh, 2012).

Vector (VT) 2 program (Wong & Vecchio, 2002) developed from University of Toronto is based on 2D plane stress finite element theory and includes most of the features present in RC members. In VT2, concrete responses were defined by using Modified Compression Field Theory (Vecchio & Collins, 1986). VT2 was used to reproduce the seismic responses of shear walls from quasi-cyclic tests (Palermo & Vecchio, 2007; Ghorbanirenani et al., 2009b; Pugh, 2012). Dynamic seismic analyses were performed with VT2 (Tremblay et al., 2008; Ghorbanirenani et al., 2009a), but no validation has yet been performed against shake table test data.

1.2 Analyses and design of RC shear walls considering higher mode effects

During severe earthquakes, a ductile RC shear wall is expected to exhibit inelastic flexural behaviour, although the shear response must remain elastic (Paulay & Priestly, 1992). For that purpose, several procedures have been proposed and/or applied in codes, such as the NZS 3101 standard in the New Zealand, EC 8, and NBCC 2010.

For details of proposed design procedures in literature review, readers are invited to firstly read section 4.2 of this thesis, "Seismic Design Guidelines Considering HMEs" (from paper number 2). The followings are to present some additional proposed design procedures considering HMEs in literature review which were not shown in section 4.2.

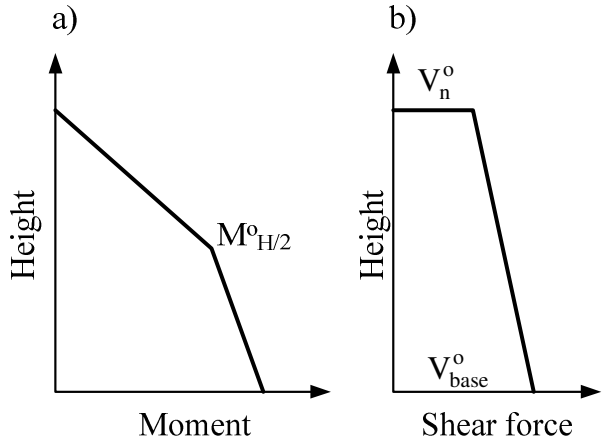

Figure 1-2: Distribution of design (a) moment and (b) shear along the height after base plastic hinge formation (Priestley et al., 2007)

Priestly et al. (2007) analyzed a series of six walls ranging from 4 to 20 storeys and designed according to the direct displacement-based design procedure. They observed increases in the intensity of shear force and bending moment envelops when increasing the applied earthquake intensity, even after the base platic hinge was formed. The authors proposed a bilinear moment envelop to take into account higher mode effects (Figure 1-2a). This envelop starts at the base with the expected flexural overstrength, ends at zero moment at the top, and passes through mid-height moment $M^0_{H/2}$ given by:

$$M^0_{H/2} = C_{1,T}\phi^0 M_b \quad \text{where} C_{1,T} = 0.4 + 0.075 T_1(\mu/\phi^0 - 1);\ C_{1,T} \geq 0.4 \qquad (1.1)$$

in which ϕ^0 is the wall base expected flexural overstrength factor, M_b is the design base bending moment, T_1 is the fundamental elastic period, and μ is the displacement ductility factor. Regarding

shear force demands, Priestly et al. (2007) proposed the shear force capacity envelop that is linear in Fig 1-2b and defined as:

$$V_{base}^{0} = \phi^{0}\omega_v V_{base} \text{ where } \omega_v = 1 + \frac{\mu}{\phi^{0}} C_{2,T}; C_{2,T} = 0.067 + 0.4(T_1 - 0.5); \omega_v \leq 1.15 \quad (1.2)$$

The design shear force at top of the wall, V_n^0 , is related to the shear at the bottom of the wall by:

$$V_n^0 = C_3 V_{Base}^0 \quad \text{where } C_3 = 0.9 - 0.3T_1; C_3 \geq 0.3 \quad (1.3)$$

In addition, Priestley et al. (2007) also proposed a modified modal superposition (MMS) technique for design forces in cantilever shear walls. For shear force envelop, a traditional multi modal analysis procedure requires calculating the contributions of all considered modes using an elastic acceleration spectrum, combining them using such a technique as the square root of the sum of the squares (SRSS), and then dividing that result by the design displacement ductility. Conversely, in the MMS method, only the first mode is reduced by the design ductility, that demand is combined with the unreduced elastic contributions of all other considered modes, and the total is not reduced. Regarding the bending moment envelop, the same method was proposed for the upper half of the wall, but multiplied by a calibration factor of 1.1, and a linear moment profile is suggested from below mid-height to the base moment capacity.

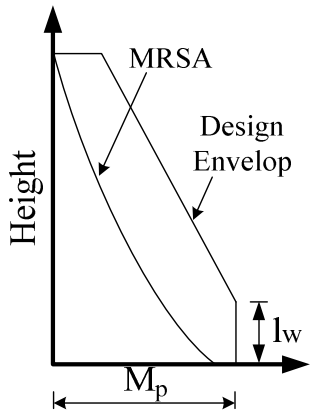

Figure 1-3: Distribution design of moment (Paulay & Priestly 1992)

Pugh (2012) studied a set of 64 reinforced concrete shear wall buildings with number of storey varying from 6 to 26 and designed according to current United State building code design (ASCE, 2010). From the obtained results, the author also proposed MMS as presented in Priestly et al. (2007) to estimate shear force design of RC shear wall buildings considering HMEs. However, Pugh (2012)

suggested to use tri-linear design envelop as presented in Paulay & Priestly (1992) for moment design envelops (Figure 1.3).

While examining shear provision of EC8 for ductile reinforced concrete shear wall, Rutterberg & Nsieri (2006) showed that allowing second plastic hinge formation in the upper part of the wall can decreases the base shear amplification. That can be more pronounced for structures with long periods and high value of ductility. Based on this observation, Panagiotou & Resprespo (2009) proposed the "dual hinge" design concept for RC shear wall buildings to consider HMEs. According to the proposed concept, the walls are allowed to develop a second plastic hinge in a predefined location in the upper part in addition to one at base while ensuring elastic response elsewhere. This mid-height plastic hinge can be designed like the base plastic hinge to meet specific requirements such as rotational ductility capacity or shear demand. Reduction of bending moment demand over wall height due to the second plastic hinge formation will be followed by a reduction in the amount of longitudinal reinforcement when compared to the wall design in accordance with the codes.

The advantage of the dual hinge design procedure was observed from the numerical study carried out by Panagiotou & Resprespo (2009) on 10, 20 and 40-storey shear walls. The walls were subjected to near-fault ground motions that have distinct strong pulses with significant frequency content in the period range of the second mode for the building considered. All walls were designed using the single plastic hinge (SPH) and dual plastic hinge (DPH) concepts. The results showed that SPH leads to an increased of flexural demand at the mid-height whereas DPH reduced significantly bending moments over wall heights. This effect will be more significant for structures with long fundamental periods. In addition, the shear forces were also reduced in DPH.

1.3 Experimental studies

To understand the true behaviour of planar (rectangular) RC shear walls under dynamically applied seismic ground motions of ENA, Ghorbanirenani et al. (2012) performed shake table tests on two identical rectangular cross section wall specimens, wall (W) 1 and wall (W) 2, designed with a scaling factor of 0.43. The specimens are representative of an individual slender reinforced concrete wall of an 8-storey residential building located in Montreal, QC, Canada, and designed according to the 2005 National Building Code of Canada (NBCC) (NRCC, 2005) with a combined inelastic force reduction factor R_dR_o of 2.8. The models have a total height of 9 m, with a uniform storey height of

1.125 m. The wall length is 1.4 m up to the 6th level and 1.2 m above this level. The wall thickness is 80 mm. The seismic weight at each floor is approximately 62 kN. The first wall (W1) was initially tested under 40% of the design EQ intensity. The intensity of the motion was subsequently increased up to 100, 80, and 120% EQ levels. The second wall (W2) was tested directly under the 100% EQ level, simulating an initially undamaged wall exhibiting uncracked stiffness when the design seismic event occurs. The earthquake record intensity of W2 was then successively increased to 120, 150, and 200% of the design earthquake. Unless otherwise noted, all analyses presented in this study were performed using the shake table acceleration feedback signals measured during the tests as input seismic motions.

The observed wall responses are presented in details in Ghorbanirenani et al. (2012). In the 100% EQ and higher level tests, plastic hinges formed at the wall base, as expected by design, as well as in the upper storeys due to higher mode response. Moreover, there was an excessive shear demand with respect to the design shear force capacity prescribed in the current building codes. In the tests, horizontal displacements, accelerations and inertia forces were directly measured at every level. Storey shear and overturning bending moments were obtained from the measured forces. Rotational demands were measured at storeys 1 and 6.

To investigate the behaviour of U shape RC shear wall, two U-shaped walls built at half scale were tested under a quasi-static cyclic loading regime (Beyer et al., 2008). The two tested walls differed mainly with regard to their wall thicknesses, the one with the thickness of 150 mm was named TUA and the other with the thickness of 100mm was named TUB. The tested specimens were not designed according to a particular code but their design for high ductility followed principles that were judged reasonable without being unnecessarily conservative with respect to the shear force and sliding shear design. The tests were focusing on the bending behaviour in different directions and therefore the walls were subjected to a bi-directional loading regime. Three actuators were used to control the horizontal movement of the top of the wall. The loading pattern imposing on the specimens was repeated at displacement ductility levels of 1, 2, 3, 4, 6, and 8 until failure occurred. For a more detailed presentation of the tests, the reader is referred to Beyer et al. (2008).

CHAPTER 2 ORGANIZATION AND OUTLINE

The introduction of this thesis presented background information on the research topic, the objectives of the research project, and the methodology that was adopted. Chapter 1 is the literature review reporting on past seismic analytical and experimental works on RC shear walls. Seismic design provisions included in current code documents are also discussed in chapter 1.

The subsequent three chapters respectively correspond to three technical papers that have either appeared or been submitted for publication in scientific journals:

Chapter 3 (Paper 1): Luu, H., Ghorbanirenani, I., Léger, P., & Tremblay, R. (2013). Numerical modelling of slender reinforced concrete shear wall shaking table tests under high-frequency ground motions. Journal of Earthquake Eng., 17, (4): 517–542.

Chapter 4 (Paper 2): Luu, H., Léger, P., & Tremblay, R. (2014). Seismic demand of moderately ductile reinforced concrete shear walls subjected to high frequency ground motions. Can. J. Civ. Eng., 41(2): 125-135.

Chapter 5 (Paper 3): Luu, H., Léger, P., & Tremblay, R. (2014). Assessing the seismic performance of 3D reinforced concrete shear wall buildings considering higher mode effects. Eng. Struct. (Submitted on 26 February 2014).

The content of these three chapters can be summarized as follows:

Chapter 3 presents the numerical modelling of large-scale shake table tests of slender 8-storey reinforced concrete (RC) shear wall specimens. Nonlinear time history analyses are carried out using reinforced concrete fibre elements (OpenSees, OS) and the finite element (FE) methods (VecTor2, VT2). The effects of the modelling assumptions are investigated, including (i) the tension stiffening effect, (ii) damping, (iii) smeared vs. lumped reinforcement, and (iv) the use of effective shear stiffness in OS. Good agreements are obtained between the numerical and experimental results. Using the proposed numerical modelling strategy, it is possible to investigate the nonlinear dynamic responses of slender RC wall structures with confidence.

Chapter 4 presents a parametric study performed to examine the seismic behaviour of MD RC shear walls designed according to Canadian code provisions, including NBCC2010 and CSA 23.3-04, when subjected to typical high-frequency ENA earthquakes. The numerical models

were experimentally validated based on large specimens shaking table test results in Chapter 3. The results obtained following the code response spectrum procedure were compared with the results from inelastic response history analyses to investigate the effect of higher modes on seismic force demands. The results indicate that current code provisions for MD shear walls need to be modified. A new base shear factor, Ω_v, and shear force design envelop are proposed to evaluate the seismic shear force demand more realistically. This study also recommends that the current CSA 23.3-04 requirements for ductile shear walls for bending moments could be applied to constrain the location of inelastic flexural deformations at the base of MD shear walls.

Chapter 5 presents three alternative design procedures to consider higher mode effects (HMEs) for an existing moderately ductile reinforced concrete shear wall building in eastern North America (ENA). Two procedures are described in (1) theinitially used (NBCC 1977) and (2) the current (NBCC 2010) versions of the National Building Code of Canada (NBCC). The third design procedure (3) (NBCC2010+) has been developed using nonlinear time history analyses for planar walls using the experimentally validated constitutive shear wall model (Chapters 3, 4). These three alternatives were implemented in the designs of an existing 10-storey shear wall building initially braced by two cores. The seismic performance of the building was assessed according to ASCE/SEI 41-13 guidelines ("Seismic Evaluation and Retrofit of Existing Buildings"). The progressive analysis procedures prescribed in ASCE/SEI 41-13 were used, including (a) linear static, (b) linear dynamic, (c) nonlinear static, and (d) nonlinear dynamic analyses. The results indicated that static procedures provided different conclusions relative to building performance compared to dynamic procedures because of significant HMEs in the ENA region. Inputting an effective wall shear stiffness derived from finite element models into fibre element models (Chapter 3) yields a better base shear force prediction than when using the shear envelop defined in ASCE/SEI 41-13. NBCC 2010+ provided the best seismic performance among the three design alternatives. NBCC 2010+ could constrain plastic deformations at the base of the walls. However, the related shear demand prediction underestimated the base shear force computed from 3D nonlinear dynamic analyses for U-shaped shear walls by approximately 70%. The shear force envelop in the upper part of the wall was significantly

affected by the irregular mass distribution but not by the effect of interactions between different walls.

Chapter 6 presents a general discussion of the results obtained from the numerical study with respect to the problems and observations discussed in the literature review. The thesis terminates with Conclusions and Recommendations for future studies on HMEs on RC shear walls.

CHAPTER 3 ARTICLE 1: NUMERICAL MODELLING OF SLENDER REINFORCED CONCRETE SHEAR WALL SHAKING TABLE TEST UNDER HIGH-FREQUENCY GROUND MOTIONS

This chapter presents the numerical modelling of large-scale shake table tests of slender 8-storey reinforced concrete (RC) shear wall specimens. Nonlinear time history analyses are carried out using reinforced concrete fibre elements (OpenSees, OS) and the finite element (FE) methods (VecTor2, VT2). The effects of the modelling assumptions are investigated, including (i) the tension stiffening effect, (ii) damping, (iii) smeared vs. lumped reinforcement, and (iv) the use of effective shear stiffness in OS. Good agreements are obtained between the numerical and experimental results. Using the proposed numerical modelling strategy, it is possible to investigate the nonlinear dynamic responses of slender RC wall structures with confidence. The content of this chapter corresponds to the article with title "numerical modelling of slender reinforced concrete shear wall shaking table tests under high-frequency ground motions" published on Journal of Earthquake Engineering in 2013, volume 17, issue 4, pages 517–542.

3.1 Introduction

Ghorbanirenani et al. (2012) performed shake table tests on two reduced scale specimens, 9 m high, of slender 8-storey moderately ductile reinforced concrete (RC) shear walls by subjecting them to the high predominant frequency ground motions, of the order of 10 Hz, typical in eastern North America (ENA). The tests showed that higher mode effects can play an important role in the seismic responses of such walls, as was predicted in past numerical studies (Filiatrault et al., 1994; Priestley & Amaris, 2002; Panneton et al., 2006; Sullivan et al., 2008; Panagiotou & Restrepo, 2009) and in recent experimental programs (Panagiotou et al. 2007, Kim et al. 2011, Panagiotou et al. 2011). In particular, the tests confirmed the possibility that an inelastic flexural response develops in the upper parts of tall walls. Moreover, base shear forces exceeded the values corresponding to the attainment of the walls' flexural strength at the base. These effects are not explicitly considered in seismic design provisions, such as ACI-318 (ACI, 2010) in the U.S or CSA A23.3 (CSA, 2004) in Canada, while an amplification of the base shear is required in New Zealand (NZS, 2006) and in Eurocode (CEN, 2004).

Large-scale shake table tests are among the best methods to understand the true behaviour of structures under dynamically applied seismic ground motions, but performing such tests is very

costly and time consuming. Therefore, experimental studies must be complemented by extensive numerical analyses to develop a better understanding of the seismic behaviour of walls. RC shear walls were often modelled in the past using elastic frame elements with hysteretic lumped plastic hinges concentrated at their ends (Clough & Johnston, 1966; Takeda et al., 1970). Although inelastic flexural seismic responses can be predicted reasonably well with these models, these analyses did not account for shear sliding deformations along large flexural cracks and the degradation of shear stiffness due to the diagonal cracking that can develop in walls subjected to large, cyclic, and inelastic deformations (Cheng et al., 1993; Thomsen IV & Wallace, 2004). The failure of the compressive zone due to the combination of shear, flexural, and axial loads in critical regions was also ignored. The prediction of the inelastic response of RC walls ideally requires the use of accurate, effective, and robust modelling and analysis tools that incorporate important material characteristics and behavioural response features, such as tension stiffening, the opening and closing of cracks, concrete confinement, and that take the interaction of axial, shear, and flexural forces into account.

Finite element analyses have been successfully used to capture most of these effects and to reproduce the shake table test responses of shear wall structures (Lu & Wu, 2000; Kazaz et al., 2006). However, there are many parameters that control the accuracy of the analysis (Loh et al., 2002; Krawinkler, 2006). Multi-fibre beam element models based on the Euler-Bernoulli theory represent an attractive alternative to finite element modelling, as they can reproduce the dominant inelastic flexural response anticipated in shear walls in detail (Orakcal & Wallace, 2006; Schotanus & Maffei, 2008; Grange et al., 2009; Kim et al., 2011), while being significantly less computationally demanding than finite element analysis, especially if 3D building models are considered. Shear deformations in fibre models are generally considered independently assuming a linear elastic shear response, without interaction with the flexural response. Fibre element models are now available in commercial software packages that are used in daily practice for the seismic analysis of RC structures (CSI, 2006; CSI, 2010; Seismosoft, 2011). Engineers would, therefore, benefit from validations performed against dynamic seismic test data that could improve the reliability of this simpler analytical technique.

This paper develops appropriate constitutive shear wall models that can reproduce the dynamic responses of the tested walls. The finite element method of the Vector 2 computer program (VT2) (Wong & Vecchio, 2002) and the fibre elements of OpenSees (OS) (Mazzoni et al., 2006) are used to quantify the effects of modelling assumptions through comparisons with the shake table test results

from Ghorbanirenani et al. (2012). VT2 is based on 2D plane stress finite element theory and includes most of the features present in RC members. VT2 was used to reproduce the seismic responses of shear walls from quasi-cyclic tests (Palermo & Vecchio, 2007; Ghorbanirenani et al., 2009b). Dynamic seismic analyses were performed with VT2 (Tremblay et al., 2008; Ghorbanirenani et al., 2009a), but no validation has yet been performed against shake table test data. The OS computer program has previously been used to predict shake table results for RC walls subjected to large inelastic demands from the ground motions expected in the western U.S. (Martinelli & Filippou, 2009). The walls studied here are of the moderately ductile category. They are subjected to the high-frequency ground motions typical of the earthquakes anticipated in ENA. The constitutive models developed in the study could then be extended with confidence to study the seismic responses of similar wall structures in large ENA urban areas located in regions of moderate seismicity, such as Boston, Montreal, and Ottawa.

3.2 Summary of the test program

The experimental program is described in (Ghorbanirenani et al., 2012) and consisted of shake table tests performed on two identical wall specimens, W1 and W2, designed with a scaling factor of 0.43 (Figure 3-1). The specimens are representative of an individual slender reinforced concrete wall of an 8-storey residential building located in Montreal, QC, Canada, and designed according to the 2005 National Building Code of Canada (NBCC) (NRCC, 2005) with a combined inelastic force reduction factor R_dR_o of 2.8. The models have a total height of 9 m, with a uniform storey height of 1.125 m. The wall length is 1.4 m up to the 6^{th} level and 1.2 m above this level. The wall thickness is 80 mm. The seismic weight at each floor is approximately 62 kN. A simulated ground motion time history developed for eastern North America seismic conditions and spectrally matched to the design spectrum was used in the test program. This motion is referred to here as 100% EQ (Figure 3-2). The first wall (W1) was initially tested under 40% EQ. The intensity of the motion was subsequently increased up to 100, 80, and 120% EQ levels. The second wall (W2) was tested directly under the 100% EQ level, simulating an initially undamaged wall exhibiting uncracked stiffness when the design seismic event occurs. The earthquake record intensity of W2 was then successively increased to 120, 150, and 200% of that of the design earthquake. Unless otherwise noted, all analyses presented in the paper were performed using the shake table acceleration feedback signals measured during the tests as input.

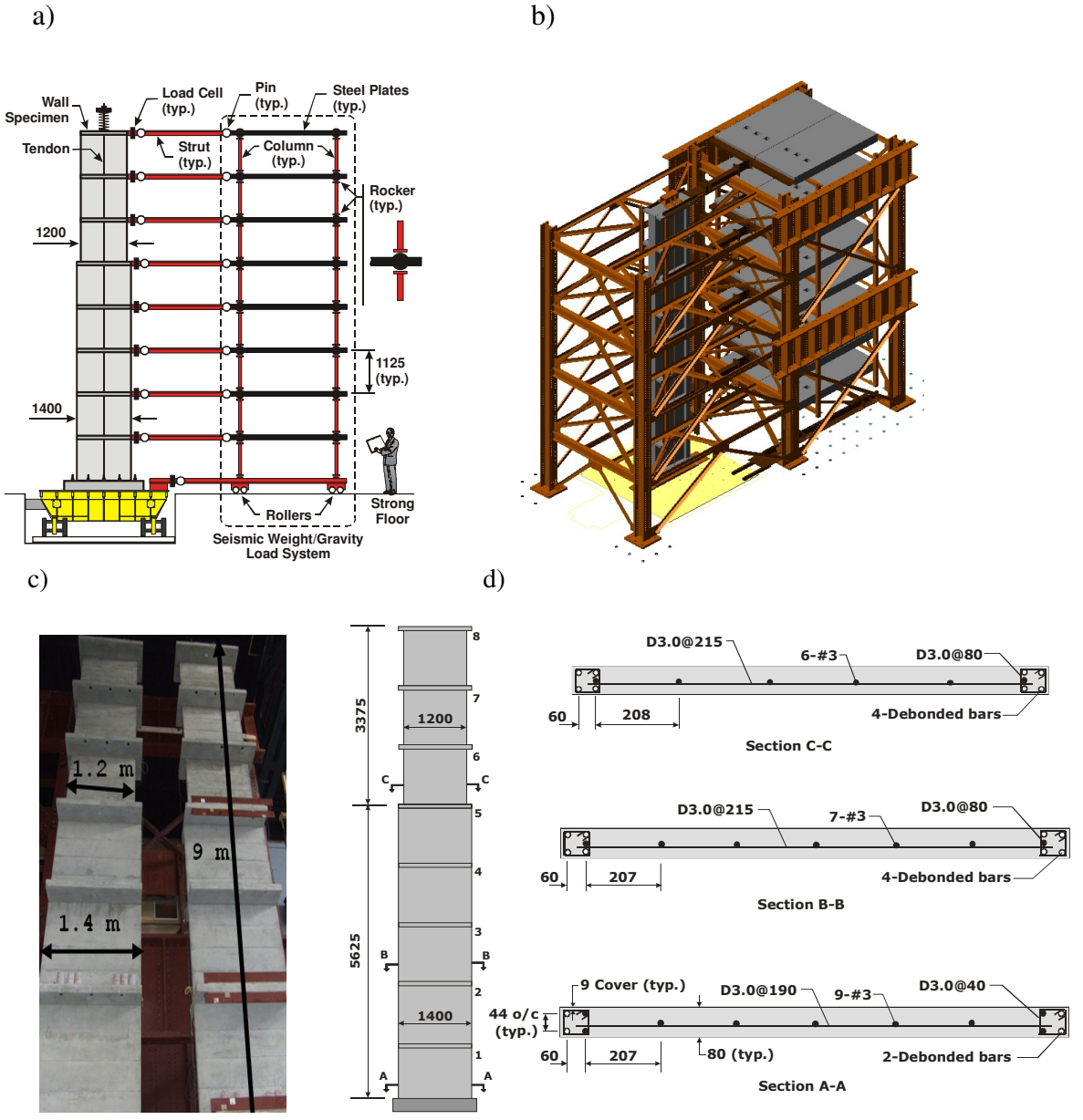

Figure 3-1 : (a) Test specimen and seismic weight/gravity load system; (b) complete test setup with a stabilising steel frame; (c) model wall; and (d) cross-section of the model wall.

The observed wall responses are also presented in Ghorbanirenani et al. (2012). In the 100% EQ and higher level tests, plastic hinges form at the wall base, as expected by design, as well as in the upper storeys due to higher mode response. Moreover, there was an exceeding of the shear demand with respect to the design shear force capacity prescribed in the current building codes. This behaviour had been also observed in several past numerical studies (Tremblay et al., 2001; Panneton et al., 2006; Panagiotou & Restrepo, 2009; Ghorbanirenani et al., 2009a; Munir & Warnitchai, 2012) and

was expected for the wall specimens. In the tests, horizontal displacements, accelerations and inertia forces were directly measured at every level. Storey shear and overturning bending moments were obtained from the measured forces. Rotational demands were measured at storeys 1 and 6.

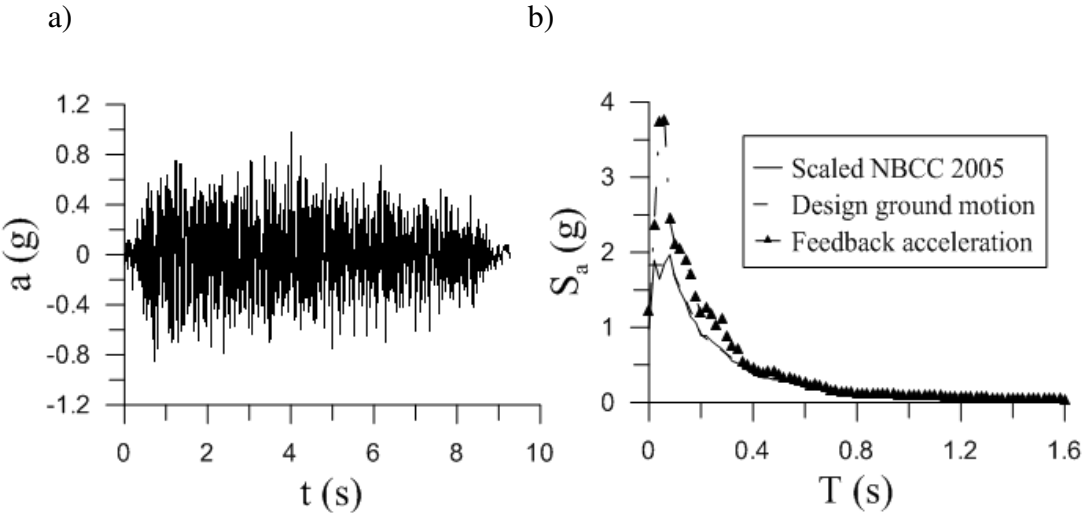

Figure 3-2: Selected ground acceleration: (a) time history; (b) response spectra.

3.3 Numerical modelling tools

3.3.1 Fibre element model

Nonlinear beam elements with fibre discretization of the cross-section are used in the OS program to model the tested walls (Figures 3-3a and c). Ten and 60 concrete fibres are used along the thickness and length, respectively (Figure 3-4a). The integration along the element is based on the Gauss-Lobatto quadrature rule. In this study, 5 integration points are selected along the height of the element. The measured material properties of the wall are used in the numerical model (Ghorbanirenani et al., 2012). The fibres and the parameters of the constitutive material models are presented in Figure 3-4. The modified Kent-Park model is used for concrete fibres (Kent & Park, 1971; Park et al., 1982) (Figure 3-4b). The slope of the tensile softening branch (E_t) of the concrete model varies linearly. Compression and tension cylinder tests were carried out separately for the walls and the boundary zones. The confinement effects on the concrete response in the regions of concentrated reinforcement were accounted for by increasing both the compressive strength and strain by 20% (Figure 3-4b). The behaviour of the confined concrete along the tension side is assumed to be the same as that of unconfined concrete (Martinelli & Filippou, 2009). The steel fibres follow the Giuffré-Menegotto-Pinto model without considering the isotropic strain hardening

(Figure 3-4c). The shear deformation is modelled by including linear shear cross-sectional stiffness coefficients. The axial force (90.7 kN) induced by post-tensioned vertical bars is considered as a static force and modelled as a point load at the top of the wall. The self-weight of the wall is considered when determining both the static axial and seismic loads. The seismic mass is lumped at each floor. P-Delta effects are not considered in the analysis as they have been shown to be insignificant in previous studies (Tremblay et al. 2001). In numerical simulations, the applied seismic excitations correspond to the measured shake table acceleration signals during the tests. Therefore, the shake table is not included in the numerical models. The integration of the equations of motions uses the Newmark method with $\beta = ¼$ and $\gamma = ½$ with a time step of 0.005 s.

A preliminary analysis showed that the predictions of the fibre element modelling are sensitive to the tension stiffening effect (TSE), damping, and the use of effective shear stiffness. Therefore, an intensive investigation of those parameters is conducted in section 3.3.4.

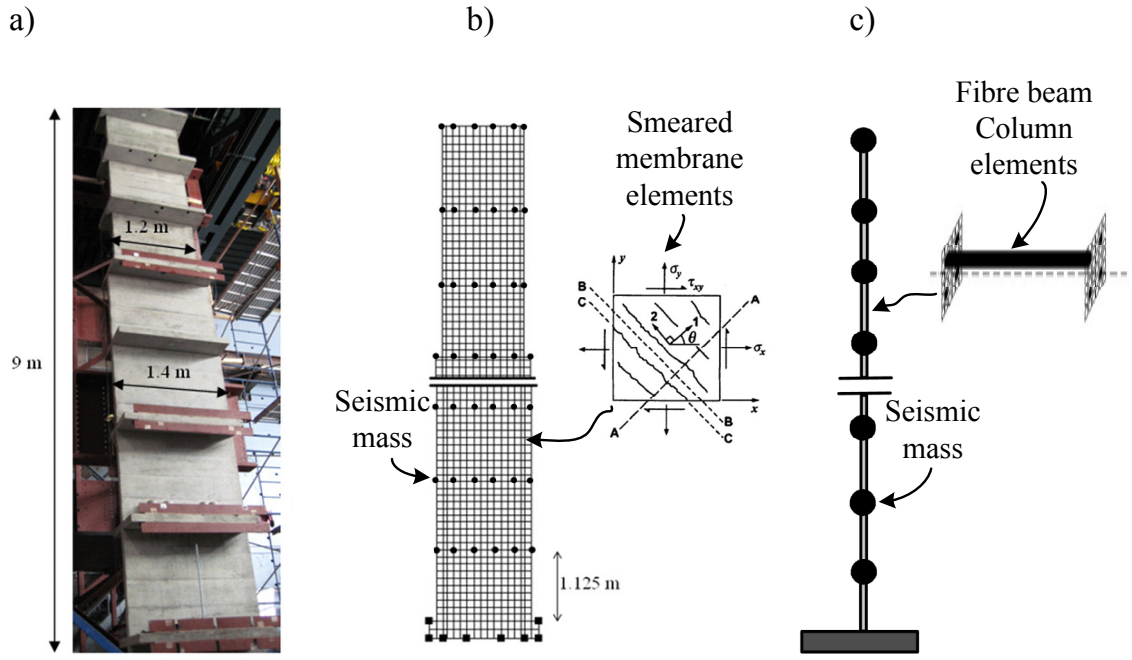

Figure 3-3: (a) Model walls tested in the laboratory; (b) FE model created in VecTor2 (VT2); and (c) fibre element model created in OpenSees (OS).

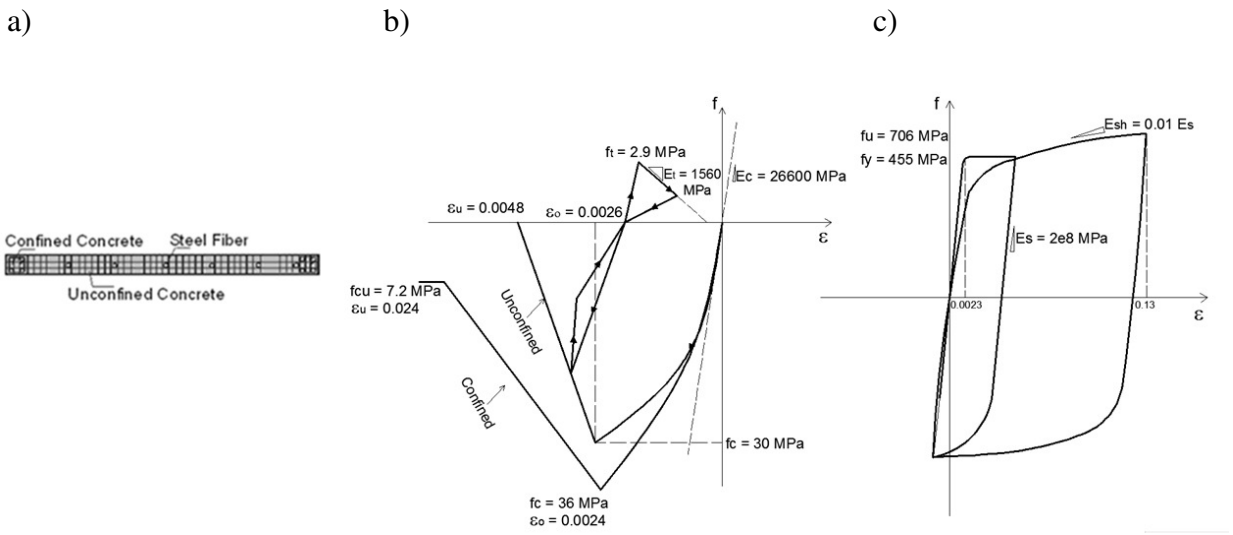

Figure 3-4: OpenSees model: (a) Cross-sectional fibre discretization; (b) concrete properties; and (c) steel properties.

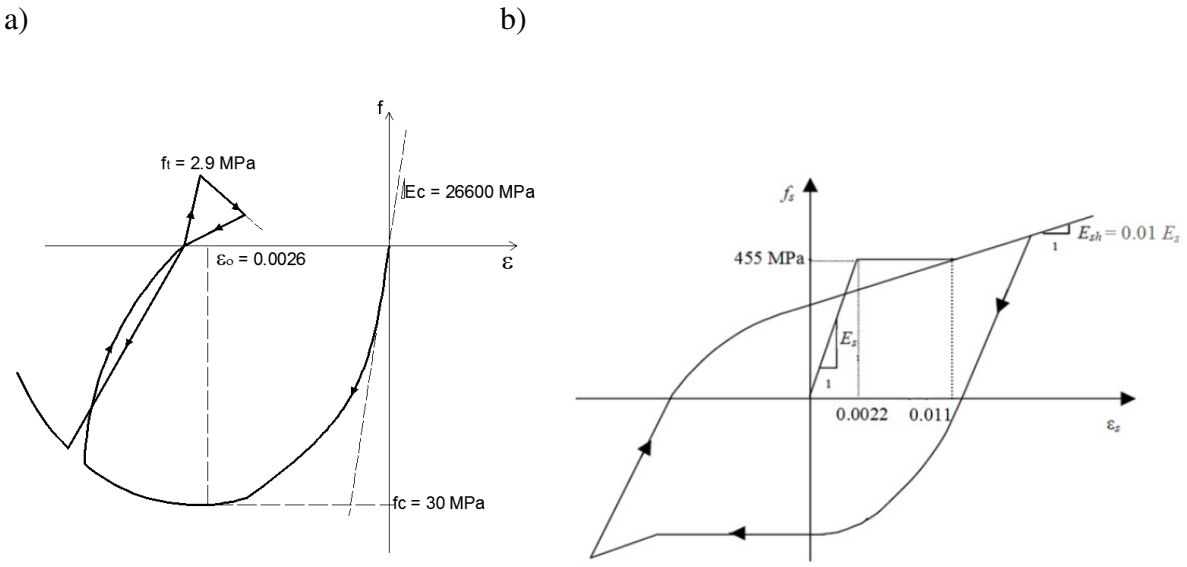

Figure 3-5: (a) Hysteretic response of concrete in the VecTor2 program; (b) hysteretic response of steel reinforcement in the VecTor2 program.

3.3.2 Comprehensive finite element model

VT2 is based on the Modified Compression Field Theory and the Disturbed Stress Field Model for the nonlinear finite element analysis of reinforced concrete membrane structures (Vecchio & Collins, 1986; Vecchio, 2000). VT2 is used to develop the finite element model of the tested walls. Two-

dimensional plane stress rectangular elements with smeared reinforcement are used, except in the flange areas, as noted in section 3.4.1. The material properties used in the FE models corresponded to the as-built material properties measured in the laboratory at the time of the tests, as described by Ghorbanirenani et al. (2012). The pre-peak compression response of the concrete is based on the Hogdnestad parabolic model (Wong & Vecchio, 2002), whereas the post-peak response followed the modified Kent-Park model (Kent & Park, 1971; Park et al., 1982) (Figure 3-5). The hysteretic response of the concrete is set according to Palermo & Vecchio (2002) (with decay). The tensile softening branch descends linearly from the cracking stress and strain to zero stress at the characteristic strain (Wong & Vecchio, 2002). The slip distortion is taken into account according to the model by Vecchio & Lai (2004). The concrete strength enhancement due to confinement is considered using the Kupfer/Richart model for concrete located in the region of concentrated reinforcement. The hysteretic model of the reinforcement is made according to the Seckin model (with the Bauschinger effect) (Seckin, 1981). Figures 3-3a and b present the test walls in the laboratory and the finite element meshes with seismic lumped masses used for the analyses of the walls in VT2. The seismic mass of each floor is distributed at the nodes of that floor. The mesh is made of 1113 rectangular elements with the horizontal size of 100 mm, a finer mesh using 50 mm horizontally does not significantly improve the results. Similar to OS model, the axial force (90.7 kN) induced by post-tensioned vertical bars is considered as a static force and modelled as a point load at the top of the wall, the self-weight of the wall is considered when determining both the static axial and seismic loads, the P-Delta effects are neglected, and the Newmark method is used for the integration of equation of motion.

Preliminary analysis showed that the predictions of the finite element model are sensitive to the tension stiffening effect, damping, and the use of smeared reinforced concrete elements. Therefore, a comprehensive investigation of those parameters is conducted in section 3.3.4.

3.4 Effects of modelling assumptions

The results shown in this section are for W2 under 100% EQ, unless stated otherwise. Similar trends are also obtained for W1 and using other EQ intensities for W2.

3.4.1 Lumped vs. smeared reinforcement

The use of smeared reinforcement instead of explicit reinforcing steel bars (which could be lumped together) is a highly convenient way to model RC structures in FE models. However, in the specimens, there are only two active vertical bars from the base to second floor and one active vertical bar from the second floor up to the top (Figure 3-1d). These bars are located in the end zones of the wall (confined areas). The debonded bars (two from the base to the second floor and four from the second floor to the top) are present only for confinement. (Figure 3-1d). These bars were wrapped in plastic thin sheets to avoid bonding with concrete and do not contribute to the flexural capacity (Ghorbanirenani et al. 2012). To study the modelling assumption for the vertical rebars of the end zones, two VT2 models are developed: one using smeared vertical end zone reinforcement and the other using lumped reinforcement. The smeared element is determined by considering only the active bonded bar areas. The lumped reinforcement is modelled by truss elements. The tension stiffening effect is neglected, and a 1.5% damping ratio is assigned for the first and third modes, as will be discussed later.

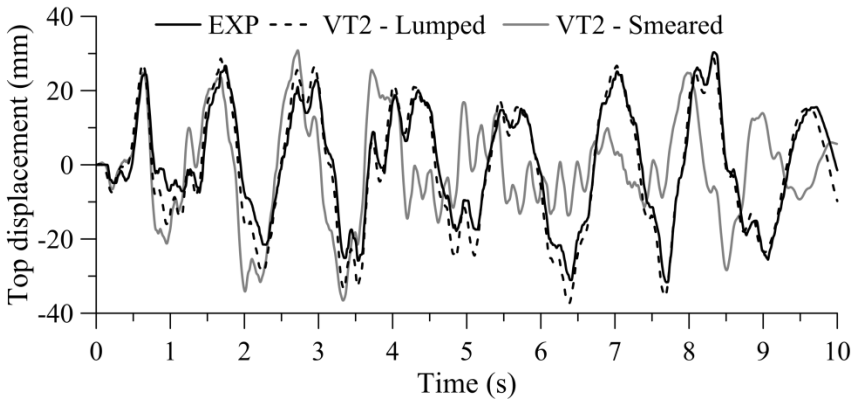

Figure 3-6: Top displacement time history of the experiment (EXP) vs. that of VT2 models using lumped and smeared steel reinforcements.

Figure 3-6 presents the lateral top displacement time history predictions from two VT2 models. From the beginning of the seismic excitation to approximately 3.8 s, there is no considerable difference between the results of the smeared and lumped reinforcements. A good agreement is obtained between the model and experimental results. However, after 3.8 s, the use of smeared vertical steel reinforcement notably underestimates the predicted top displacement of the wall. On the other hand, the use of lumped steel reinforcement more accurately predicts the experimental results.

This result suggests that the modelling assumption of the end zones using concentrated steel reinforcement significantly affects the response predictions of the tested walls. For a scaled specimen whose reinforcement is non-uniformly distributed, the approximation of using a smeared reinforcement may result in inaccurate predictions. For the tested wall in this study, the lumped reinforcement approach is used for the end zones of the wall.

3.4.2 Tension stiffening effect (TSE)

The TSE in reinforced concrete is the increase in stiffness of a cracked member due to the development of tensile stresses between cracks in the concrete, and it plays an important role in RC member responses. TSE can be modelled in VT2 using the Bentz 1999 model (Bentz, 1999). The VT2 model presented a good agreement with the experimental data from the monotonic and cyclic tests (Ghorbanirenani et al., 2009b). However, under the dynamic hysteretic inelastic response, there is deterioration in the bonding between the reinforcement and concrete. The TSE can be reduced significantly compared with the TSE associated with the monotonic response.

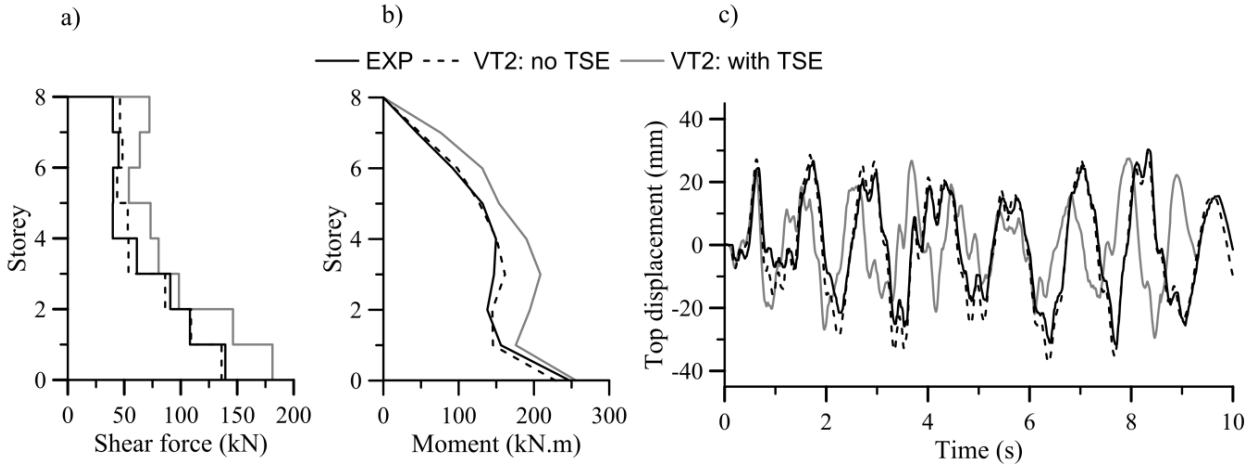

Figure 3-7: VT2 model with and without the TSE vs. experiment: (a) shear force envelop; (b) moment envelops; and (c) lateral top displacement time history

To investigate the TSE, two models are developed using VT2. The first considers the TSE (Bentz, 1999), while the second neglects it. Rayleigh viscous damping at 1.5% for the first and third modes is employed in the VT2 model. Figure 3-7 presents the wall responses based on two VT2 models compared with the experimental results. The TSE significantly overestimates the shear force and moment envelop distributions. This overestimation is most critical with respect to the base shear forces, which are 181 kN in the VT2 model including TSE and 140 kN in the experiment. A

significant moment difference also occurs in the third floor, namely 195 kN-m in the VT2 model considering TSE versus 138 kN-m in the experiment. The model without TSE produces excellent predictions of both the moment and shear force envelop distributions (Figures 3-7a and b). Considering the lateral top displacement time history, the same conclusion is obtained. There is a considerable discrepancy between the prediction of the model with the TSE and the experimental results. However, the model without the TSE follows the experimental displacement pattern (Figure 3-7c). As a corollary, the TSE is neglected in the tested wall models developed further in this study.

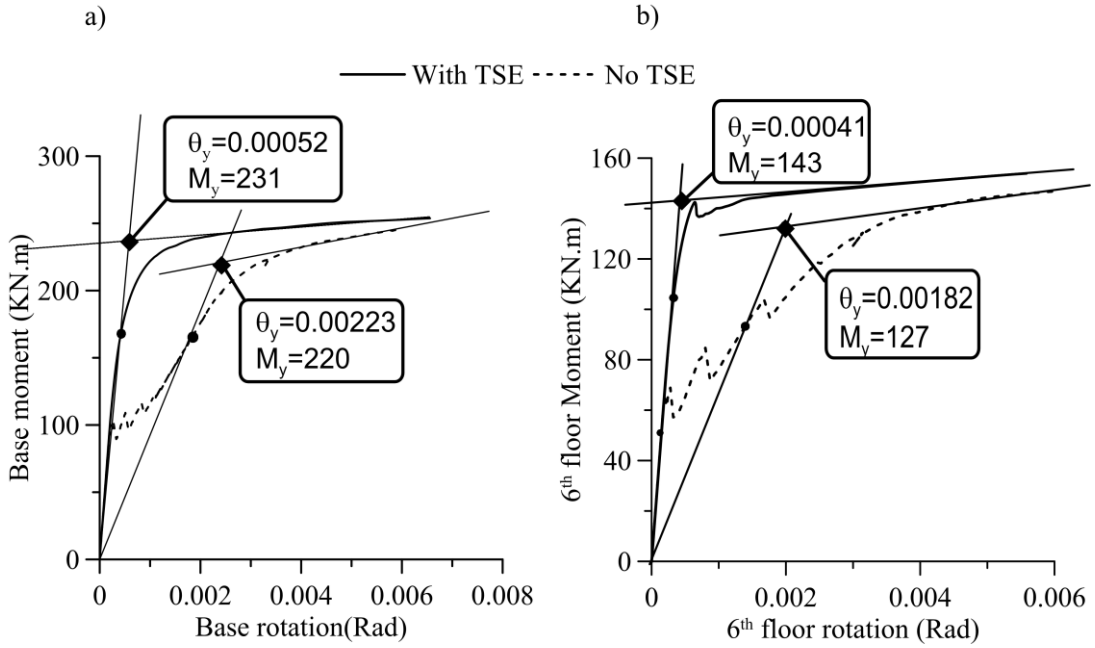

Figure 3-8: Effect of considering the TSE on pushover analysis to determine the moment and yielding rotations at (a) the 1st floor and (b) the sixth floor.

The inclusion of the TSE in the OS model (not shown here) results in similar conclusions. Consideration of the TSE results in widely different storey displacements, shear forces and moment envelop distributions compared with the experimental results. Conversely, the model without the TSE produced a good agreement with the experiment for all three examined parameters. In the OS model, 2% Rayleigh viscous damping is assigned for the first two modes and effective shear stiffness of 25% and 5% are used for the base and middle-height regions (5th, 6th , and 7th storeys) of the wall, respectively.

The effect of considering the TSE is also quantified in a pushover analysis (Figure 3-8). The results in Figure 3-8 are taken from a pushover analysis conducted with an OS model using an inverted triangular load pattern and fixity at the studied storey for cases with and without inclusion of the

TSE. The yielding rotations are evaluated herein using the method presented by Paulay & Priestly (1992) for the 1st and 6th storeys of the tested wall. A secant is drawn from the origin to the point corresponding to 0.75 M_y, and a tangent to the response at larger rotations is then extrapolated to intersect the secant line and define θ_y.

Consideration of the TSE results in rotational yielding predictions for both the 1st and 6th storeys that are nearly 4.3 times lower than those in the case that does not consider the TSE (Figure 3-8). Considering the TSE in the analysis might lead to a large rotational ductility demand in the upper part of the wall.

3.4.3 Effect of the selected viscous damping model and damping ratio

The damping matrix [C] can be defined in a variety of ways. For ease of application, it is usually defined as a linear combination of the mass (M) and stiffness (K) matrices using the Rayleigh damping formula: $[C]=a_M[M]+b_K[K]$. However, in non-linear analysis under strong ground motion, classical damping may be inappropriate and may need to be re-evaluated. This is particularly the case for tall buildings subjected to earthquakes. This is because the data and observations from past earthquakes are limited, as is the experience in using nonlinear analysis for building design.

Table 3-1: Effective modal mass (% of total mass) of tested wall W2.

Mode	1	2	3
Period (s)	0.73	0.14	0.054
Accumulated mass (%)	68.9	18.6	7.4

In OS, three approaches are available to model damping:

Approach I: $[C]_{ini}= a_M[M] + b_K[K]_{ini}$ (3.1)

Approach II: $[C]_{tan} = a_M[M] + b_K[K]_{tan}$ (3.2)

Approach III: $[C]_{com} = a_M[M] + b_K[K]_{com}$ (3.3)

where a_M and b_K are pre-defined constant coefficients that depend on the periods of the vibration modes and selected damping ratios, and $[K]_{ini}$ and $[K]_{tan}$ are the initial elastic and tangent stiffness matrices, respectively. The tangent stiffness matrix represents the state at the current analysis time step, and it is updated during each iteration step. $[K]_{com}$ is the "committed" stiffness matrix. It is a feature of OS that is defined as follows. Considering the i^{th} and $(i+1)^{th}$ steps of the analysis and noting that $[K]_{tan-i}$ is the tangent stiffness matrix for the i^{th} step of the analysis, this matrix is used to

obtain the solution for the next analysis step $(i+1)^{th}$ and is not updated during the iterations for that analysis step. This means that a modified Newton-Raphson iteration procedure is used for convergence in each analysis step. After solving the $(i+1)^{th}$ step of the analysis, the tangent stiffness matrix is updated to $[K]_{tan\text{-}i+1}$. This stiffness matrix is called the "committed" stiffness matrix and is used in the next step of the analysis.

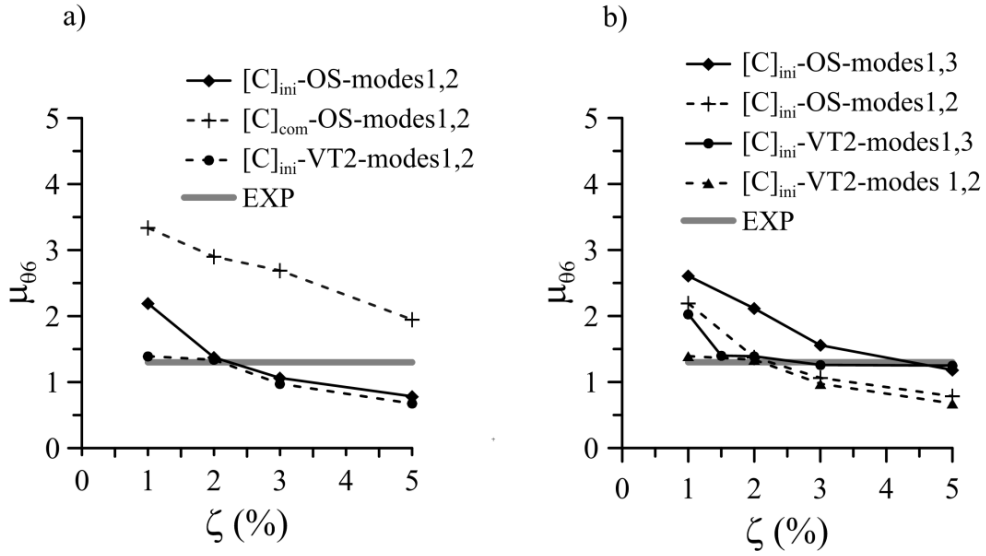

Figure 3-9: Rotational ductility at the sixth floor vs. damping values of damping models assigned for (a) modes 1 and 2 and (b) modes 1 and 3.

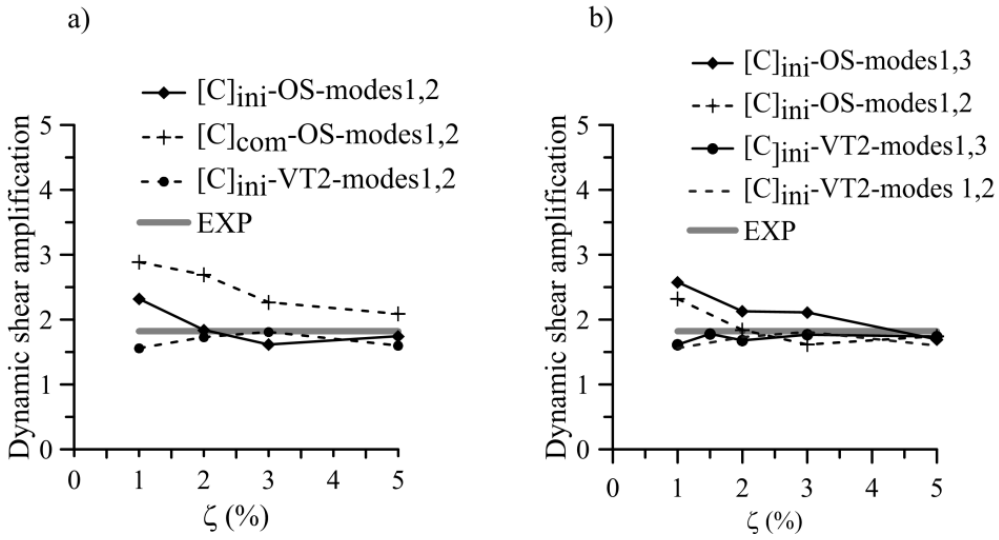

Figure 3-10: Dynamic base shear force vs. damping values of damping models assigned for (a) modes 1 and 2 and (b) modes 1 and 3.

While using the OS program, the authors observed that there is no significant difference between the results determined using $[K]_{tan}$ and $[K]_{com}$ for the tested wall models. However, $[K]_{tan}$ requires a significantly greater computational effort than $[K]_{com}$ to obtain convergence. As a consequence, $[K]_{com}$ is selected for parametric numerical analyses.

In VT2, only the initial stiffness based Rayleigh viscous damping model is implemented. Thus, the investigation is conducted with only that model.

The damping ratio for the n^{th} mode of a multi-degree-of-freedom (MDOF) system is as follows:

$$\zeta_n = \frac{a_M}{2}\frac{1}{\omega_n} + \frac{b_K}{2}\omega_n \tag{3.4}$$

Herein, ω_i and ω_j are the frequencies in mode i and j, respectively.

The coefficients a_M and b_K can be determined from the specified damping ratios ζ. If both modes i and j are assumed to have the same damping ratio, then

$$a_M = \zeta\frac{2\omega_i\omega_j}{\omega_i + \omega_j} \;\; ; \quad b_K = \zeta\frac{2}{\omega_i + \omega_j} \tag{3.5}$$

Figures 3-9 and 3-10 present the responses of the tested wall model compared with those obtained from different types of Rayleigh damping models. Figure 3-9 shows the rotational ductility measured at storey 6 due to the formation of the plastic hinge at this location (Ghorbanirenani et al., 2012). In Figure 3-10, the base shear amplification factor corresponds to the ratio between the base shears from nonlinear time history OS or VT2 analyses and from response spectrum analysis using the shake table feedback accelerations. The horizontal lines (EXP) in the figures represent the values measured in the tests. In the analyses, damping ratios ranging from 1 to 5% were considered for both OS and VT2. Based on findings in section 3.4.2, models with no TSE were used.

According to section 3.4.2, the results from the tested wall are in good agreement with the OS model using 2% initial Rayleigh viscous damping for the first two modes($[C]_{ini}$-OS-modes 1,2). The predictions from that OS model are also very close to experimental lines (EXP) in both rotational ductility at 6^{th} storey and dynamic amplification at base (Figures 3-9 and 3-10). In the VT2 model, using 1.5% damping for modes 1 and 3, the mass- and initial stiffness-based proportional Rayleigh damping ($[C]_{ini}$-VT2-modes 1,3) offers an accurate agreement with the experimental results (see

section 3.4.2). Once again, that VT2 model can produce close values to experiment in the matter of rotational ductility at 6th storey and base shear force (Figures 3-9b and 3-10b).

The utilisation of $[C]_{com}$ gives a larger base shear force prediction than using $[C]_{ini}$ (Figure 3-10a). This trend is consistent with the observed rotational ductility at the 6th storey for the tested wall (Figure 3-9a). However, $[C]_{ini}$ leads to a better prediction than $[C]_{com}$ between the numerical and experimental results. The utilisation of $[C]_{com}$ is conservative in this application as it results in larger structural response quantities (Figures 3-9a and 3-10a).

According to Figures 3-9a and b, a second plastic hinge has formed in the upper part of the wall. In Figure 3-9b, where damping is assigned for modes 1 and 3, the formation of an upper hinge is possible even if the damping ratio is 5% for both the VT2 and OS models, the damping value implicitly assumed in building codes (NRCC, 2005). Figures 3-9a and 3-10a show that there is no significant difference between the OS and VT2 predictions of the rotational ductility and base shear amplification factor when the damping value used is larger than 2%.

Table 3-2: Viscous damping ratios assumed in OpenSees for W1 and W2.

Wall	W1			W2			
EQ	40%	100%	120%	100%	120%	150%	200%
ξ(%)	5.0	1.5	1.5	2.0	1.5	1.0	1.0

In Rayleigh damping, using eq. (5), two modes must be selected with the specified damping ratios to compute a_M and b_K. For the MDOF structures, different pairs of modes can be selected, which further complicates the modelling. The first specified damping ratio should be assigned to the fundamental mode because it dominates the seismic structural responses such as roof displacements and base moments. The question lies in the selection of the second mode to be used to specify the damping. If a high mode is employed, the lower modes will be under-damped. Conversely, if a low mode is employed, the higher modes will be over-damped. In their analysis of ductile cantilever wall systems, Ruttenberg et al. (2006) employed the first and fifth modes with 5% Rayleigh damping. Grange et al. (2009) used Rayleigh damping with 2% damping specified in the first and fourth modes to analyse a full-scale 7-storey RC wall. Kazaz et al. (2006) adopted Rayleigh damping with 2% damping specified in the first two modes to study a 1/3-scale 5-storey RC structural wall.

In Figures 3-9b and 3-10b, there is no significant variation in the rotational ductility and base shear amplification with respect to two selected mode pairs: modes 1 and 2 or modes 1 and 3. Frequently,

the first mode and the mode for which the accumulated modal mass participation reaches more than 90% of the total mass are selected. For the tested wall in Table 3-1, three modes are needed to reach a minimum of 90% of the total mass and one could select modes 1 and 3 to compute a_M and b_K. This is consistent with the mode selection in the VT2 model, which provides the best agreement with the experimental results when 1.5% damping ratio is assigned to modes 1 and 3. However, Figures 3-9a and 3-10a illustrate that Rayleigh damping using modes 1 and 2 in the OS model provides a better agreement with the experimental data. This result is due to the under-damped contribution of mode 2 when modes 1 and 3 are adopted for Rayleigh damping in the OS model. Note that a smaller damping percentage is used in the VT2 model, as this model more closely reproduces the energy dissipation experienced by the structure and, hence, presents a relatively greater dissipated hysteretic energy than that produced by the OS model (Ghorbanirenani et al., 2009a).

The effect of EQ intensities on selected damping ratios is also studied. Different damping values are selected for the OS models to obtain the best match for each specific intensity. The results are shown in Table 3-2. The matrix $(C)_{ini}$ and damping ratios assigned to the first 2 modes are used.

Following Table 3-2, the damping ratios must be adjusted based on the EQ intensities. The value of 5% damping prescribed in most building codes (NRCC, 2005; NZS, 2006; CEN, 2004) is selected for W1 under 40% EQ intensity. However, W1 is still in the elastic range under this low EQ intensity. For higher EQ intensity levels (from 100 to 200%), the selected damping values are between 1.0 and 2%. These results are consistent with suggestions made by Wilson (2000) and Martinelli & Filippou (2009). Moreover, as indicated in Table 3-2, low damping values are employed for the wall under high EQ intensity levels because, under such high levels, the wall models experienced significant inelastic behaviour, and the EQ energy was dissipated through hysteretic responses.

3.4.4 Effect of effective shear stiffness

VT2 utilises an FE code that is able to account for inelastic shear deformation and shear-flexural-axial force interactions. On the other hand, the fibre element model (OS) considers shear deformation simply by including linear shear cross-sectional stiffness coefficients. It asks the user to select an appropriate effective shear stiffness value. Based on a study analysing reinforced concrete membrane elements with shear tests under reversed cyclic loading, Rad (2009) proposed using 10-20% of the gross shear stiffness. However, determining the most appropriate shear stiffness value in an OS model of a shake table-tested wall requires additional investigation.

A set of OS shear wall models with different shear stiffness values varying from 5 to 100% over the height are developed. The shear stiffness is defined here as the product of the shear modulus G and the wall cross-sectional area A_w. Some numerical analyses (Panagiotou & Restrepo, 2009; Ghorbanirenani et al., 2009a; Munir & Warnitchai, 2012) and experimental data (Ghorbanirenani et al., 2012) have shown that there is a second plastic hinge formation located at the middle height of the wall in addition to the hinge formation at the base. These hinges result in significant shear stiffness degradation at the middle height (the 5th, 6th, and 7th storeys) and base of the wall. Therefore, the variations in shear stiffness are only studied at those locations.

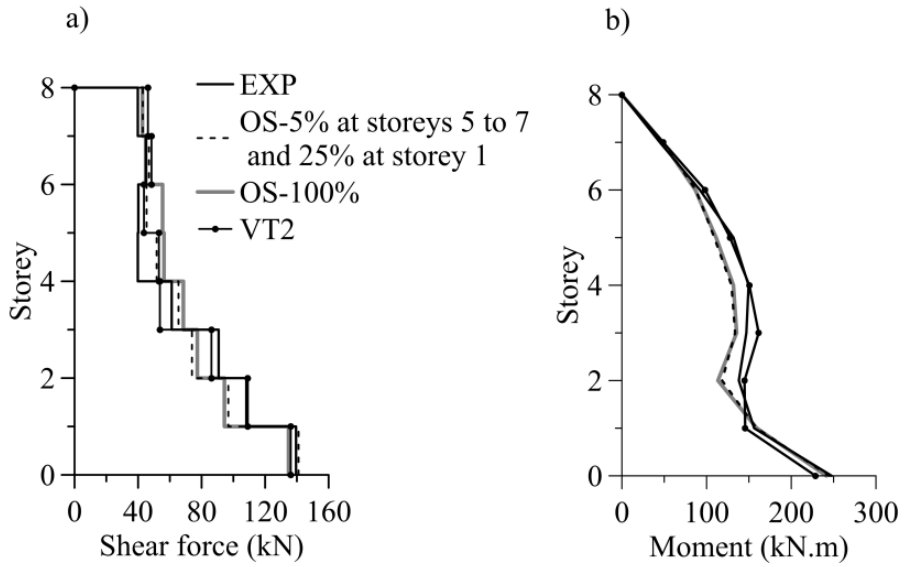

Figure 3-11: Dynamic structural responses due to different effective shear stiffnesses: (a) shear envelop and (b) moment envelop.

Table 3-3: Base and 6th storey shear forces, as well as Standard Deviations (SDs) of the shear force envelops from OS models with different shear effective stiffnesses vs. the experimental results.

	OS 100%	OS 50%	OS 30%	OS 10%	OS 5%	**OS 25% in storey 1 and 5% in storeys 5 to 7**	VT2	EXP
V_6 (kN)	55	54	50	50	45	**45**	43	40
V_b (kN)	137	141	140	150	146	**141**	136	140
SD (%)	22.2	20.5	15.4	14.9	15.1	**13.1**	13.6	-

Figure 3-11 presents the dynamic responses obtained from the OS wall models. Generally, the moment envelop distributions are not sensitive to shear stiffness assumptions (Figure 3-11b). However, all of the models slightly underestimate the moment demands with respect to the experimental results. Regarding the shear envelop distribution, the shear stiffness also slightly

influences the predicted values (Figure 3-11a). Table 3-3 presents the peak shear forces at the 6th storey, V_6, and at the base, V_b. The standard deviation (SD) of the ratios between the OS and experimental shear results at all 8 floors is also given in the table. The model using the low shear stiffness (10% of gross stiffness) provides an acceptable shear force envelop distribution with the smallest error over the wall height (SD = 14.9%). However, that model significantly overestimates the base shear force at 150 kN compared with 140 kN in the experiment. On the contrary, the OS model with 100% shear stiffness produces a good base shear prediction (137 kN vs. 140 kN in the experiment) but a poor shear force envelop distribution prediction (SD = 22.2%). These results suggest that the model with a high shear stiffness at the base and a low stiffness at the middle height could produce a better prediction of the tested wall response. After a few trials, it was found that an OS model with 25% of gross shear stiffness at the first storey and 5% of gross shear stiffness at the 5th, 6th, and 7th storeys could lead to very good shear force envelop distribution and reasonable base and 6th storey shear force predictions, as shown in Figure 3-11 and Table 3-3. Therefore, this model was selected as the OS model in this study.

The results obtained from the VT2 model, which takes into consideration nonlinear shear behaviour, are given in Figure 3-11 and Table 3-3. An excellent agreement between VT2 and the experiment is observed. The use of the VT2 results could provide a good shear force envelop distribution prediction under seismic event when no experimental data are available.

3.5 Nonlinear finite and fibre element seismic response

VT2 and OS models have been investigated under different modelling assumptions. The most appropriate assumptions that provide the best agreement with the experimental results are summarised with comments in Tables 3-4 and 3-5 for the VT2 and OS programs, respectively. In section 3.4, results were presented for W2 under 100% EQ intensity. Complementary studies were also conducted for W1 and different EQ intensities and are presented in this section. Similar conclusions to W2 under 100% EQ intensity regarding the TSE, damping, lumped vs. smeared reinforcement and effective shear stiffness are also obtained.

Table 3-4: Effects of modelling assumptions on VT2 model results (W2 under 100% EQ).

	Model 1	Model 2	Model 3	Model 4	**Model 5**
TSE	No	No	No	Yes	**No**
Lumped steel	Yes	Yes	No	Yes	**Yes**
Rayleigh damping	$[C]_{ini}$; modes 1, 3; 1 to 5%	$[C]_{ini}$; modes 1, 2; 1 to 5%	$[C]_{ini}$; modes 1, 3; 1.5%	$[C]_{ini}$; modes 1, 3; 1.5%	**$[C]_{ini}$; modes 1, 3; 1.5%**
Results/ comments	Good matches in shear force and moment envelops.	Poor match in the time history of the top displacement; good matches in the shear force and moment envelops.	Poor match in the time history displacement; good matches in the shear force and moment envelop distributions.	Poor matches in the time history of the top displacement, shear force and moment envelop distributions.	**The best matches in the time history displacement, shear force and moment envelop distributions.**

Table 3-5: Effects of modelling assumptions on OS model results (W2 under 100% EQ).

	Model 1	Model 2	Model 3	Model 4	**Model 5**
TSE	No	No	No	Yes	**No**
Rayleigh damping	$[C]_{com}$; modes 1, 2 and modes 1, 3; 1 to 5%	$[C]_{ini}$; modes 1, 3; 1 to 5%	$[C]_{ini}$; modes 1, 2; 2%	$[C]_{ini}$; modes 1, 2; 2%	**$[C]_{ini}$; modes 1, 2; 2%**
Effective shear stiffness	5% at the 5th, 6th and 7th storeys; 25% at the base	5% at the 5th, 6th and 7th storeys; 25% at the base	5, 10, 20, 50 and 100%	5% at the 5th, 6th and 7th storeys; 25% at the base	**5% at the 5th, 6th and 7th storeys; 25% at the base**
Results/ comments	Overestimates the shear force and moment envelop distributions.	Overestimates the shear force and moment envelop distributions.	Good matches in the time history displacement, shear force and moment envelop distributions.	Poor match in the time history of the top displacement; overestimates the shear force and moment envelop distributions.	**Good match in the time history displacement; the best matches in the shear force and moment envelop distributions.**

3.5.1 Dynamic characteristics

Table 3-6 compares the dynamic characteristics and peak responses of the walls obtained from the experiment and the numerical models 5 (Tables 3-4 and 3-5). The first natural periods are generally close to the values obtained from the free vibration response of the wall specimens in free vibration impact tests. The lower values obtained from the OS model are due to the use of effective shear stiffness. As nonlinearity increased in the VT2 and OS models, the natural periods of the walls elongated approximately in the same proportion as the experimental values. This indicates that the cracking and level of damage in the wall are well captured by the constitutive RC models.

Although a 1.5% constant viscous damping for the first and third modes was used in the VT2 analyses, the damping calculated using the VT2 model from the free vibration response at the end of each test is significantly larger. The additional damping in the VT2 model could be due to the accumulated damage in the steel and concrete materials, the energy dissipation caused by the opening and closing of the cracks, and the tangential crack motions modelled in VT2.

3.5.2 Damage crack patterns

Under 100% EQ, the crack patterns observed in the tests and computed from the VT2 analysis are in fair agreement but damage to the specimen under this ground motion level was limited. The program's ability to predict cracking and damage is better evaluated under 200% EQ test (the maximum intensity), as illustrated in Figure 3-12 for W2. The distributions of the cracks at the base and the 6^{th} level span the storey height in both the test observations and the FE model. In Figure 3-12c, the cracks at the base are a combination of inclined shear cracks and horizontal flexure cracks, which is well predicted by the FE model (Figure 3-12d). In the tests, shear cracks were not observed at the 6^{th} level (Figure 3-12b), and the crack pattern obtained from the FE analysis (VT2) agrees well with the test results (Figure 3-12c).

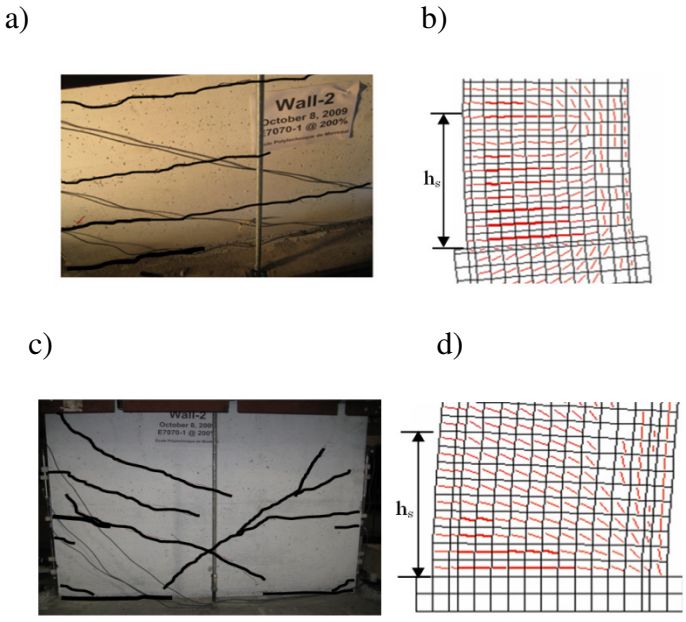

Figure 3-12: Cumulative crack patterns in W2 under 200% EQ: (a) 6th level based on the test; (b) 6th level based on the VT2 model; (c) at the base based on the test; and (d) at the base based on the VT2 model.

3.5.3 Displacement response

Table 3-6 presents the maximum top displacements ($\Delta_{max\ (top)}$) for W2 and W1 under different EQ intensities. All of the predictions from OS and VT2 are close to the experimental values. This is especially the case for W2 under 100% EQ, which was initially undamaged, and W1 under 40% EQ, which remained in the elastic regime. Figure 3-13 compares the top displacement histories of W1 and W2 under 100% EQ with those obtained from the OS and VT2 models. VT2 predictions in Figures 3-13c and d follow the same displacement patterns as those obtained in the experiment. The results of the OS model shown in Figures 3-13 a and b also agree well with the experimental values. Figures 3-14a and b compare the distributions of the drifts along the heights of W1 and W2 under 100% EQ. Both VT2 and OS produce values that are very close to those obtained from the experiment.

Table 3-6: Experimental and numerical dynamic characteristics and peak responses for W1 and W2.

		W1			W2			
Parameter	Method	40%	100%	120%	100%	120%	150%	200%
T_1(s)[1]	EXP	0.72	0.90	0.96	0.96	1.0	1.03	1.31
	OS	0.58	0.87	0.88	0.81	0.87	1.15	1.24
	VT2	0.62	0.90	0.92	0.94	0.97	0.98	1.03
ξ(%)[1]								
	OS	5.1	3.7	4.5	4.5	3.5	2.1	1.6
	VT2	3.8	4.3	4.6	4.4	4.6	4.8	5.6
$V_{b\ max}$ (kN)	EXP	57	118	139	140	140	172	183
	OS	71	128	149	141	149	165	187
	VT2	88	130	132	136	135	175	182
$V_{6\ max}$ (kN)	EXP	21	40	46	40	45	46	66
	OS	34	56	47	45	59	85	77
	VT2	35	41	66	43	56	60	57
M_{max} (kN.m)	EXP	111	241	261	250	225	243	253
	OS	124	240	251	243	249	258	260
	VT2	158	224	217	221	213	221	227
$\Delta_{max\ (top)}$ (mm)	EXP	10	36	41	31	38	52	71
	OS	9	35	38	34	39	47	63
	VT2	10	40	48	37	46	51	53
$\mu_{\theta 6}$	EXP	0.2	1.6	2.1	1.3	1.5	3.2	4.8
	OS	0.4	1.5	1.5	1.3	2.0	2.7	4.2
	VT2	0.8	1.9	2.6	1.4	2.8	3.2	3.9
$\mu_{\theta b}$	EXP	0.2	1.1	1.2	1.2	1.1	1.6	1.7
	OS	0.3	1.3	1.3	1.3	1.1	1.8	1.8
	VT2	0.3	1.6	1.1	1.3	1.1	1.2	1.2

(1) Free vibration in the damaged condition

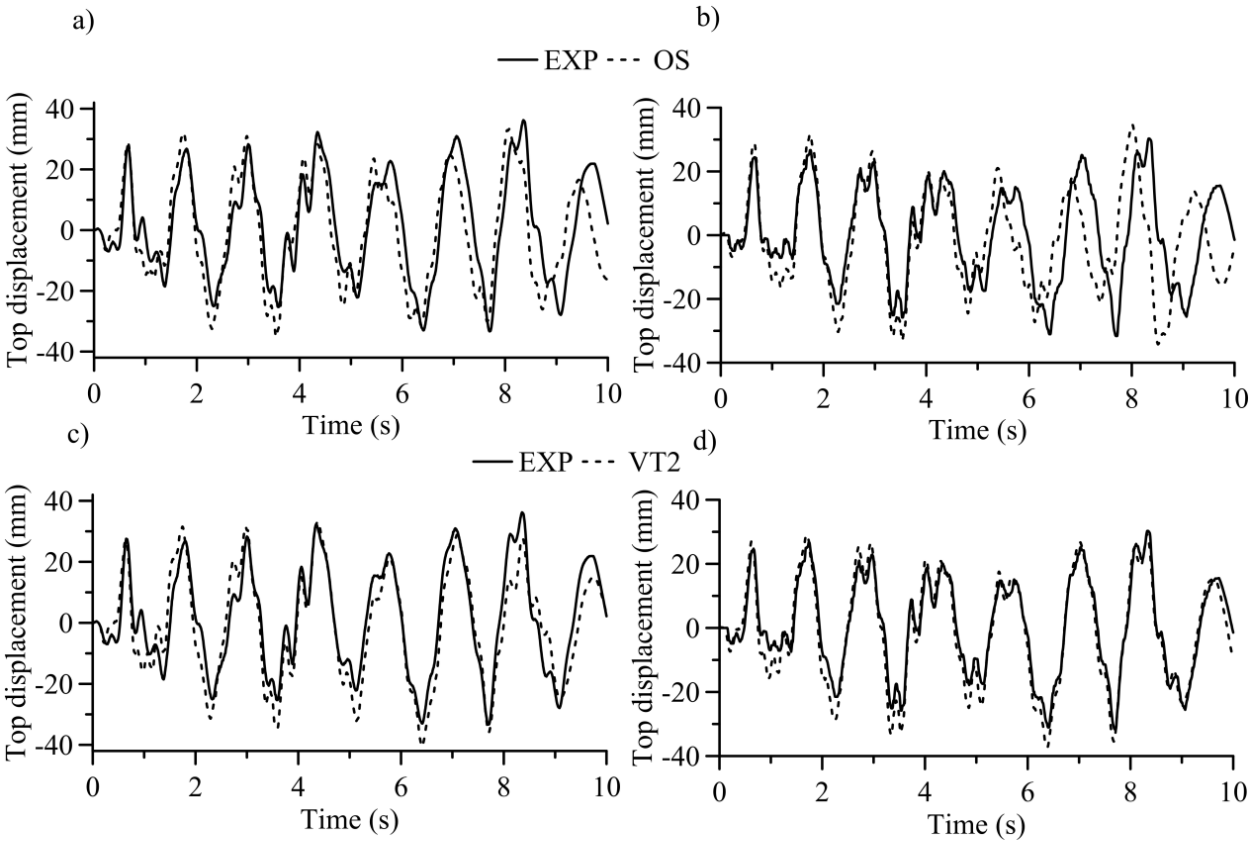

Figure 3-13: Top displacement history for W1 and W2 under 100% EQ: (a) OS vs. test for W1; (b) OS vs. test for W2; (c) VT2 vs. test for W1; and (d) VT2 vs. test for W2.

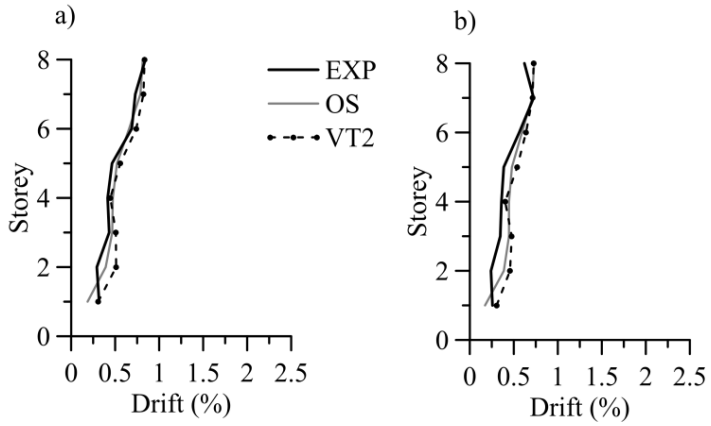

Figure 3-14: Vertical distribution of drifts under 100% EQ for (a) W1 and (b) W2.

3.5.4 Flexural and shear responses

In Table 3-6, the shear forces obtained from both OS and VT2 models are in good agreement with the experimental results, especially at the base. The moments at the bases of W1 and W2 obtained

from both models are very similar to the experimental results. Figures 3-15 and 3-16 compare the shear and moment envelops along the heights of W1 and W2 between the experiments and the numerical models under 100% EQ. The moment distributions obtained from both OS and VT2 in Figures 3-15b and d and Figures 3-16b and d are nearly identical to the test values. VT2 slightly underestimates the value of the base moment, but it predicts an excellent moment distribution pattern in the upper part of the wall. In Figure 3-16a, the base shear force obtained from VT2 for W1 is approximately 10% greater than that obtained in the test. This could be due to the previously damaged condition of W1. For W2, which was initially undamaged, VT2 provides an excellent distribution of the shear forces (Figure 3-16c). The OS predictions of the shear force envelop distribution along the wall height in Figures 3-15a and c for W1 and W2 are similar to the experimental values. Due to higher mode effects, the base shears in the walls were amplified in the tests and were much higher than the values predicted by the response spectrum analysis using the feedback (fbk) input-response spectrum (Figures 3-15a and c and Figures 3-16a and c). These effects are captured very well by both the OS and VT2 numerical models.

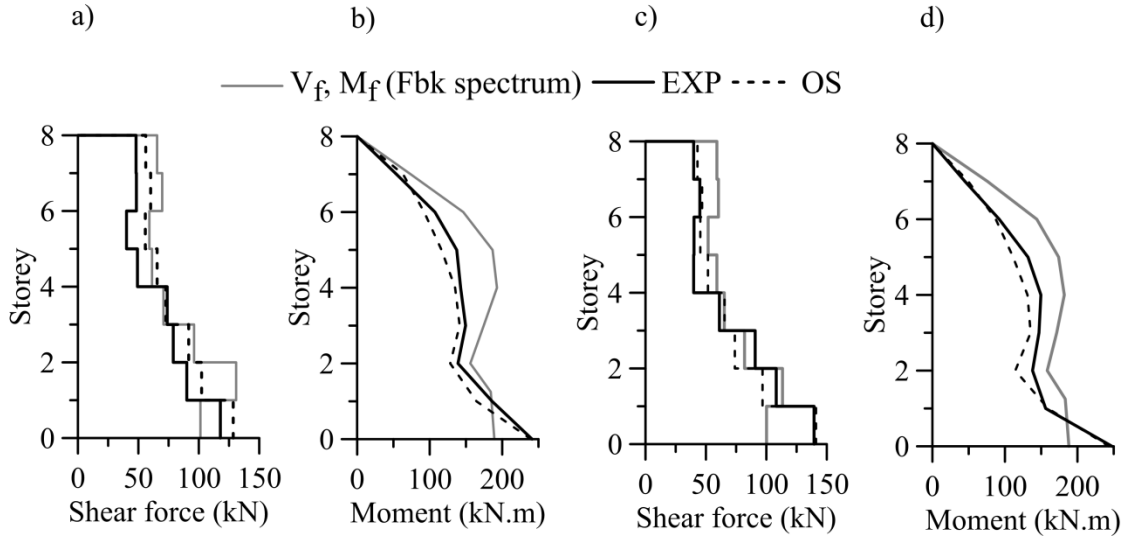

Figure 3-15: Vertical force distribution under 100% EQ in the OS models: (a) shear distribution for W1; (b) moment distribution for W1; (c) shear distribution for W2; and (d) moment distribution for W2.

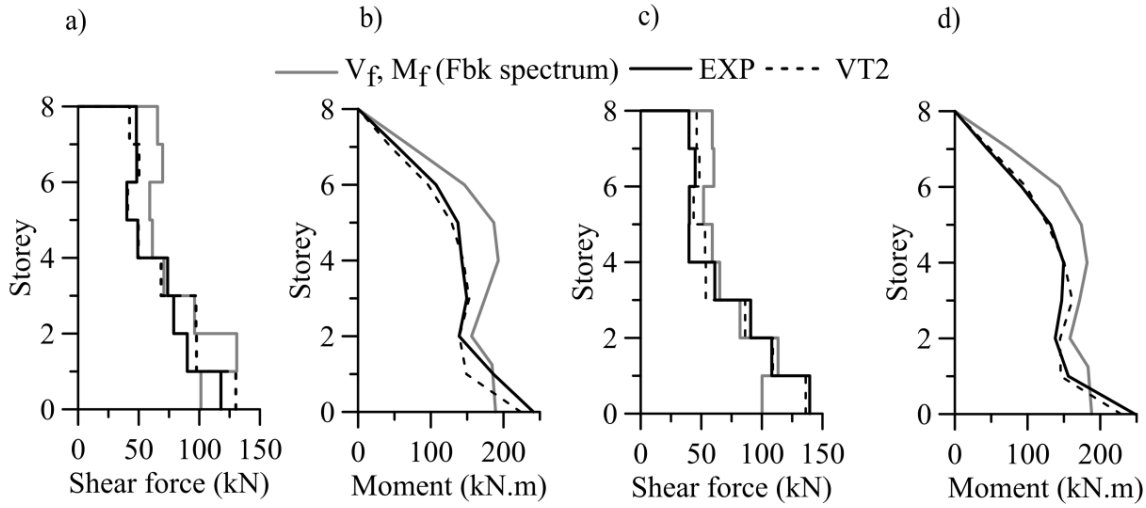

Figure 3-16: Vertical force distribution under 100% EQ in the VT2 models: (a) shear distribution for W1; (b) moment distribution for W1; (c) shear distribution for W2; and (d) moment distribution for W2.

Figures 3-17a and b present the vertical distributions of the horizontal accelerations along the heights of W1 and W2 at the time of the maximum base shear and under 100% EQ. Lateral inertial forces, or seismic loads, acting on the walls directly correspond to the accelerations shown. The lateral force patterns obtained from the tests show significant contributions from the second and third vibration modes. Both OS and VT2 predict the same patterns, especially for W1.

3.5.5 Hysteretic responses

Figures 3-18 and 19 present comparisons of the moment-rotation responses obtained from the models and experiments for W1 and W2 under 100% EQ. In both walls, inelastic rotations could be observed at the base and at the 6th level. Both the VT2 and OS models yield flexural stiffnesses that are close to the measured values. In Figure 3-18a, the OS results match well those of the test with respect to hysteric responses at the 6th level. The computed force demand and rotational ductility are very close to the test results. VT2 also provided a good match to the experimental hysteretic moment-rotation curves, especially for W2 (Figures 3-19b and d). In Figures 3-18b and c, the moments and rotations obtained from the VT2 and OS analyses at the base and 6th level, respectively, of W1 are slightly larger than the corresponding experimental values.

The VT2 model has the ability to predict cracking due to shear and bending, the interaction of these cracks in concrete members, and the shear deformation responses, including the reduction in shear stiffness due to bending and shear cracks. This stiffness degradation can be reproduced well with the

VT2 model, and it is evident considering prediction of the relations between moments and rotations for W2 at the 6th storey (Figure 3-19b).

3.5.6 Time history of Base Shear vs. Plastic Rotation Demand

According to Ghorbanirenani et al. (2012), the maximum base shear reached in W2 under 100% EQ was approximately 1.15 times the nominal wall shear strength obtained using the actual material properties. No shear failure was observed in that test. The wall could even resist the 30% greater shear demand imposed when applying 200% EQ. In CSA-A23.3 (CSA, 2004), the contribution of the cracked concrete to the shear resistance varies with the expected hinge inelastic rotation. The concrete shear resistance is the maximum up to an inelastic rotation of 0.005 rad and decreases linearly to zero as the inelastic rotation reaches and exceeds 0.015 rad; the shear resistance of concrete is neglected for plastic rotations greater than 0.015 rad.

The shear and rotation measured at the base of W2 are plotted in Figure 3-20 for the 100% EQ test. The predictions derived from VT2 are also provided in the graphs. According to both VT2 and the experimental results, the maximum base shear occurred before the maximum plastic rotation. The time lag between the maximum rotation and maximum base shear is occurring because the former is dominated by the first mode response, whereas the second is governed by the second and higher mode responses. This behaviour may be of significance when assessing the performance of shear wall structures, as the concrete's contribution to the shear resistance depends on the sequence of these peak rotations and the shear demand values. An additional study of OS model, not shown here, also demonstrates that this model is capable of accurately predicting this behaviour.

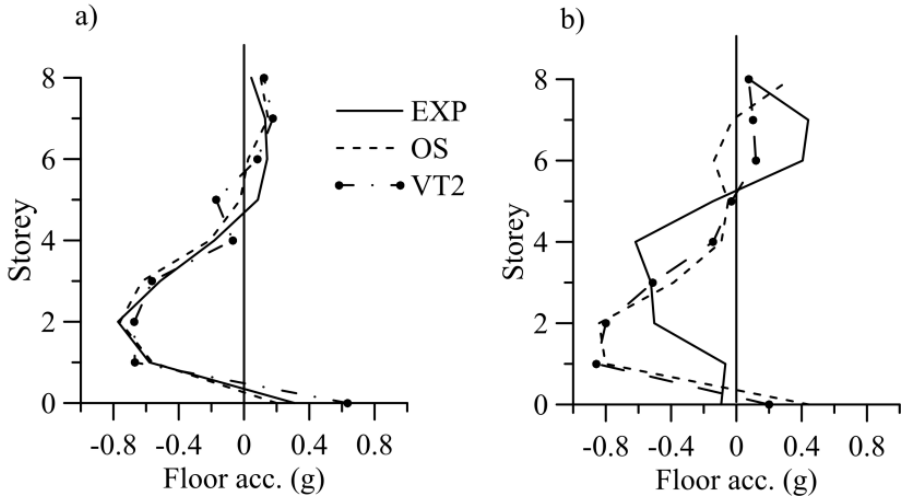

Figure 3-17: Vertical distributions of horizontal accelerations under 100% EQ for (a) W1 and (b) W2.

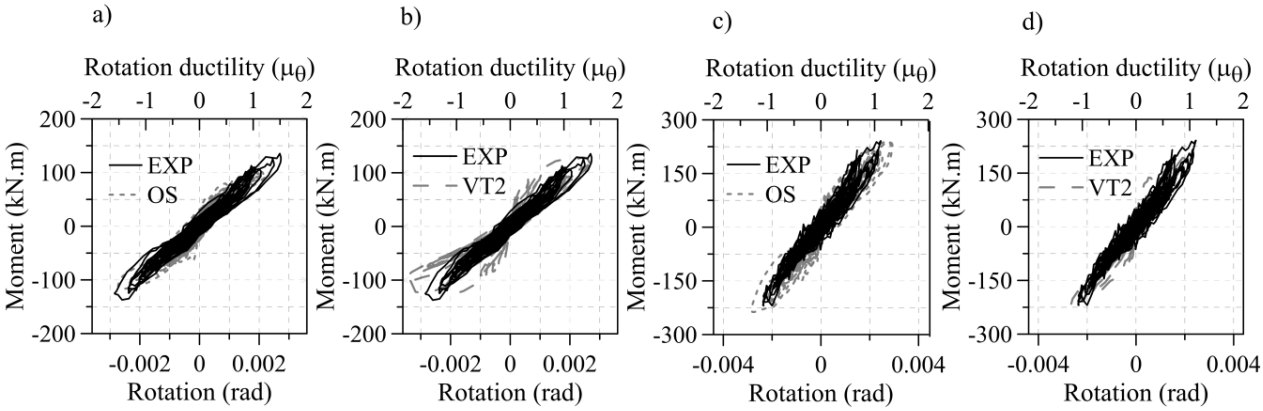

Figure 3-18 : Moment-rotation response of W1 under 100% EQ: (a) OS vs. the test at the 6th level; (b) VT2 vs. the test at the 6th level; (c) OS vs. the test at the base; and (d) VT2 vs. the test at the base.

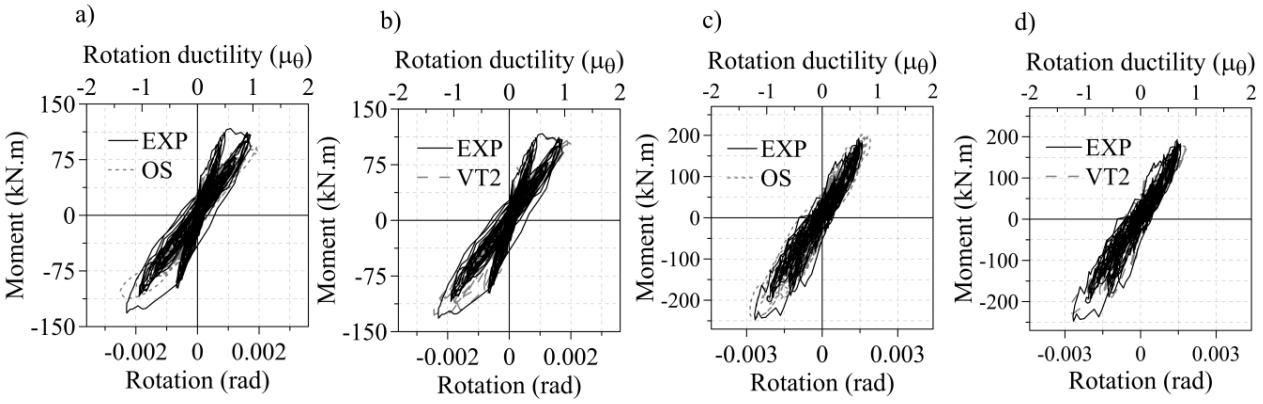

Figure 3-19 : Moment-rotation response of W2 under 100% EQ: (a) OS vs. the test at the 6th level; (b) VT2 vs. the test at the 6th level; (c) OS vs. the test at the base; and (d) VT2 vs. the test at the base.

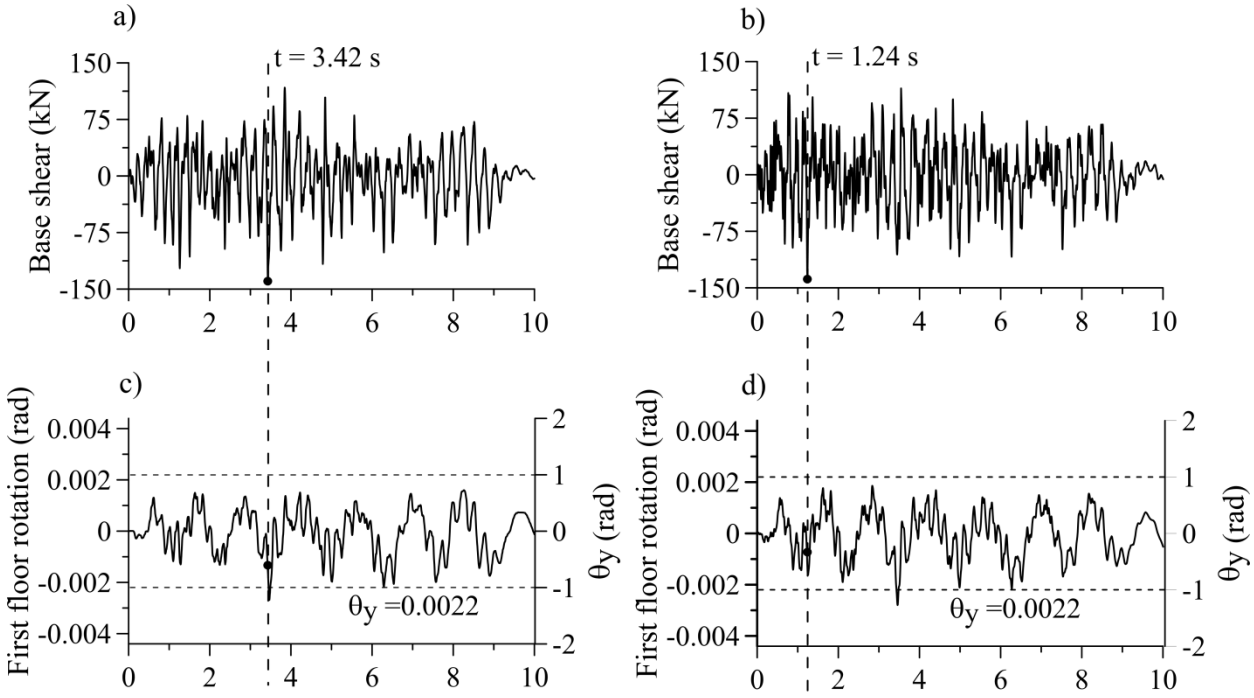

Figure 3-20: (a) Base shear history of W2 under 100% EQ from the experiment; (b) base shear history of W2 under 100% EQ from VT2; (c) base rotation time history of W2 under 100% EQ from the experiment; and (d) base rotation time history of W2 under 100% EQ from VT2.

3.6 Conclusions

In this chapter, the results of two series of shake table tests on slender reinforced concrete walls are analysed using numerical simulations. The walls are modelled with the finite element method using the VecTor2 (VT2) computer program and with the fibre element method using the OpenSees (OS) program. The effects of different modelling assumptions are investigated. The following conclusions and recommendations can be drawn from this study:

1- The tension stiffening effect (TSE) should not be considered in developing seismic numerical models of slender RC shear walls. Consideration of the TSE may result in inaccurate estimations of the structural responses of the wall.

2- The utilisation of an initial stiffness proportional to the Rayleigh viscous damping in both finite (VT2) and fibre (OS) element models provides the closest match between the numerical and experimental results for the analysed system. The damping ratio assigned for the FE program should be slightly smaller than the value used in the fibre element program. The suggested damping ratio for VT2 is 1.5% for modes 1 and 3, while the value for OS is 2% for the first two modes.

3- The finite element (VT2) model can predict the natural periods of the walls for the tests under elastic or damaged conditions. VT2 models can predict the top displacement time history, moment and shear envelop distributions and hysteretic responses well for all the test series in the elastic range or under damaged conditions. This is especially important for W2, which was in an undamaged condition when the designed seismic excitation was applied.

4- The fibre element (OS) model can predict the dynamic responses of the tested wall in the areas of the top displacement time history, shear and moment envelop distributions. Comparisons between results obtained from the experiment and results obtained from the different effective shear stiffness models confirmed that a good estimate of shear force demand can be achieved using a small value (5-30%) of effective shear stiffness at the base and at the middle height of the wall. For the studied walls, the use of an elastic shear stiffness value of 5% at the 5^{th}, 6^{th} and 7^{th} storeys and a value of 25% at the 1^{st} storey produces the best agreement with the experiment.

5- The damping ratios computed at the end of the VT2 analyses by free vibration in a damaged condition gradually increase with the applied EQ intensity due to the accumulation of damage.

6- The VT2 program is able to predict the combined shear-flexural cracks at the base and the bending cracks at the 6^{th} level. A very good match is obtained with the observed crack patterns in the tests.

7- The tests showed that a second plastic hinge formed at the 6^{th} level of the walls in addition to the formation of the base hinge due to the higher mode effects. This behaviour is also computed using the OS and VT2 modelling techniques, and there is good agreement in the moment-rotation responses between the test results and numerical model results.

References

CI (2010) "ACI-318-08, Building Code Requirements for Structural Concrete (ACI 318-08) and Commentary," American Concrete Institute, Farmington Hills, MI, USA.

Bentz, E. C. (1999) "Sectional Analysis of Reinforced Concrete Members," Ph.D. thesis, Department of Civil Engineering, University of Toronto.

CEN (2004) "Eurocode 8: Design of structure of earthquake resistance. Part 1 General rules, seismic action and rules for buildings (EN 1998-1)," Brussels.

Cheng, F. Y., Mertz, G. E., Sheu, M. S. & Ger, J. F. (1993) "Computed versus observed inelastic seismic low-rise RC shear walls," ASCE J. Struct. Eng., 119(11), 3352-3275.

Clough, R. W. & Johnston, S. B. (1966) "Effect of stiffness degradation on earthquake ductility requirements," Proceedings of the Japan Earthquake Engineering Symposium, Tokyo, Japan, 195-198.

CSA (2004) " CSA A23.3-04, Design of concrete structures," Canadian Standards Association, Mississauga, ON, Canada.

CSI (2006) "Perform 3D: Nonlinear Analysis and Performance Assessment for 3D Structures," Computer and Structures, Inc., Berkeley, CA

CSI (2010) "SAP 2000: Structural Analysis Program,V15.1.0/1," Computer and Structures, Inc., Berkeley, CA

Filiatrault, A., D'Aronco, D. & Tinawi, R. (1994) "Seismic shear demand of ductile cantilever walls: a Canadian perspective," Can. J. Civ. Eng., 21(3), 363-376.

Ghorbanirenani, I., Tremblay, R., Léger, P. & Leclerc, M. (2012) ”Shake Table Testing of Slender RC Shear Walls Subjected to Eastern North America Seismic Ground Motions,” ASCE J. Struct. Eng., 138(12), 1515–1529. DOI: 10.1061/(ASCE)ST.1943-541X.0000581

Ghorbanirenani, I., Rallu, A., Tremblay, R. & Léger, P. (2009a) "Distribution of Inelastic Demand in Slender R/C Shear Walls Subjected to Eastern North America Ground Motions," ATC-SEI Conference on Improving the Seismic Performance of Existing Buildings and Other Structures, San Francisco, CA, pp. 1-13.

Ghorbanirenani, I., Velev, N., Tremblay, R., Palermo, D., Massicotte, B. & Léger, P. (2009b) "Modelling and Testing Influence of Scaling Effects on Inelastic Response of Shear Walls,"ACI Structural Journal, 106(3), 358-367.

Grange, S., Kotronis, P. & Mazars, J. (2009) "Numerical modelling of the seismic behaviour of 7-story building: NEES benchmark," Materials and Structure, 42, 10.1617/s11527-008-9462-y. 1433-1442.

Kazaz, I., Ahmet, Y. & Polat, G. (2006) "Numerical simulation of dynamic shear wall tests: A benchmark study," Computer and Structures, 84(8-9), 10.1016/j.compstruc.

Kent, D. & Park, R. (1971) "Flexural member with confined concrete," Journal of Structural Division, Proceedings of the American Society of Civil Engineers, 97(ST7), 1969–1990.

Kim, Y., Kabeyasawa, T., Matsumori, T. & Kabeyasawa, T. (2011) "Numerical study of a full-scale six-storey reinforced concrete wall-frame structure tested at E-Defense," Earthquake Engng Struct. Dyn., DOI: 10.1002/eqe.1179.

Krawinkler, H. (2006) "Important of good nonlinear analysis," Struct. Design Tall Spec. Build., 15, 10.1002/tal.379. 515-531.

Loh, C.-H., Wan, S. & Liao, W.-I. (2002) "Effects of hysteretic model on seismic demands consideration of near-fault ground motions," Struct. Design Tall Spec. Build., 11, 10.1002/tal.182. 155-169.

Lu, X. & Wu, X. (2000) "Study on a new shear wall system with shaking table test and finite element analysis," Earthquake Engng Struct. Dyn., 29(10), 1425-1440.

Martinelli, P. & Filippou, P. C. (2009) "Simulation of the shaking table test of a seven-story shear wall building," Earthquake Engng Struct. Dyn., 38(5), 587-607.

Mazzoni, S., McKenna, F., Scott, M. H. & Fenves, G. L. (2006) "OpenSees Command Language, Manual, Open System for Earthquake Engineering Simulation (OpenSees)," Pacific Earthquake Engineering Research Center, University of California Berkeley, CA.

Munir, A. & Warnitchai, P. (2012) “The cause of unproportionately large higher mode contributions in the inelastic seismic responses of high-rise core-wall buildings,” Earthquake Engng Struct. Dyn. DOI: 10.1002/eqe.2182.

NRCC (2005) "National Building Code of Canada, 12th ed," National Research Council of Canada, Ottawa, ON, Canada.

NZS (2006) "NZS 3101.1&2:2006, Concrete Structures Standard: Part 1 – The Design of Concrete Structures Standards New Zealand," Wellington, New Zealand.

Orakcal, K. & Wallace, W. (2006) "Flexural modelling of reinforced concrete walls experimental verification," ACI Structural Journal, 103(2), 196-206.

Palermo, D. & Vecchio, F. J. (2002) "Behavior of three-dimensional reinforced concrete shear walls," ACI Structural Journal, 99(1), 81-89.

Palermo, D. & Vecchio, F. J. (2007) "Simulation of Cyclically Loaded Concrete Structures Based on the Finite-Element Method," ASCE J. Struct. Eng., 133(5), 728-738.

Panagiotou, M. & Restrepo, J. I. (2009) "Dual-plastic hinge design concept for reducing higher-mode effects on high-rise cantilever wall buildings," Earthquake Engng Struct. Dyn., 38(12), 1359-1380.

Panagiotou, M., Restrepo, J. I. & Conte, J. P. (2007) “Shake table test of a 7-story full scale reinforced concrete structural wall building slice phase II: T-wall,” SSRP 07-08 Report Dept. of Struct. Eng., Univ. of California at San Diego,CA.

Panagiotou, M., Restrepo, J. I. & J.P., C. (2011) "Shake table test of a 7-story full scale reinforced concrete structural wall building slice phase I: rectangular wall," ASCE J. Struct. Eng., 137(6), 691-701.

Panneton, M., Léger, P. & Tremblay, R. (2006) "Inelastic analysis of a reinforced concrete shear wall building according to the NBCC 2005," Can. J. Civ. Eng., 33(7), 854-871.

Park, R., Priestley, M. J. N. & Gill, W. (1982) "Ductility of square-confined concrete columns", ASCE J. Struct. Eng., 108(4), 929–950.

Paulay, T & Priestley, M. N. J. (1992) Seismic Design of Reinforced Concrete and Masonry Buildings, John Wiley & Sons, Inc., New York.

Priestley, M. J. & Amaris, A. D. (2002) “Dynamic amplification of seismic moments and shear forces in cantilever walls,” Research Report ROSE No. 01 Rose School, University of Pavia, Pavia, Italy.

Rad, B. R. (2009) "Seismic shear demand in high-rise concrete walls," Ph.D. thesis Civil Engineering, The University of British Columbia.

Ruttenberg, A. & Nsieri, E. (2006) "The seismic shear demand in ductile cantilever wall systems and the EC8 provisions," Bull Earthquake Eng., 4, 10.1007/s10518-005-5407-9. 1-21.

Schotanus, M. I. & Maffei, J. R. (2008) "Computer modelling and effective stiffness of concrete wall buildings," Tailor Made Concrete Structures – Walraven & Stoelhorst (eds). Taylor & Francis Group, London, ISBN 978-0-415-47535-8.

Seckin, M. (1981) "Hysteretic Behaviour of Cast-in-Place Exterior Beam-Column-Slab Subassemblies," Department of Civil Engineering, University of Toronto, Ph.D, 266.

Seismosoft (2011) “SeismoStruct: Software applications for analysis of structures subjected to seismic actions,” Pavia, Italy

Sullivan, T. J., Priestley, M. J. N. & Calvi, G. M. (2008) "Estimating the higher-mode response of ductile structures," Journal of Earthquake Eng., 12(3), 456–472.

Takeda, T., Sozen, M. A. & Nielsen, N. N. (1970) "Reinforced concrete response to simulated earthquakes," ASCE J. Struct. Eng., 96(12), 2557-2573.

Thomsen IV, J. H. & Wallace, J. W. (2004) "Displacement-based design of slender reinforced concrete structural walls - experimental verification," ASCE J. Struct. Eng., 130(4), 618-630.

Tremblay, R., Ghorbanirenani, I., Velev, N., Léger, P., Leclerc, M., Koboevic, S., Bouaanani, N., Galal, K. & Palermo, D. (2008) "Seismic response of multi-storey reinforced concrete walls subjected to Eastern North America high frequency ground motions," Proc. 14WCEE., Beijing, China, Paper no. 05-01-0526.

Tremblay, R., Léger, P. & Tu, J. (2001) “Inelastic Seismic Response of Concrete Shear Walls Considering P-Delta Effects,” Can. J. Civ. Eng., 28(4), 640-655.

Vecchio, F. J. (2000) "Disturbed Stress Field Model for Reinforced Concrete: Formulation," ASCE J. Struct. Eng., 126(9), 1070-1077.

Vecchio, F. J. & Collins, M. P. (1986) "The modified compression-field theory for reinforced concrete elements subjected to shear," ACI Structural Journal, 83(2), 219-231.

Vecchio, F. J. & Lai, D. (2004) "Crack shear-slip in reinforced concrete elements," Journal of Advanced Concrete Technology, 2(3), 289-300.

Wong, P. S. & Vecchio, F. J. (2002) "VecTor2 & Formworks user’s manuals," Department of Civil Engineering, University of Toronto, pp.213.

CHAPTER 4 ARTICLE 2: SEISMIC DEMAND OF MODERATELY DUCTILE REINFORCED CONCRETE SHEAR WALLS SUBJECTED TO HIGH-FREQUENCY GROUND MOTIONS

This chapter presents a parametric study performed to examine the seismic behaviour of moderately ductile (MD) reinforced concrete (RC) shear walls designed according to Canadian code provisions, including National Building Code of Canada (NBCC) 2010 and Canadian Standards Association (CSA) 23.3-04, when subjected to typical high-frequency eastern North America (ENA) earthquakes. The numerical models were experimentally validated based on large specimens shaking table test results. The results obtained following the code response spectrum procedure were compared with the results from inelastic response history analyses to investigate the effect of higher modes on seismic force demands. The results indicate that current code provisions for MD shear walls need to be modified. A new base shear factor and shear force design envelop are proposed to evaluate the seismic shear force demand more realistically. This study also recommends that the current CSA 23.3-04 requirements for ductile shear walls for bending moments could be applied to constrain the location of inelastic flexural deformations at the base of MD shear walls. The content of this chapter corresponds to the article with title "seismic demand of moderately ductile reinforced concrete shear walls subjected to high frequency ground motions" published on Canadian Journal of Civil Engineer, volume 41, issue 2, pages125-135.

4.1 Introduction

Most seismic design codes for shear walls, including the NBCC 2010 (NRCC, 2010), New Zealand codes (NZS, 2006), and Eurocode (EC) 8 (CEN, 2004), are based on capacity design principle. The wall is allowed to behave nonlinearly by forming a plastic flexural hinge at the base, and the upper part must remain in the elastic regime.

Response spectrum modal analysis (RSMA) is the most preferable technique prescribed in NBCC 2010 to predict structural wall responses for design. This technique provides an accurate and adequate estimate of response parameters when the shear wall structure behaves within the linear range. However, the wall is expected to respond in a nonlinear manner (base plastic hinge), and flexural and shear stiffness will vary during strong ground motions.

To account for nonlinear behaviour in design, the computed force demand from an elastic analysis is simply reduced by applying inelastic response modification coefficients (R_dR_0 in NBCC 2010);

however, elastic modal analysis does not consider the force redistribution as the structure becomes inelastic. At that point, the shear wall responds like a pinned-base structure after base hinging, with relatively greater importance of higher mode effects (HMEs) (Paulay & Priestly, 1992). This response may cause inaccuracies in seismic shear wall response predictions.

Recent numerical studies (Boivin & Paultre, 2012a; Velev, 2007; Rutenberg & Nsieri, 2006) have investigated the importance of HMEs in structural wall response. These studies demonstrated that the current code requirements may underestimate the seismic shear at the base and flexural strength demands in the middle height; and may thus lead to shear failure at the wall base and unintended plastic hinge formation in the upper part of the wall.

Seismic design provisions (NRCC, 2010; NZS, 2006; CEN, 2004) and researchers (Boivin & Paultre, 2012b; Rejec et al., 2012; Velev, 2007; Ruttenberg & Nsieri, 2006) have proposed methods to consider HMEs. However, most of the proposed methods were based on numerical studies using simple finite element structural analysis program with lumped plasticity beam elements or finite element models with assumptions that have not been validated using dynamic tests. Modelling assumptions may affect HME predictions in numerical analysis results (Luu et al., 2013). Therefore, an investigation of HMEs using experimentally verified constitutive shear wall models is necessary.

Shaking table tests were conducted on 0.43 scaled, 9m high wall models of an 8-storey MD shear walls designed according to Canadian codes under high-frequency-content ENA earthquakes (Ghorbanirenani et al., 2012). The tests indicated that shear and flexural demands from the code were underestimated. Inelastic behaviour was observed at the base and in the sixth storey of the specimens. Following this test program, Luu et al. (2013) developed constitutive shear wall models using nonlinear reinforced concrete (RC) fibre elements in the OpenSees (OS) software (Mazzoni et al. 2006) and finite elements in the Vector 2 (VT2) program (Wong & Vecchio 2002). Back analyses of 7 test results with different earthquake intensities varying from 40% to 200% indicated that both OS and VT2 adequately reproduced the experimental data. Therefore, the developed modelling procedures were used as the representative constitutive shear wall model for the ENA region.

In this paper, the developed OS and VT2 modelling procedures are used as representative constitutive shear wall models to investigate HMEs and propose new code-type procedures to assess the seismic demand on structural walls under high-frequency-content ENA earthquakes. A nonlinear time history analysis (NTHA) parametric study was performed to investigate the influence of design parameters on the higher mode amplification effects on the seismic force demand. The results are

used to propose a new simplified method to determine the magnitude and distribution over the wall height of the shear and bending moments considering HMEs. This research focuses on MD shear walls, which is the most commonly used shear wall category for the moderate and low seismic demand in ENA. A new capacity design method considering higher mode amplification effects is proposed to determine capacity design envelops for flexural and shear strength demands to achieve a single base plastic hinge response at the wall base.

The paper is organised as follows: first, a literature review of HMEs on RC shear walls identifies key parameters controlling wall seismic responses. Next, a parametric study, conducted using NTHA, quantifies HMEs for a series of designed shear wall prototypes located in Montreal for different parameters. These are (1) site classes (C, D, and E), (2) fundamental periods (T) ranging from 0.5 s to 3.5 s, (3) numbers of storeys (n), varying from 5 to 25, (4) wall flexural base overstrength factors (γ_w), ranging between 1.2 and 2.4, and (5) axial load ratios, ranging from 5% to 13% (the ratio between the base axial load to the product of the concrete compressive strength and the wall base cross section area, $P/(A_g f_c^{'})$). Finally, a new simplified design method is proposed for MD shear walls located in ENA.

4.2 Seismic Design Guidelines Considering HMEs

During severe earthquakes, a ductile RC shear wall is expected to exhibit inelastic flexural behaviour, although the shear response must remain elastic (Paulay & Priestly, 1992). For that purpose, several procedures have been proposed and/or applied in codes, such as the NZS 3101 standard in the New Zealand, EC 8, and NBCC 2010.

Appendix D1 of NZS 3101 (NZS 2006) outlines the method of a modified shear force design envelop (V) by multiplying the shear force envelop from the equivalent static force procedure (ESFP), V_E, by a dynamic amplification factor for shear, ω_v, and the flexural overstrength factor, ϕ_0:

$$V = \omega_v \phi_0 V_E \tag{4.1}$$

The factor ω_v depends on the number of storeys, n:

$$\omega_v = \begin{cases} 0.9 + n/10 & \text{for } n \le 6 \\ 1.3 + n/30 \le 1.8 & \text{for } n > 6 \end{cases} \tag{4.2}$$

The overstrength factor ϕ_0 corresponds to the ratio of the flexural wall resistance obtained with increased reinforcing steel yield stress (1.25 f_y for grade 300 steel) and concrete compressive strength (f'_c + 15 MPa) to the factored moment demand, M_f.

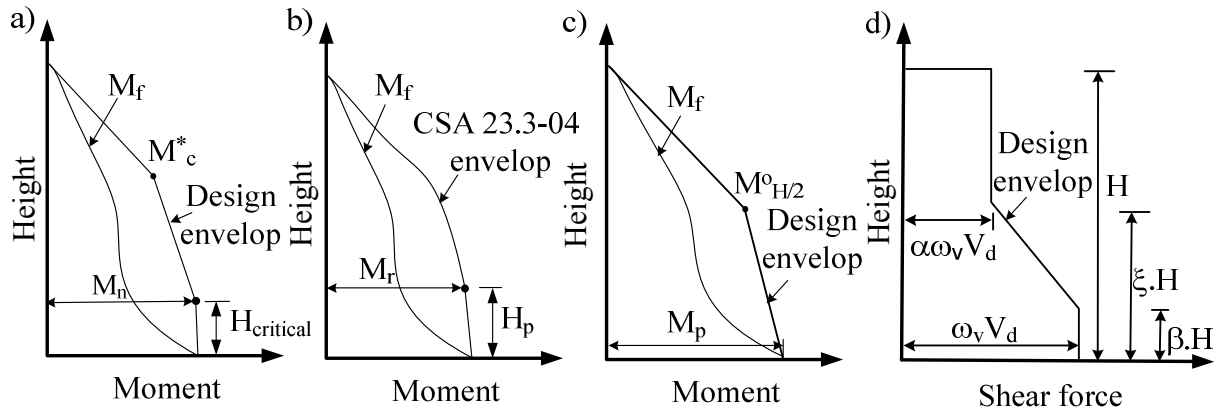

Figure 4-1: Proposed capacity design: (a) moment envelop in the New Zealand code; (b) moment envelop in the Canadian code for ductile shear walls; (c) bilinear moment envelop; and (d) tri-linear shear force envelop.

NZS 3101 also includes a design moment envelop above the plastic hinge region that accounts for HMEs on flexural demand. As illustrated in Figure 4-1a, the design moment, which is used to determine the wall nominal flexural resistance, comprises two straight line segments: one segment extending from the nominal flexural strength at the critical section of the base plastic hinge, M_n, to a moment M_c^* at the wall mid-height, and a second line varying from the moment M_c^* at the wall mid-height to zero at the wall top. The moment M_c^* is taken as

$$M_c^* = \frac{M_{E,C}}{0.85}\left[1+\frac{n-1}{4}\right];\ M_c^* \geq 0.5M_n \text{ at the base} \qquad (4.3)$$

where $M_{E,C}$ is the moment at the mid-height of the wall from static or modal response spectrum analysis.

EC 8 (CEN, 2004) proposes a similar approach to the New Zealand code with a shear amplification factor for HMEs on base shear force demand. Two ductility classes are defined in EC 8 for concrete shear walls: ductility class high (DCH), with a behaviour (ductility) factor q = 4, and ductility class medium (DCM), with a ductility factor q = 3. A different seismic design approach is specified for

each class. For DCH, the amplification factor depends on both the flexural overstrength at the base and the contribution of higher modes on base shears:

$$\varepsilon = q\sqrt{\left(\frac{\gamma_{Rd}}{q}\frac{M_{Rd}}{M_{Ed}}\right)^2 + 0.1\left(\frac{S_e(T_c)}{S_e(T_1)}\right)^2} \leq q \qquad (4.4)$$

where, for flexural overstrength, M_{Ed} and M_{Rd} are the design bending moment and design flexural resistance at the base of the wall, respectively, and γ_{Rd} is the factor accounting for overstrength due to steel strain-hardening. In the term for higher mode response, $S_e(T_c)$ is the ordinate of the constant spectral acceleration region of the spectrum at short periods, and $S_e(T_1)$ is the ordinate of the elastic response spectrum at the fundamental period of vibration of the building, T_1. In Eq. (4.4), the amplification factor ε is limited to the behaviour factor, q, such that the demand does not exceed the elastic response. For DCM, the design shear forces are simply taken as 1.5 times the shear forces obtained analytically. Thus, as opposed to DCH class walls, the flexural overstrength and HMEs need not be evaluated when determining design shears. In EC 8, no recommendation exists to avoid the second hinge formation in the mid-height of the wall due to HMEs.

Table 4-1**:** Proposed amplification factor (a) M_v and J from NBCC 2010; and (b) ω_v and α_M values adapted from Boivin & Paultre (2012b).

a)

		M_v		J		
$S_a(0.2)$ /$S_a(2.0)$	T ≤ 1.0	T = 2.0	T ≥ 4.0	T ≤ 0.5	T = 2.0	T ≥ 4.0
< 8.0	1.0	1.2	1.6	1.0	0.7	0.5
> 8.0	1.0	2.2	3.0	1.0	0.4	0.3

Note: For the intermediate period, the values of M_v and J are obtained by linear interpolation

b)

	ω_v		α_M	
R_dR_o/γ_w	T ≤ 0.5	T ≥ 1	T ≤ 0.5	T ≥ 1
2.8	1.0	2.0	0.5	0.62
1.87	1.0	1.5	0.5	0.55
≤ 1.4	1.0	1.0	0.5	0.5

Note: For the intermediate period, the values of ω_v and α_M are obtained by linear interpolation

In NBCC 2010, the HMEs are explicitly considered when using the ESFP by applying the factors M_v and J to the base shear and moment envelop distribution, respectively. These factors depend on the shape of the seismic design spectrum at the site and the fundamental period (T), as indicated in Table 4-1a. In addition to NBCC 2010, the CSA-A23.3-04 Design of Concrete Structures standard also contains specific seismic design provisions for shear walls. For ductile shear walls, the factored shear

resistance shall not be less than the shear corresponding to the development of the probable moment capacity, M_p, of the wall at its base. The moment M_p is calculated using 1.25 f_y as the probable reinforcing steel yield strength. For MD shear walls, the shear corresponding to the nominal wall base moment capacity, M_n, must be used to determine the design shears. Thus, the design shears are obtained by multiplying the factored shear forces from the analysis by the flexural overstrength factor, $\gamma_w = M_n/M_f$, where M_f is the factored bending moment at the base obtained from the analysis.

In CSA A23.3, for ductile shear walls, the bending moment above the plastic hinge region, as obtained from linear analysis, M_f, is amplified to prevent inelastic response in the upper part of the walls. The design moment envelop is obtained by multiplying the moment M_f by the ratio of the factored moment resistance, M_r, to the factored moment demand, M_f. Both of these parameters are calculated at the top of the assumed plastic hinge region (elevation H_p in Figure 4-1b). However, no such recommendation is given for the design moments for MD shear walls.

Ruttenberg & Nsieri (2006) studied DCH walls designed according to EC 8 to investigate the shear at the base and the shear envelop along the structure height. The authors included the behaviour factor q and the fundamental period of the structure, T, to evaluate a base shear amplification factor, ε, considering HMEs:

$$\varepsilon = 0.75 + 0.22\,(T + q + Tq) \tag{4.5}$$

A new method was also proposed to define the design shear force envelop considering HMEs in the upper part of the wall. The proposed envelop is tri-linear, as indicated in Figure 4-1d, with α, ξ, and β:

$$\begin{cases} \xi = 1.0 - 0.3\,T;\ \xi \geq 0.5 \\ \alpha = 0.5;\ \beta = 0.1 \end{cases} \tag{4.6}$$

Rejec et al. (2012) studied DCH and DCM shear walls designed according to EC 8 and found that the current EC 8 amplification factor from Eq. (4.4) would apply to DCH and DCM shear walls by imposing an upper limit of 1.0 to the term associated with flexural overstrength and a minimum ε value of 1.5:

$$\varepsilon = q\sqrt{\left(\min\left[\frac{\gamma_{Rd}}{q}\frac{M_{Rd}}{M_{Ed}};1\right]\right)^2 + 0.1\left(\frac{S_e(T_c)}{S_e(T_1)}\right)^2} \geq 1.5 \tag{4.7}$$

Velev (2007) analysed ductile shear walls located in Vancouver, Canada, and MD shear walls in Montreal, Canada, that were designed according to NBCC 2005 and CSA 23.3-04. The authors proposed two different dynamic base shear amplification factors (ω_v) as function of the number of storeys, n, for each site:

$$\omega_v = 1.5 + n/40 \quad \text{for Vancouver (ductile shear walls)} \tag{4.8}$$

$$\omega_v = 1.4 - n/100 \quad \text{for Montreal (MD shear walls)} \tag{4.9}$$

Boivin & Paultre (2012a, b) conducted a parametric study for ductile shear walls under Western North America (WNA) ground motions. The authors concluded that the wall overstrength factor and fundamental period primarily influenced the seismic base shear force demand. A new dynamic base shear force amplification factor value, ω_v, was proposed, as indicated in Table 4-1b. The authors also suggested using the design shear force envelop proposed by Ruttenberg & Nsieri (2006) with a tri-linear shear force envelop, as displayed in Figure 4-1d, with the same value for α and β but with a new equation for the height ratio, ξ:

$$\begin{cases} \xi = 1.5 - T; 0.5 \le \xi \le 1.0 \\ \alpha = 0.5; \beta = 0.1 \end{cases} \tag{4.10}$$

In Table 4-1b, ω_v appears to depend on the overstrength and ductility-related force modification factors, R_o and R_d, but in fact, the parametric study by Boivin & Paultre (2012a) was restricted to ductile shear walls. Boivin & Paultre (2012b) also proposed a bilinear design moment envelop, as shown in Figure 4-1c, with α_M interpolated from Table 4-1b. This envelop is similar to that proposed by Priestly et al. (2007) for direct displacement based seismic design of concrete buildings.

4.3 Key controlling parameters

The previous review indicated several key parameters that had the greatest influence on HMEs for the dynamic base shear in RC shear walls, including: (1) the fundamental period, T, (2) the number of storeys, n, (3) the flexural overstrength at the base, γ_w, (4) the ductility of the structure, as expressed using R_d, q, μ, or R, and (5) the characteristics of the ground motions (intensity and frequency content). In the upper part of the walls, HMEs are influenced by T for the shear force envelops and by γ_w for the bending moment envelops (Boivin & Paultre, 2012a; Rutenberg & Nsieri, 2006).

Most of the above studies were performed using structural analysis programs with lumped plasticity beam elements that could develop flexural plastic hinges at their ends. In these models, bi-linear moment curvature hysteretic behaviour was considered, shear load-deformation response was assumed to be linear elastic, and axial-flexure interaction is only partially accounted. With such modelling assumptions, important nonlinear physical phenomena that occur in actual RC shear walls are omitted, such as shear-flexure-axial interaction and the effects of shear sliding deformations along flexural cracks and shear stiffness degradation. Those effects might cause an inaccurate assessment of HMEs on the structural wall response.

Boivin & Paultre (2012a, b) used the nonlinear finite element program VT2 (Wong & Vecchio, 2002) that better reproduces nonlinear RC responses, but they made several assumptions in their numerical models, particularly in their consideration of tension stiffening effects. Using data from shake table tests on 9-m-tall wall specimens, Luu et al. (2013) found that considering tension stiffening effects in VT2 analyses could overestimate shear and moment demands. The study by Boivin & Paultre (2012b) was restricted to ductile shear walls subjected to WNA earthquakes and did not investigate MD shear walls, which are expected to sustain reduced inelastic demand compared to ductile shear walls when subjected to high-dominant-frequency (≅ 10 Hz) ENA ground motions.

4.4 Nonlinear Time History Analyses – Input Parameters

4.4.1 Parameters studied and the design of walls

The walls studied for nonlinear dynamic analysis are MD walls designed with the force modification factors $R_d = 2.0$ and $R_o = 1.4$. The walls are assumed to be located in Montreal, Québec, in ENA. The following parameters were considered in the study: (1) number of storeys, (2) lateral fundamental period, T, (3) flexural overstrength factor at wall base, γ_w, (4) axial load ratio, $P/(A_g f_c')$, and (5) site class (SC).

Table 4-2 provides the values of the parameters studied and their ranges. The number of storeys was limited to 25 because the wall design for buildings with more than for 25-storey is typically governed by wind loading rather than by seismic loads in Montreal. For each building height, two values of T were selected to cover the range of corresponding un-cracked fundamental periods, T_{uncr}, of shear wall buildings as measured in ambient vibration tests (Gilles, 2010). Three different site classes were investigated: C, D, and E. The effect of site class was only studied for $n \leq 10$ because soil

amplification effects are limited for high-rise buildings (Figure 4-2). Site class A was excluded in this study because it led to low seismic demand in the Montreal region. The flexural overstrength at the wall base, γ_w, varied from the minimum possible value to a value resulting in nearly elastic base shear response. The parameter γ_w was varied by modifying the amount of longitudinal steel reinforcement. The values of $P/(A_g f_c')$ were selected to reflect practical wall designs.

Table 4-2 : Parameters studied.

n	Height (m)	T_{uncr} (s)	T (s)	T_a (s)	Wall cross-section type	Wall length (m)	Site class	Overstrength factor, γ_w	$P/(A_g f_c')$ (%)	Computer program
5	17.5	0.4	0.5	0.50	I	4	D	1.2,1.6,2.0	5	OS
		0.7	1.0	0.86	I	4	C,D,E	1.2,1.6,2.0	5,8,12	OS and VT2
10	35.0	1.2	1.5	1.44	I	6	D	1.2,1.6,2.0	7	OS
		1.6	2.0	1.44	I	6	C,D,E	1.2,1.6,2.0	7,10,12	OS and VT2
15	52.5	1.6	2.0	1.95	I	8	D	1.6,2.0	7	OS
		2.0	2.5	1.95	I	8	D	1.6,2.0	8,10,13	OS and VT2
20	70.0	2.1	2.5	2.42	[	8	D	2.0,2.4	9	VT2
		2.5	3.0	2.42	[	8	D	2.0,2.4	14	VT2
25	87.5	2.5	3.0	2.86	[	10	D	2.0,2.4	11	VT2
		3.0	3.5	2.86	[	10	D	2.0,2.4	15	VT2

The wall cross sections are rectangular for $n \leq 15$ and have a C shape for the 20- and 25-storey buildings. The height of each storey is 3.5 m. The thickness of the walls equals 0.35 m from the base to the top of the walls. The compressive strength of the concrete is 30 MPa for $n \leq 15$ MPa and 40 MPa for the taller walls.

A total of 35 shear walls were individually designed according to NBCC 2010 and CSA A23.3-04 requirements for MD shear walls. The seismic mass was selected to obtain the cracked fundamental periods shown in Table 4-2. In design, concrete cracking was accounted for by using the effective flexural properties recommended in CSA A23.3-04, which depend on axial load, concrete strength, and wall cross-sectional area. The resulting effective (cracked) fundamental periods using modal analysis, T, are given in Table 4-2. For each wall, the design period, T_a, was then taken as the minimum of T and two times the period obtained from the empirical expression specified in NBCC 2010, $T_{emp} = 0.05\ H^{0.75}$. As indicated in Table 4-2, the latter governed for all structures except for the 5-storey wall with T = 0.5 s; however, the differences between T and T_a values were generally small. Accidental torsion was considered by increasing the design spectrum prescribed in NBCC 2010 by

10% (Figure 4-2). The results obtained from modal response spectrum analysis were calibrated such that the base shear (V_d) was equal to 100% of the base shear from the ESFP. As specified in the NBCC 2010, the M_v factor (Table 4-1a) included in the calculation of V_d is equal to 1.0 for walls with T = 0.5 and 1.0 s, and it varied from 1.25 to 2.42 for T ranging from 1.5 s to 3.5 s. According to CSA A23.3-04 for MD shear walls, the calibrated base shear, V_d, was then amplified by γ_w to obtain the design base shear. The shear force and moment design values in the upper part of the walls were taken directly from modal response spectrum analysis. The reinforcement design of each wall was verified to satisfy all requirements in CSA A23.3-04 by using the S-concrete computer program (S-Frame, 2012).

4.4.2 Selected Ground Motions

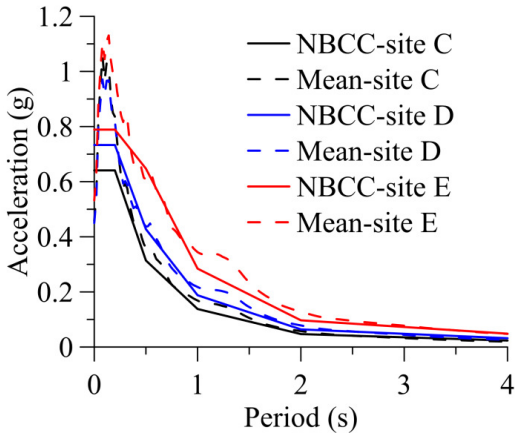

Figure 4-2: Mean acceleration response spectra of the selected ground motions versus NBCC 2010 design spectra.

Atkinson (2009) simulated 45 statistically independent ground motion time histories for each of the following magnitude-distance (M-R) scenarios for ENA earthquakes: (1) M 6.0 at R = 10 km, (2) M 6.0 at R = 30 km, (3) M 7.0 at R = 25 km, and (4) M 7.0 at R = 100 km. For this study, three of these records were selected from each M-R bin and scaled to match the NBCC 2010 Montreal uniform hazard spectra (UHS). Therefore, for each site class studied (C, D, and E), 12 ground motions were selected and scaled according to the recommendations from Atkinson (2009). The mean acceleration response spectra of the scaled ground motions are described in Figure 4-2. The mean spectra are in good agreement with the design spectrum prescribed in NBCC 2010.

4.4.3 Constitutive shear wall models

Luu et al. (2013) developed shear wall models for the ENA region using nonlinear fibre elements with OS (Mazzoni et al., 2006) and finite elements with VT2 (Wong & Vecchio, 2002). The authors used data from the shake table experiments performed on two 1:0.43-scaled, 9-m-tall MD shear wall specimens representative of an 8-storey structure (20.97 m in height) designed according to Canadian code (Ghorbanirenani et al., 2012). The results indicated that the OS and VT2 numerical models could adequately reproduce the experimental data. Figure 4-3 illustrates good agreements between OS, VT2 and experiment for time history top displacement, shear force and moment envelops. The standard deviations of shear force and moment envelops between proposed numerical modelling (both OS and VT2) predictions and experiment are all smaller than 14% and 10%, respectively. In addition, Luu et al. (2013) revealed that the models adequately predicted the HMEs that resulted in amplification of the base shear (Figure 4-3b), second hinge formation in the upper wall region, redistribution of shear forces, and a time lag between maximum base shear and maximum bending moment. A summary of the OS and VT2 modelling assumptions are provided in Table 4-3.

Table 4-3: Selected parameters for the VT2 and OS models.

	Model parameters	
	VT2	**OS**
Concrete	Compression pre-peak: Hogdnestad parabolic; compression post-peak: modified Kent-Park	Modified Kent-Park
	Confined strength: Kupfer/Richart	Confined strength: Increase 20%
	Hysteretic response: Palermo 2002 (with decay)	Hysteretic response: Palermo 2002 (with decay)
Steel	Hysteretic response: Seckin (with Bauschinger effect)	Giuffré-Menegotto-Pinto (with Baushinger effect)
ζ	$[C]_{ini}$[1]; 1.5% modes 1 and 3	$[C]_{ini}$[1]; 2% for modes 1 and 2
Shear stiffness	Nonlinear	5-30% at base and mid-height
TSEs[2]	No	No

[1] $[C]_{ini}$: Initial stiffness proportional Rayleigh damping

[2] TSEs = Tension stiffening effects

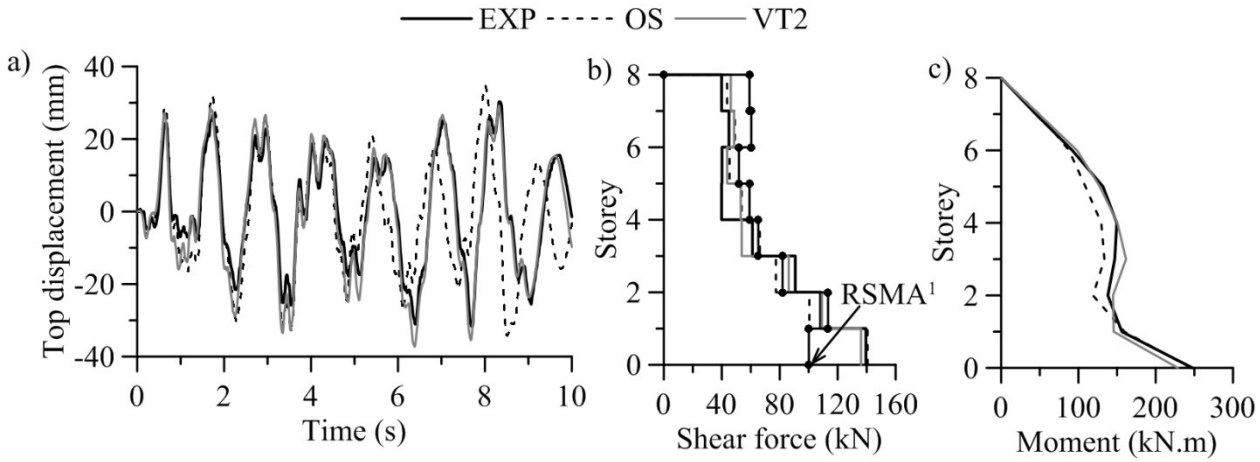

Note: [1]obtained from linear response spectrum modal analysis.

Figure 4-3 : OS and VT2 predictions compared to the experimental data from shaking table test: (a) time history of top displacements; (b) shear force envelop; and (c) bending moment envelop.

This parametric study employed these wall constitutive models, but most of the analyses were conducted with the OS models because they require significantly less computational resources than the VT2 models. Luu et al. (2013) observed that the effective shear stiffness must be carefully defined in the OS models and suggested using a small percentage (5-30%) of the gross shear stiffness at the base and middle height. Using effective shear stiffness in this range will give standard

deviations between OS predictions and test results under 100% earthquake intensity being less than 15%. However, the proper value of the effective shear stiffness can vary significantly with the ground motion intensity or fundamental period of the wall. In this parametric study, the OS models were developed based on the response obtained from VT2 models, considering the latter as benchmarks for developing OS models. This calibration was performed for one five-, 10-, and 15-storey walls subjected to one ground motion. For the five- and 10-storey walls, the three site classes, C, D, and E, were considered. In each case, the procedure was as follows:

- Develop a VT2 model using the VT2 modelling assumptions validated from the experiments.
- Run the VT2 model to obtain the top displacement time history and shear envelops distribution.
- Calibrate the damping ratio in the corresponding OS model to best match the VT2 top displacement time history.
- In the OS model, calibrate the effective shear stiffness at the wall base and mid-height, following Luu et al. (2013), to best match the shear force envelop distribution from VT2.

Table 4-4 presents the results of calibrated damping and shear stiffness of OS models. Figure 4-4 illustrates the good correlation between the OS and VT2 predictions of shear force envelops. For each building height, the calibrated damping and effective shear stiffness properties of the OS model were then applied to all walls having that height. For $n \geq 20$, the proposed procedure for calibrating OS models called for the use of a questionable (unrealistic) Rayleigh damping model with the selection of modes 1 and 20. This damping model might under-damp important modes that contribute significantly to the wall responses. The dubious OS calibration of damping parameters for $n = 20$ and 25 were due to the complex shear and flexure responses of the high-rise shear wall, and an effective shear stiffness from OS models may not properly substitute the nonlinear shear behaviours. Consequently, all analyses were conducted using VT2 models for the cases $n = 20$ and 25 in this study.

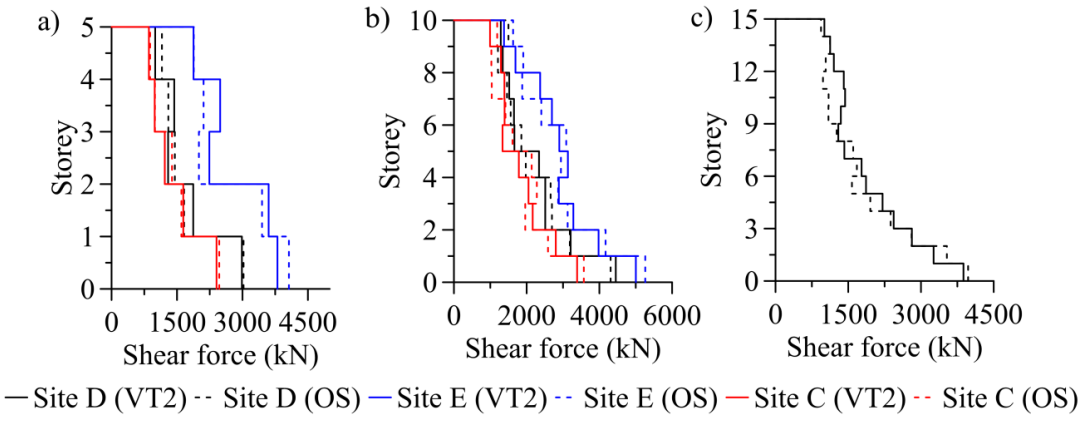

Figure 4-4 : Calibration of the OS model for shear force distribution based on VT2 model predictions: (a) 5-storeys, T = 1.0 s, $\gamma_w = 1.2$; (b) 10-storey, T = 2.0 s, $\gamma_w = 1.2$; and (c) 15-storey, T = 2.5 s, $\gamma_w = 1.6$.

Table 4-4: Selected shear stiffness and Rayleigh damping model for the OS models of the walls under consideration.

Storey	**Site Class**	**Shear stiffness (%)**	**ζ (%)**
n=5; T=0.5s; γ=1.2	C	60% at base; 30% at 3rd storey	$[C]_{ini}$; 2% for modes 1,3
	D	19% at base; 5% at 3rd storey	$[C]_{ini}$; 2% for modes 1,2
	E	10% from base to the top	$[C]_{ini}$; 2% for modes 1,3
n=10; T=2.0s; γ=1.2	C	60% at base; 30% at 5th, 6th and 7th storeys	$[C]_{ini}$; 1.5% for modes 1,3
	D	50% at base ; 20% at 5th, 6th and 7th storeys	$[C]_{ini}$; 1.5% for modes 1,3
	E	18% at base; 7% at 4th and 5th storeys	$[C]_{ini}$; 1.5% for modes 1,2
n=15; T=2.5s; γ=1.6	D	18% at base; 20% at 7th and 8th storeys	$[C]_{ini}$; 1.5% for modes 1,2

4.5 Nonlinear time history analysis – Results

The mean results for each ensemble of 12 ground motions, as obtained from the OS models for $n \leq 15$ and VT2 models for $n \geq 20$, except for cases with special notes, were used to evaluate the seismic demand of the walls designed. A base shear factor, referred to as Ω_v, was defined as the ratio of the base shear forces from NTHA, V_{NL}, to the base shear, V_d, considered in the design:

$$\Omega_v = V_{NL}/V_d \tag{4.11}$$

The reference base shear V_d used to calculate Ω_v was not amplified by $\gamma_w = M_n/M_f$. The bending moments and storey shear force demands along the wall height were normalised relative to the wall nominal flexural resistance at the base, M_n, and the base shear from NTHA, V_{NL}, respectively. The rotational ductility at each storey, μ_θ, was determined as the ratio of the computed rotation demand to the yield rotation at that storey. The yield rotation, θ_y, was evaluated using the method presented by Paulay & Priestly (1992) and used in previous studies by Ghorbanirenani et al. (2012) and Luu et al. (2013). From moment rotation plot obtained from pushover analysis, a secant is drawn from the origin to the point corresponding to $0.75M_y$, and a tangent to the response at larger rotations is then extrapolated to intersect the secant line and define θ_y.

4.5.1 Effect of axial load ($P/(A_g f_c')$)

In Figure 4-5a, no noticeable effect can be observed for the axial load ratio $P/(A_g f_c')$ on Ω_v for the five-, 10-, and 15-storey buildings. A linear increase is observed for the 15-storey walls, but this increase is limited to 10% for the studied range of $P/(A_g f_c') = 8\%$ to 13%. The effects of $P/(A_g f_c')$ on shear force and moment demand distributions along the wall height are presented in Figures. 4-5b and 5c, respectively, for n = 15, $\gamma_w = 1.6$, and T = 2.5 s. The very small differences indicate that $P/(A_g f_c')$ does not significantly affect the distribution or magnitude of the shear force and moment demands. An additional study using VT2 for n = 15 is illustrated in Figure 4-5a. The result re-confirms no effect of axial loading on Ω_v as seen from OS prediction, indicating good agreement between the OS and VT2 predictions, and demonstrating the validity of the proposed OS model calibration.

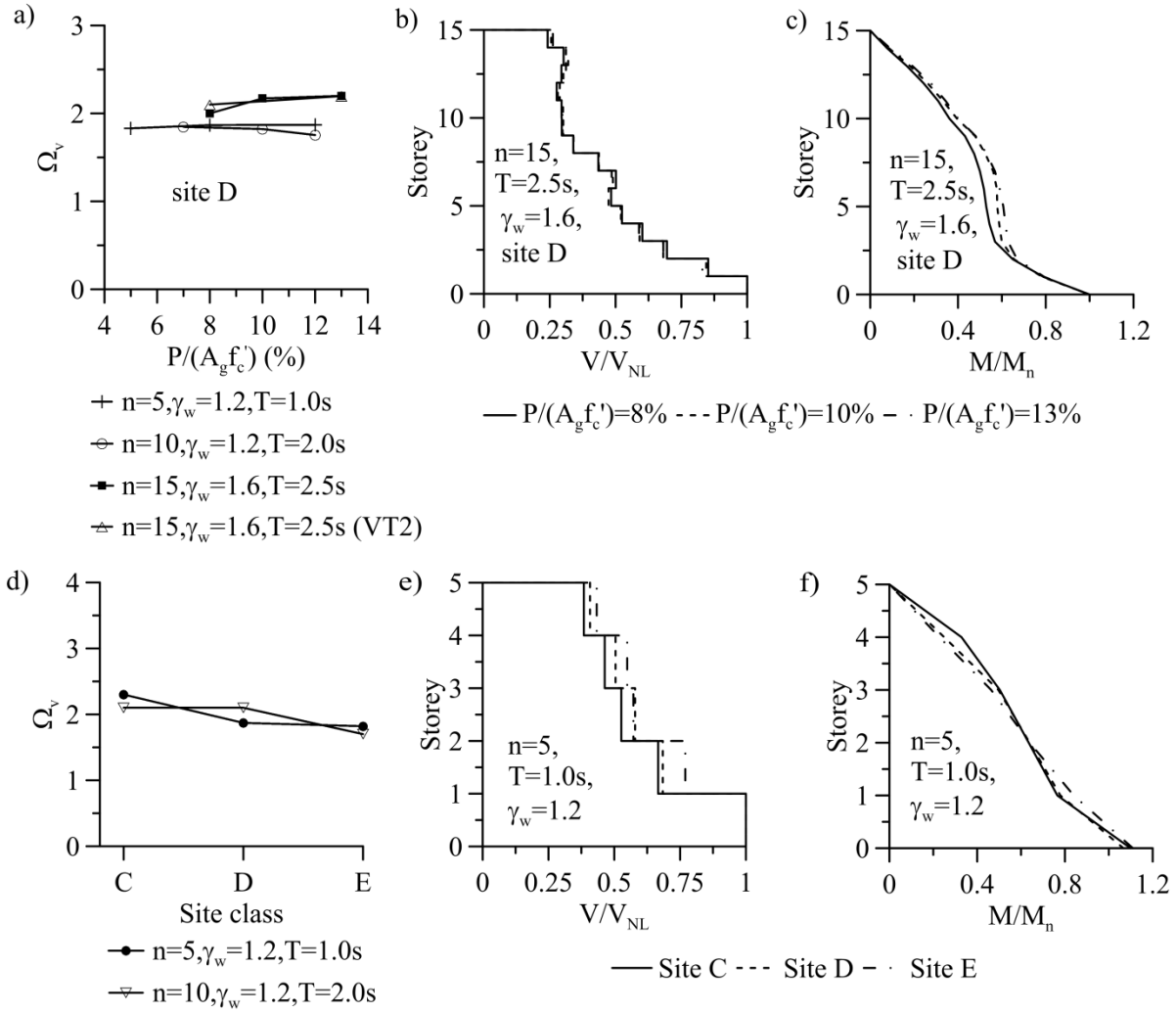

Figure 4-5**:** Influence of the axial load ratio on the (a) mean base shear factor, (b) shear force envelop, and (c) bending moment envelop; and influence of the site class on the (d) mean base shear factor, (e) shear force envelop, and (f) bending moment envelop.

4.5.2 Effect of site class

The effects of the site class on Ω_v, the shear force envelop, and the bending moment envelop are examined for n = 5, T = 1.0 s, and γ_w = 1.2 in Figures. 4-5d, 4-5e, and 4-5f, respectively. In Figures. 4-5e and 4-5f, the site class has no significant influence on the shear force or moment distribution demands. The storey averages of variation between cases with different site classes for shear and moment distributions are all less than 8%. Each wall was designed for the site class considered. The base shear factor, $\Omega_{v,}$ appears to be slightly more sensitive to the site class (Figure 4-5d) due to the relatively higher first mode contribution to the base shear from ESFP used for the calibration of V_d

for site E compared to site C. The ratios between base shear obtain from modal response spectrum analysis and ESFP of the cases n=5, T=1s with site classes C and E are 1.1 and 1.8, respectively. A similar conclusion is drawn for n = 10, T = 2.0 s, and $\gamma_w = 1.2$.

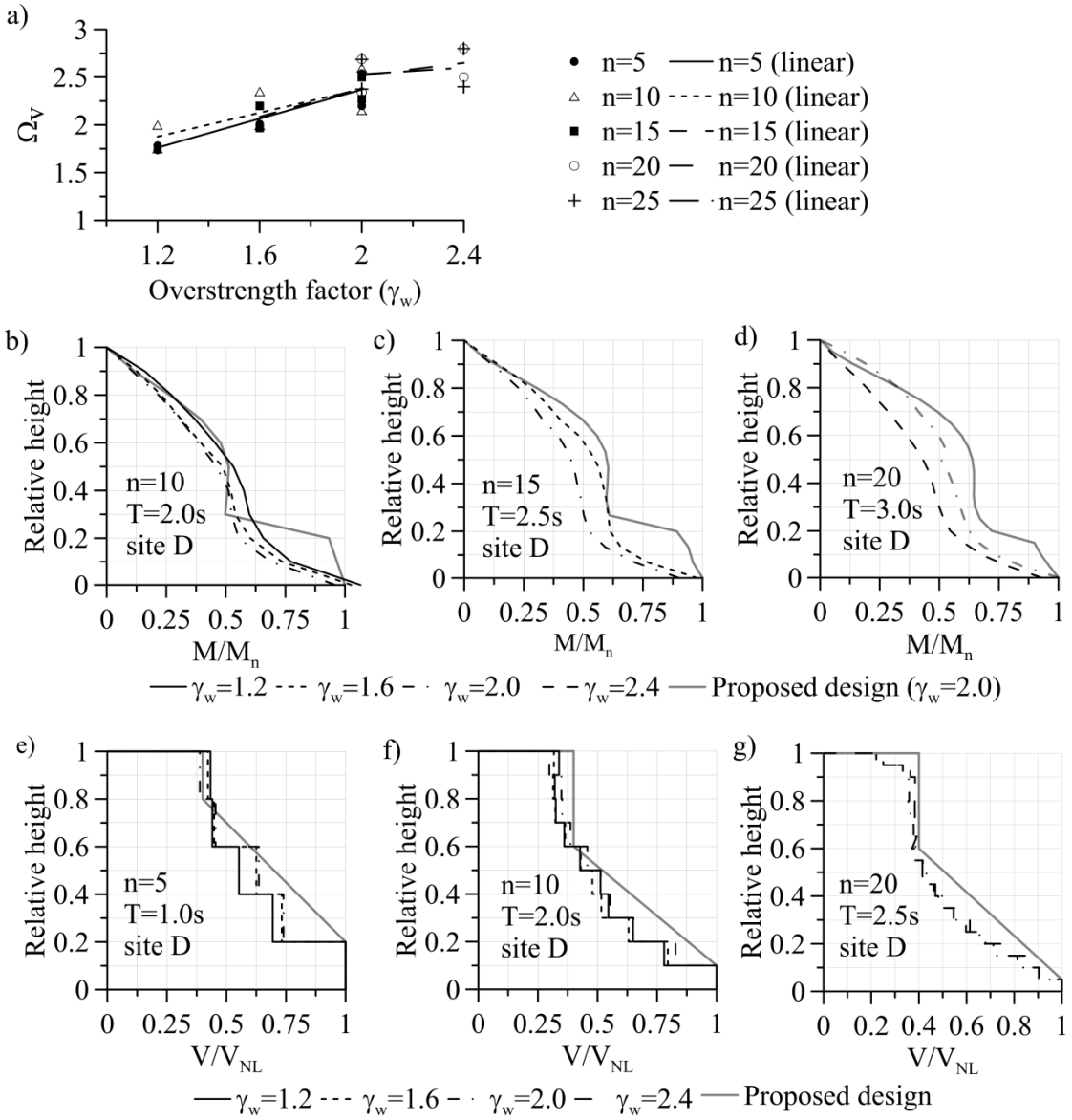

Figure 4-6: Influence of the flexural overstrength on the (a) base shear factor; (b), (c), and (d) mean moment demand envelops; and (e), (f), and (g) mean shear demand envelops.

4.5.3 Effect of the base overstrength factor (γ_w)

The influence of the base overstrength factor, γ_w, on the base shear factor, Ω_v, is illustrated in Figure 4-6a. In view of the previous observations, there is no significant influence of site classes and axial

loads on higher mode effects, so only the results for site class D and for the lowest of three axial load ratios are presented in Figure 4-6a and the following figures. The values of γ_w range from 1.2 to 2.4. Linear trends for each of the building height (n = 5, 10, 15, 20, and 25) are also plotted in Figure 4-6a. For each building height, the base shear factor generally linearly increases as a function of the base flexural overstrength γ_w. The slope of the linear trends varies between 0.15 and 0.76, with an average of 0.70. This ratio is less than 1.0 and indicates that the base shear forces are not directly proportional to the base flexural overstrength. However, for ductile shear walls located in high seismic regions, as studied by Boivin & Paultre (2012a), γ_w can be larger than 2.4, and the effect of γ_w on Ω_v could be more important than what is observed in this study on MD walls located in ENA.

The normalised bending moment envelop distribution along the wall height is presented in Figures. 4-6b, c, and d for n = 10, 15, and 20, respectively. In all three cases, the normalized bending moment in the middle height is increase with the decrease of γ_w. Therefore, the amplification of the moment demand near the wall mid-height is maximum for the walls with low flexural overstrength ($\gamma_w = 1.2$). However, the magnitude of the moments along the wall height is only slightly influenced by the value of γ_w for MD shear walls. In Figures. 4-6e, f, and g, the effect of γ_w on shear force envelops is presented for n = 5, 10, and 20, respectively. The shear forces along the wall height are normalised with respect to the base shear V_{NL}. The results demonstrate that γ_w has no noticeable effects on the shear force envelops.

4.5.4 Effect of the number of storeys and fundamental period

In Figure 4-7a, the relationship between the number of storeys, n, and Ω_v is presented. For each value of n, the average was taken for the case having two values of T to get the linear trends. The results indicate that the base shear factor is not directly affected by the number of storeys.

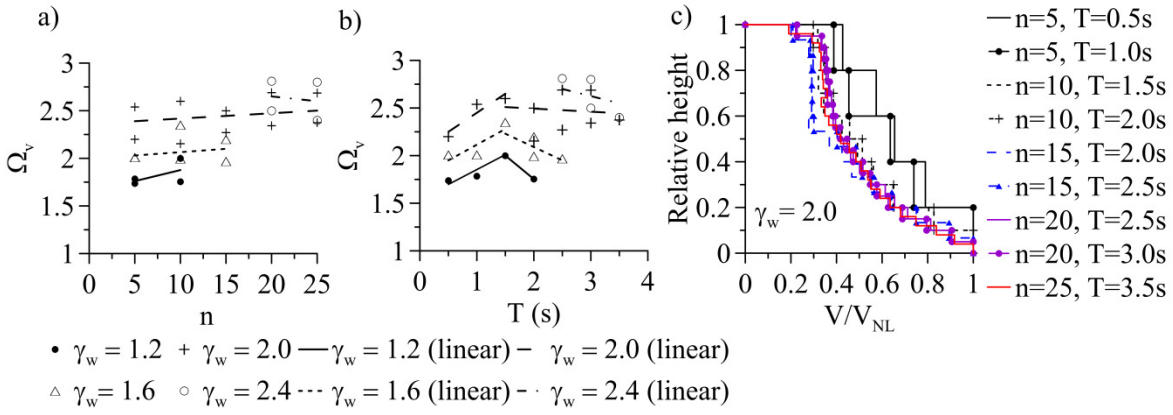

Figure 4-7**:** Influence on base shear factor on the (a) number of storey (n) and (b) fundamental period (T); and (c) influence of the shear force envelop on the fundamental period and number of storeys.

In Figure 4-7b, the base shear factor, Ω_v, is plotted against the fundamental period, T. For each value of T, the average is taken for the cases having more than one value of n to get the linear trends. The results show a linear increase of Ω_v for the range 0.5 s $\leq$ T $\leq$ 1.5 s and a linear decrease for T $\geq$ 1.5 s. The slopes of the linear increasing and decreasing segments of the curves are approximately 0.2 and -0.1, respectively.

In Figures 4-6b, c, and d, very similar bending moment profiles along the wall height are obtained for cases with different fundamental periods and numbers of storeys, suggesting that there is no noticeable effect of T and n on the moment envelop. The effect of the same two parameters on the shear force envelop is illustrated in Figure 4-7c, which indicates that for n > 5 or T > 1.0 s, the shear demands appear to decrease linearly from V_{NL} at the base to 0.4 V_{NL} at the height 0.6H and then remain constant to the top of the wall. For 5-storey buildings with T = 0.5 and 1.0 s, the shear force envelops are nearly linear.

4.5.5 Formation of a second plastic hinge

The mean rotational ductility demand along the walls is presented in Figure 4-8 for four wall cases: n = 5, 10, 15, and 20. The OS program can replace VT2 to study rotational ductility demand along the wall because of its capability of considering flexural nonlinearity behaviours. Therefore, the OS model taken from the case n = 15 was used for the case n = 20 in this study. Figure 4-8 indicates that there is a possibility of a second plastic hinge formation in the upper part of the four walls as designed (current design case). In Figure 4-8d, the rotational ductility demand is even larger at the wall mid-height than at the base for a tall wall with large γ_w. The same four walls were redesigned by

increasing the bending moment demand above the plastic hinge by the ratio of the factored moment resistance (M_r) to the factored moment (M_f), both calculated at the top of the plastic hinge region, as prescribed in clause 21.6.2.2 (c) of CSA 23.3-04 for ductile walls (proposed design case). Examples of such amplified bending moment distributions are illustrated in Figure 4-1b. As shown in Figure 4-8, plastic hinges are not expected in the upper part of the wall when adopting this design approach.

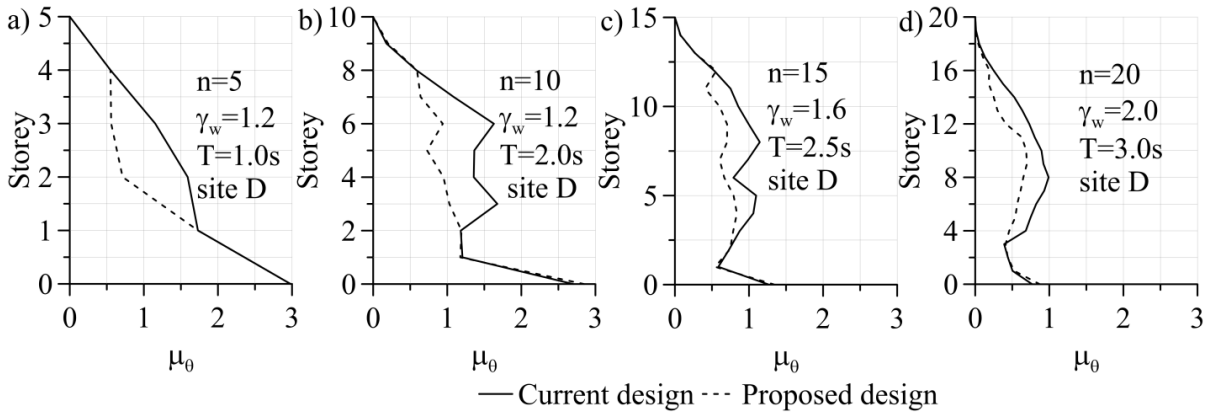

Figure 4-8 : Mean rotational ductility demand over wall height for: (a) 5-storey; (b) 10-storey; (c) 15-storey; and (d) 20-storey.

4.6 Design Recommendations

Drawing on the results and observations, the following recommendations are proposed for the seismic design of MD RC shear walls subjected to ENA ground motions:

4.6.1 Base shear amplification factor

The base shear demands for MD shear walls under ENA earthquakes do not appear to be influenced by the axial loading or number of storeys and appear to be only slightly influenced by site class, base overstrength factor, and fundamental period. As discussed, for MD walls, it is preferable to include flexural overstrength and fundamental period effects in a base shear factor Ω_v applied to the base shear V_d obtained from the NBCC analysis procedure. The results presented in Figures. 4-6 and 4-7 are plotted in detail in Figure 4-9a. Based on these data, the following empirical expression can be used to determine Ω_v:

$$\begin{cases} \Omega_v = 1.6 + 0.7(\gamma_w - 1) + 0.2(T - 0.5), \text{ if } 0.5 \le T \le 1.5 \\ \Omega_v = 1.8 + 0.7(\gamma_w - 1) - 0.1(T - 1.5), \text{ if } 1.5 < T \le 3.5 \end{cases} \quad (4.12)$$

The Ω_V predictions from Eq. (4.12) are compared to the values obtained from NTHA in Figure 4-9b. The mean value and coefficient of variation (COV) of the ratios between the predictions and the NTHA results are respectively equal to 1.02 and 7%. For simplicity, the two expressions of Eq. (4.12) can be replaced by a conservative value of $\Omega_v = 2.5$. This simplified proposal results in a mean predicted-to-analysis ratio of 1.11, and a COV of 15% (Figure 4-9a).

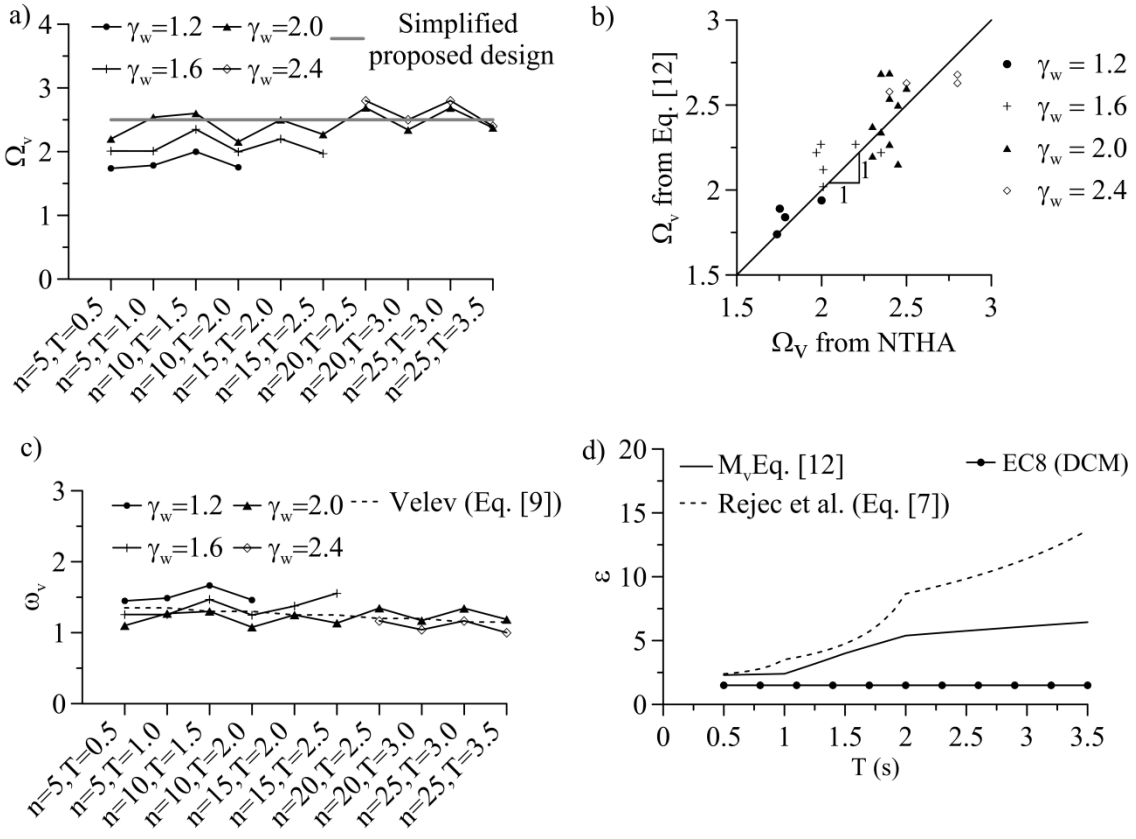

Figure 4-9**:** Mean base shear force demand versus: (a) Simplified proposed base shear factor; (b) proposed base shear factor from Eq. (4.12); (c) dynamic amplification factor ω_v predicted by Eq. (4.9); and (d) shear amplification factor ε predicted by EC 8 and Eq. (4.7).

In this study, the maximum value of Ω_v from NTHA was 2.84 for the 20- and 25-storey buildings with $\gamma_w = 2.4$ (Figure 4-6a). Because higher flexural overstrength level is unlikely for typical MD shear walls, the base shear factor could be limited $\Omega_v = R_d R_o = 2.8$ so that the design base shear

forces would not exceed the elastic forces corresponding to $R_dR_o = 1.0$. However, shear wall structures may exhibit much lower damping than the 5% level assumed in the NBCC design spectrum. In addition, peak base shear typically occurs early during a seismic ground motion, before the wall has sustained extensive cracking and yielding. The wall vibration periods governing the response up to that point may then be close to the values obtained using gross section properties, resulting in higher force demand. For these reasons, it is recommended not to limit Ω_v to $R_dR_o = 2.8$.

Values of the dynamic base shear amplification factor, ω_v, are plotted in Figure 4-9b for all of the structures studied. This factor corresponds to the ratio of the base shear forces from NTHA and the base shear corresponding to the development of nominal moment capacity of the wall system at its plastic hinge location:

$$\omega_v = V_{NL}/(\gamma_w V_d) \tag{4.13}$$

This magnification factor is consistent with the format adopted in CSA 23.3-04. The values of ω_v obtained in this study are plotted in Figure 4-9c. As shown, ω_v is not influenced significantly by the number of storeys or the period. The values are compared to those predicted using Eq. (4.9) proposed by Velev (2007) for MD shear walls under ENA earthquakes. The agreement is very good for $\gamma_w = 2.0$ and 2.4; however, Eq. (4.9) is found to underestimate the base shear dynamic amplification by as much as 25% for cases where $\gamma_w = 1.2$ or 1.6. This indicates that the factor ω_v should also be a function of the wall base overstrength.

Shear magnification as defined in Eq. (4.13) assumes that the maximum base shear is directly proportional to the wall flexural resistance, implying that peak base shear during a ground motion occurs at the same time as the maximum bending moment develops in the base plastic hinge. In reality, numerical and experimental studies (Luu et al., 2013; Ghorbanirenani et al., 2012) have revealed that the maximum base moment is dominated by first mode response, while second and higher mode response contributes the maximum base shear. Thus, both parameters may not be directly correlated and determining design base shears using a base shear factor Ω_v that only partially accounts for flexural overstrength could more closely represent the reality than the approach following the current CSA A23.3, using ω_v, which calls for specifying design base shears corresponding to the development of the nominal moment capacity of the wall.

In Figure 4-9d, the factor ε from Eq. (4.7) is compared to the product $M_v\ \Omega_v$, where Ω_v is obtained from Eq. (4.12), for walls having periods varying from 0.5 s to 3.5 s. In Eq. (4.7), q is set equal to 2.0

(= R_d for MD walls), the term $\gamma_{Rd}\ M_{Rd}/M_{Ed} = 2.0$ (overstrength), $S_e(T_c) = S_a(0.2\text{ s})$ and $S_e(T_1) = S_a(T)$. In Figure 4-9d, the amplification factor of 1.5 as currently specified for DCM in EC8 is also plotted. As shown, both Eq. (4.7) and this study give much higher base shear forces compared to current EC8. The ε factor from Eq. (4.7) is generally more conservative compared to $M_v\ \Omega_v$. The two parameters are similar up to a period of 1.5 s, beyond which base shears from Rejec et al. (2012) would be much higher. The significant overestimation of Rejec et al. (2012) stems from the large ratio of $S(T_c)/S(T_1)$ due to ENA earthquake ground motions that possess a high amount of energy in the short period range.

4.6.2 Shear force envelop

The analysis results indicate that the fundamental period T primarily controls the shear force envelop. Trial and error revealed that a shear force envelop similar to that proposed by Ruttenberg & Nsieri (2006) and Boivin & Paultre (2012b) can accurately reproduce the analysis results when using the parameters α, ξ, and β given by

$$\begin{cases} \alpha = 0.4 \\ 0.6 \le \xi = 1.2 - 0.4T \le 1 \\ \beta = 1/n \end{cases} \qquad (4.14)$$

When applying these expressions, βH and ξH should be adjusted to match the elevation of the next storey. The proposed envelop is compared to analysis results in Figures. 4-6e, f, and g.

4.6.3 Bending moment envelop

As observed, the current design method for MD shear walls may lead to inelastic flexural response in the upper part of the walls. To avoid this behaviour, this study suggests determining the design moments above the base plastic hinge region as currently prescribed in CSA A23.3 for ductile shear walls, i.e., amplifying the bending moments from analysis by the M_r/M_f ratio calculated at the top of the plastic hinge region.

4.7 Summary and Conclusions

This paper presented a parametric study of the seismic response of MD RC shear walls ranging from 5- to 25-storey when subjected to high-frequency-content earthquakes expected in ENA. More specifically, this study examined the base shear and the envelops of shear forces and bending

moments along the wall height and investigated the influences of five parameters: the fundamental period, number of storeys, site class, axial load ratio, and base flexural overstrength. NTHAs were conducted using both fibre (OS program) and finite element (VT2 program) constitutive numerical models that were developed and calibrated using results from shaking table tests performed on large-scale, 9-m-tall, RC MD shear wall specimens. The analyses were conducted with OS models that had been developed using VT2 finite element benchmark solutions for $n \leq 15$ and by VT2 for $n > 15$.

The results indicate that the design provisions in current the NBCC 2010 and CSA 23.3 standards could underestimate from 15% to 70% the base shear force demand and there is possibility of plastic behaviour in the upper part for MD walls. The shear force demand is primarily influenced by the flexural overstrength and fundamental period. A base shear factor Ω_v was proposed to estimate the base shear demand, including these effects, and was applied directly to the base shear V_d obtained from the NBCC analysis procedure. The shear force envelop is mostly influenced by the building fundamental period, and a tri-linear envelop was proposed to determine storey shears above the first level. The study indicated that the design bending moments above the base plastic region must be amplified in the manner prescribed for ductile walls to constrain the plastic deformation at the base of the wall.

Additional studies are needed to determine the force demand on MD shear walls subjected to ground motions expected in WNA. The influence of the wall cross-section type must also be investigated further in future work.

References

Atkinson, G.M. 2009a. Earthquake time histories compatible with the 2005 NBCC uniform hazard spectrum. Can. J. Civ. Eng., **36**(6): 991-1000.

Boivin, Y. et Paultre, P. 2012a. Seismic force demand on ductile RC shear walls subjected to western North American ground motions: Part 2 - New capacity design methods. Can. J. of Civ. Eng., **39**(7), 1157–1170, doi:10.1139/L2012-044

Boivin, Y. et Paultre, P. 2012b. Seismic force demand on ductile RC shear walls subjected to western North American ground motions: Part 1 - Parametric study. Can. J. of Civ. Eng., **39**(7), 1157–1170, doi:10.1139/L2012-043

CEN. 2004. Eurocode (EC) 8 - Design of structures for earthquake resistance Part 1: General rules, seismic actions and rules for buildings, EN 1998-1. European Committee for Standardization (CEN), Brussels, Belgium.

CSA. 2004. Design of concrete structures. CSA standard A23.3-04 (Update No. 3, August 2009), Canadian Standards Association, Toronto, Ont.

Gilles, D. 2011. In situ dynamic properties of building in Montréal determined from ambient vibration records. PhD. Thesis. Department of Civil Engineering and Applied Mechanics, McGill University, Montréal, Que.

Ghorbanirenani, I., Tremblay, R., Léger, P. & Leclerc, M. 2012. Shake table testing of slender RC shear walls subjected to Eastern North America seismic ground motions. ASCE J. Struct. Eng., **138**(12):1515-1529.

Luu, H., Ghorbanirenani, I., Léger, P., & Tremblay, R. (2013). Numerical modelling of slender reinforced concrete shear wall shaking table tests under high-frequency ground motions. Journal of Earthquake Eng., 17, (4), 517–542.

Mazzoni, S., McKenna, F., Scott, M.H., & Fenves, G.L. 2006. OpenSees Command Language Manual. Open System for Earthquake Engineering Simulation (OpenSees), Pacific Earthquake Engineering Research (PEER) Center, University of California, Berkeley, California, USA.

NRCC. 2010. National Building Code of Canada; Part 4: Structural Design. Canadian Commission on Building and Fire Codes, National Research Council of Canada (NRCC), Ottawa, Ont.

NZS. 2006. NZS 3101 Concrete structures standard, Part 1: The design of concrete structures; Part 2: Commentary on the design of concrete structures. Standards New Zealand, Wellington, New Zealand.

Rejec, K., Isaković, T. & Fischinger, M. 2012. Seismic shear force magnification in RC cantilever structural walls, designed according to Eurocode 8. Bull Earthquake Eng, **10**.1007/s10518-011-9294-y. 1-20.

Ruttenberg, A. & Nsieri, E. 2006. The seismic shear demand in ductile cantilever wall systems and the EC8 provisions. Bull Earthquake Eng., **4**, 10.1007/s10518-005-5407-9. 1-21.

Paulay, T., & Priestley, M.J.N. 1992. Seismic design of reinforced concrete and masonry buildings. John Wiley & Sons Inc., New York, United States of America.

Priestley, M.J.N., Calvi, G.M., & Kowalsky, M.J. 2007. Displacement-Based Seismic Design of Structures. Institute Universitariodi Studi Superiori (IUSS) Press, Pavia, Italy.

S-Frame software inc. 2012. S-concrete: Concrete Section Design, version 10.00.40. Maycrest WayRichmond, B.C., Canada.

Velev , N. 2007. Influences of higher modes of vibration on the behaviour of reinforced concrete shear walls structures. Master thesis, École Polytechnique de Montréal, Département des génies civil, géologique et des mines, Montréal, Que.

Wong, P.S., & Vecchio, F.J. 2002. VecTor2 and Formworks User's Manual. Civil Engineering, University of Toronto, Toronto, Ont.

CHAPTER 5 ARTICLE 3: ASSESSING THE SEISMIC PERFORMANCE OF 3D REINFORCED CONCRETE SHEAR WALL BUILDINGS CONSIDERING HIGHER MODE EFFECTS

This chapter presents three alternative design procedures to consider higher mode effects (HMEs) for a moderately ductile reinforced concrete shear wall in eastern North America (ENA). Two procedures are described in (1) the previous (NBCC 1977) and (2) the current (NBCC 2010) versions of the National Building Code of Canada (NBCC). The third design procedure (3) (NBCC2010+) has been developed using nonlinear time history analyses for planar walls using an experimentally validated constitutive shear wall model. These three alternatives were implemented in the designs of an existing 10-storey shear wall building initially braced by two cores. The seismic performance of the building was assessed according to ASCE/SEI 41-13 guidelines ("Seismic Evaluation and Retrofit of Existing Buildings"). The progressive analysis procedures prescribed in ASCE/SEI 41-13 were used, including (a) linear static, (b) linear dynamic, (c) nonlinear static, and (d) nonlinear dynamic analyses. The results indicated that static procedures provided different conclusions relative to building performance compared to dynamic procedures because of significant HMEs in the ENA region. Inputting an effective wall shear stiffness derived from finite element models into fibre element models yields a better base shear force prediction than when using the shear envelop defined in ASCE/SEI 41-13. NBCC 2010+ provided the best seismic performance among the three design alternatives. NBCC 2010+ could constrain plastic deformations at the base of the walls. However, the related shear demand prediction underestimated the base shear force computed from 3D nonlinear dynamic analyses for U-shaped shear walls by approximately 70%. The shear force envelop in the upper part of the wall was significantly affected by the irregular mass distribution but not by the effect of interactions between different walls. The content of this chapter corresponds to the article with title “assessing the seismic performance of 3D reinforced concrete shear wall buildings considering higher mode effects” submitted to Engineering Structure on 26 February 2014.

5.1 Introduction

The basic seismic design objective is that a building should remain stable and have significant reserve capacity under the extreme earthquake loading condition. This design objective is refined in performance-based design (ASCE/SEI 41-13) by defining the damage threshold to achieve immediate occupancy (IO), life safety (LS), and collapse prevention (CP). The selected LS and CP

performance levels could be achieved with the development of ductile inelastic responses in predefined locations (Paulay & Priestly, 1992). The seismic building codes (NRCC 2010; NZS 2006; CEN 2004) provide detailing requirements and capacity design provisions aimed at controlling the development and stability of these inelastic response mechanisms (i.e., plastic hinges).

In Canada, for RC shear wall structures, the requirements of the National Building Code of Canada (NBCC) 2010 (NRCC 2010) and Canadian Standards Association (CSA) 23.3-04 (CSA 2004) are intended to constrain inelastic deformations in a single plastic hinge formed at the wall base, whereas the upper part of the wall remains in the elastic regime. However, recent numerical studies (Boivin and Paultre, 2012a; Rejec et al., 2012; Rutenberg & Nsieri,2006) demonstrated that current code requirements may underestimate the seismic shear and flexural strength demands and may thus lead to shear failure at the wall base and unintended plastic hinge formation in the upper part of the wall. This underestimation is attributed to the inaccuracy of considering higher mode effects (HMEs) when slender shear wall structures are in the inelastic regime (Powel 2010; Wiebe et al., 2012)

Luu et al. (Luu et al., 2014) conducted an intensive investigation of the seismic responses of thirty-five walls of different heights, overstrength factors, fundamental periods, soil classes, and axial load levels at the base to consider nonlinear HMEs in the seismic design of moderately ductile (MD) planar reinforced concrete (RC) shear walls in eastern North America (ENA). Nonlinear time history analyses (NTHAs) were conducted using constitutive numerical models that were developed and calibrated using results from shaking table tests performed on large-scale, 9-m-tall RC MD shear wall specimens (Luu et al., 2013). Luu et al. (2014) proposed that to consider HMEs in the design of MD RC shear walls, (i) the base shear force must be amplified by a base shear factor Ω_v that depends on the fundamental period T and overstrength factor γ_w (the ratio of the nominal moment resistance to the applied factored moment); (ii) the shear force in the upper part must be designed with a trilinear envelop that depends on the fundamental period T; and (iii) design bending moments in the upper part must be amplified by the ratio between the factor moment resistance, M_r, and factor moment demand, M_f, both of which are calculated at the top of the plastic hinge region. This approach is similar to the approach prescribed for ductile walls in CSA 23.3-04 to constrain the plastic deformation at the base of the wall.

However, the study by Luu et al. (2014) was restricted to isolated and two-dimensional RC shear wall models without considering the cross-sectional torsional effect. The implementation of the proposal of Luu et al. (2014) must be verified in the three-dimensional context of a building because

structural wall responses under EQ loading are different in the context of a real three-dimensional building with irregular structural properties, cross-sectional torsional effects and considering interaction with the other shear walls (Rutenberg & Nsieri, 2006).

This study examined the expected performance of a RC shear wall configuration designed by the proposed approach of Luu et al. (2014) (labelled as "NBCC 2010+") in the context of a real three-dimensional building located in ENA. The performance was compared with two other design alternatives: i) NBCC 2010 and CSA 23.3-04 (labelled as "NBCC 2010") and ii) NBCC 1977 (NRCC, 1977) and CSA 23.3-1973 (CSA, 1973) (labelled as "NBCC 1977").

The design/evaluation analyses were implemented considering a 10-storey existing RC shear wall building located in Montreal, Quebec, Canada, where the building is expected to be subjected to high-predominant-frequency seismic ground motions on the order of 10 Hz. The building was designed according to NBCC 1977 (Figure 5-2a) and contains two central RC cores as the seismic force resisting system (SFRS). Two other designs were implemented: one design following NBCC 2010 and the other design following NBCC 2010+. The designs were implemented to respect the architectural decisions of the existing building designed according to NBCC 1977. The stairway and elevator positions must be maintained at the same location but redesigned according to NBCC 2010 and NBCC 2010+, and additional exterior shear walls are allowed if necessary.

The seismic assessments were conducted using the linear ETABS (CSI 2010) and nonlinear finite (fibre) element PERFORM 3D (CSI, 2013) programs. All linear static, nonlinear static, linear dynamic, and nonlinear dynamic analysis methods were considered. The evaluation procedure and acceptance criteria followed the provisions prescribed in ASCE/SEI 41-13, "Seismic Evaluation and Retrofit of Existing Buildings" (ASCE, 2013).

This paper is organised as follows. First, a literature review of three design alternatives for RC shear walls according to NBCC 1977, NBCC 2010, and NBCC 2010+ is presented. Next, the seismic performance assessments using linear, nonlinear, static, and dynamic analysis procedures for the three design alternatives are conducted and compared with one another. Finally, recommendations for seismic safety assessment procedures for existing structures are formulated, and a suitable design approach for new RC shear wall buildings located in ENA is proposed.

5.2 Different approaches for considering HMEs in RC shear wall analysis and design

During severe earthquakes, a ductile RC shear wall must exhibit inelastic flexural behaviour in a predefined location at the wall base, while the shear response must remain elastic (Paulay & Priestly, 1992). However, numerical (Luu et al., 2014; Boivin and Paultre, 2012a; Rutenberg and Nsieri, 2006,) and experimental studies (Ghobarirenani et al., 2012) have indicated the potential for the formation of a second hinge in the upper part and shear failure at the base of the wall due to the presence of HMEs when a structure behaves inelastically. Therefore, the control of HMEs to avoid base shear failure and actions against an unintended inelastic response have been progressively proposed for or applied in NBCC and CSA for the design of concrete structures. The following sections present one previous ("NBCC 1977"), one current ("NBCC 2010"), and one proposed ("NBCC 2010+") version of NBCC for MD RC shear wall design considering HMEs on a rational basis.

In NBCC 1977, the seismic design of shear walls was based on a probabilistic seismic zoning map. There was no constraint regarding the use of the equivalent static force procedure (ESFP) for RC shear walls. The minimum lateral seismic force (base shear), V, was given as

$$V_b = ASKIFW \tag{5.1}$$

$$S = 0.5T^{1/3} \leq 1.0 \tag{5.2}$$

$$T = 0.05h_n D^{1/2} \tag{5.3}$$

where A is the horizontal design ground acceleration determined from the location of the structure (its seismic zone), S is the seismic response factor defined in Eq. (5.2), T is the fundamental period of vibration of the building in seconds in the direction under consideration defined in Eq. (5.3), h_n is the height of the structure, and D is the dimension of the building in a direction parallel to the applied forces), K is a coefficient that reflects the material and type of construction, damping, ductility, and/or energy-absorptive capacity of the structure, I is the importance factor, F is the foundation factor, and W is the seismic weight of the structure.

The HMEs on the shear force demand distribution were accounted for through the application of a portion of the lateral force, V, acting as a concentrated force, F_t, at the top of the structure. F_t is defined as

$$F_t = \begin{cases} 0.004V\left(\frac{h_n}{D_s}\right)^2 \le 0.15V & \text{if } \frac{h_n}{D_s} > 3 \\ 0 & \text{if } \frac{h_n}{D_s} \le 3 \end{cases} \quad (5.4)$$

where D_s is the dimension of the lateral force-resisting system acting parallel to the applied forces.

The remaining force resultant, V-F_t, is distributed along the height of the building, including the top level, as follows:

$$F_x = (V_b - F_t)\frac{W_x h_x}{\sum_{i=1}^{n} W_i h_i} \quad (5.5)$$

where "i" and "x" represent levels "i" and "x", respectively.

Regarding the moment distribution considering HMEs, NBCC 1977 specified that the overturning moment, M, at the base of the structure be multiplied by a reduction coefficient, J, where

$$\begin{cases} J = 1 & \text{if } T < 0.5\,s \\ J = 1.1 - 0.2T & \text{if } 0.5\,s \le T \le 1.5\,s \\ J = 0.8 & \text{if } T > 1.5\,s \end{cases} \quad (5.6)$$

The overturning moment M_x at any level x shall be multiplied by J_x, where

$$J_x = J + (1 - J)\left(\frac{h_x}{h_n}\right)^3 \quad (5.7)$$

CSA A23.3-1973 also contains specific seismic design provisions for shear walls. The ductile flexural walls shall be designed in any section for a shear force of

$$V_{uc} = 1.1FV_u \quad (5.8)$$

$$F = M_{uc}/M_u \quad (5.9)$$

where M_{uc} and M_u are the moment capacity of the wall and the moment obtained by elastic analysis and multiplied by the specified ultimate load combination factor, respectively. Both M_{uc} and M_u are calculated at the wall base.

In NBCC 2010, the uniform hazard spectrum (UHS) approach was adopted for seismic design. The modal response spectrum method (MRSM) became the preferred method of analysis and must be used for structures with irregularities.

The minimum lateral earthquake design force, V, at the base of the structure according to the ESFP is:

$$V_b = \frac{S(T)M_v IW}{R_d R_0} \tag{5.10}$$

where S(T) is the design spectral response acceleration, in g, for the fundamental period T divided by g to become unitless; R_d is the ductility-related factor; and R_0 is the overstrength-related factor. R_d=3.5 and R_0=1.5 for a ductile shear wall, whereas R_d=2.0 and R_0=1.4 for a MD shear wall.

In Eq. (5.9), M_v accounts for the HMEs in the base shear in NBCC 2010. M_v is determined from the fundamental period (T), type of structure, and shape of the UHS (ratio between S(0.2) and S(2.0)), as shown in Table 5-1.

The developments leading to parameters M_v, F_t, J, and J_x can be found in the work of Humar & Mahgoub (2003). However, Humar & Mahgoub (2003) used linear modal response spectrum analyses for their study. The results could change significantly when shear wall structures behave nonlinearly, which is accounted by using coefficients R_dR_o>1. Moreover, using Eq. (5.10) following NBCC 2005 (NRCC 2010), which is similar to NBCC 2010, could yield almost a two-fold increase in the predicted base shear force, V, compared to using Eq. (5.1) following NBCC 1977 (Mitchell et al. 2010).

Regarding shear force distribution, NBCC 2010 specified procedures similar to NBCC 1977 to account for HMEs. A portion of the base shear force, F_t, as determined in Eq. (5.11), is assigned to the top of the wall, and the remaining shear force is distributed along the wall according to Eq. (5.5).

$$F_t = \begin{cases} 0 & \text{if } T \le 0.7\,\text{s} \\ 0.07TV_b & \text{if } 0.7\,\text{s} < T \le 3\,\text{s} \\ 0.25V_b & \text{if } T \ge 3.6\,\text{s} \end{cases} \tag{5.11}$$

For the moment envelop considering HMEs, NBCC 2010 prescribes that the base moment and storey level moments, M_x, be adjusted by the overturning moment factors J and J_x, as follows:

$$M_x = J_x \sum_{i=x}^{n} F_x (H - h_x) \tag{5.12}$$

$$\begin{cases} J = 1 & \text{if } h_x \geq 0.6H \\ J = J + (1 - J)\dfrac{h_x}{H} & \text{if } h_x < 0.6H \end{cases} \tag{5.13}$$

In addition to NBCC 2010, CSA-A23.3-04 also contains specific seismic design provisions for shear walls. For ductile shear walls, the factored shear resistance shall not be less than the shear corresponding to the development of the probable moment capacity, M_p, of the wall at its base. M_p is calculated using 1.25 f_y as the probable reinforcing steel yield strength. For MD shear walls, the shear corresponding to the nominal wall base moment capacity, M_n, must be used to determine the design shears. Thus, the design shears are obtained by multiplying the factored shear forces from the analysis by the flexural overstrength factor, $\gamma_w = M_n/M_f$, where M_f is the factored bending moment demand at the base obtained from the analysis.

In CSA A23.3, for ductile shear walls, the bending moment above the plastic hinge region obtained from linear analysis, M_f, is amplified to prevent an inelastic response in the upper part of the walls. The design moment envelop is obtained by multiplying the moment M_f by the ratio of the factored moment resistance, M_r, to the factored moment demand, M_f. Both of these parameters are calculated at the top of the assumed plastic hinge region (elevation H_p in Figure 5-1a). However, no such recommendation is given for design moments for MD shear walls.

Luu et al. (2014) conducted a parametric study using NTHA to quantify nonlinear HMEs for a series of thirty-five 2D MD shear wall prototypes designed according to NBCC 2010 located in Montreal for five different parameters. These parameters are: (1) site classes (C, D, and E), (2) fundamental periods (T; ranging from 0.5 s to 3.5 s), (3) number of storeys (n; varying from 5 to 25), (4) wall flexural base overstrength factors (γ_w; ranging between 1.2 and 2.4), and (5) axial load ratios (the ratio between the base axial load to the product of the concrete compressive strength and the wall base cross sectional area, $P/(A_g f_c')$; ranging from 5% to 13%).

The results of this investigation indicate that the design provisions in NBCC 2010 and CSA 23.3-04 standards could underestimate the base shear force demand by 15% to 70%, and plastic behaviour occurs in the upper part for several MD walls. The shear force demand is primarily influenced by the flexural overstrength and fundamental period. The shear force envelop is largely influenced by the building fundamental period. The study also indicated that the design bending moments above the

base plastic region must be amplified in the manner prescribed for ductile walls to constrain the plastic deformation at the base of the wall.

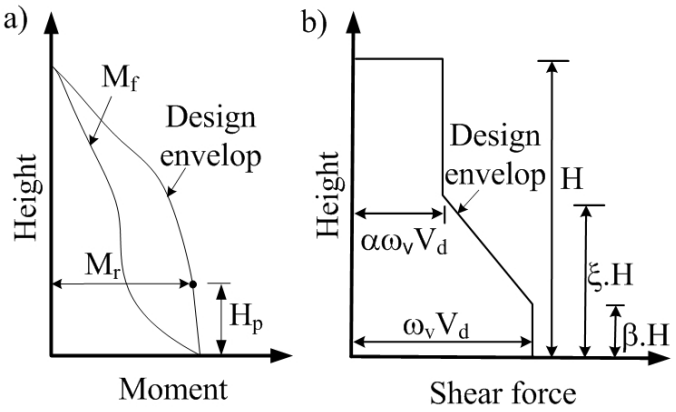

Figure 5-1 : Design envelops of (a) moment and (b) shear.

Table 5-1: Proposed amplification factors, M_v and J, from NBCC 2010

		M_v		J		
S(0.2)/S(2.0)	T[1]≤1.0	T=2.0	T≥4.0	T≤0.5	T=2.0	T≥4.0
<8.0	1.0	1.2	1.6	1.0	0.7	0.5
>8.0	1.0	2.2	3.0	1.0	0.4	0.3

Note: (1) T is in second(s); for the intermediate period, the values of M_v and J are obtained by linear interpolation.

A new design procedure for MD RC shear wall considering HMEs labelled as NBCC 2010+ was proposed. Following NBCC 2010+, the following steps shall be implemented when designing a MD RC shear wall:

a) Determine the number of storeys (n), fundamental period (T), and site class.

b) Perform a MRSA and ESFP according to NBCC 2010 to obtain the shear demand (V_f) and moment demand (M_f).

c) Apply the base shear factor (Ω_v), Eq. (5.14) to V_f to obtain the design base shear V_d. Clause 21.7.3.4.1 of CSA-A23.3-04, which states that the design shear corresponds to the development of the nominal moment capacity of the wall system, need not be applied.

$$\begin{cases} \Omega_v = 1.6+0.7(\gamma_w - 1)+0.2(T-0.5), \text{ if } 0.5 \le T \le 1.5 \\ \Omega_v = 1.8+0.7(\gamma_w - 1)-0.1(T-1.5), \text{ if } 1.5 < T \le 3.5 \end{cases} \quad (5.14)$$

d) Construct the trilinear design shear envelop, as shown in Figure 5-1b, with the parameters α, ξ, and β given by

$$\begin{cases} \alpha = 0.4 \\ 0.6 \le \xi = 1.2 - 0.4T \le 1 \\ \beta = 1/n \end{cases} \tag{5.15}$$

When applying these expressions, βH and ξH should be adjusted to match the elevation of the next storey.

e) Construct the moment envelop for the elastic part of the wall by applying the ratio of the factored moment resistance (M_r) to the factored moment (M_f), both of which are calculated at the top of the plastic hinge region (Figure 5-1a).

f) Design the steel reinforcement for flexure and shear.

5.3 Building studied

The building selected for study is located in Montreal, Quebec, Canada. The building is a typical residential building using flat slabs designed according to NBCC 1977 and CSA 23.3-1973 (Figure5-2a). The building is located on a site with class C soil according to NBCC 2010. The SFRS of the existing building includes two RC cores (stairway and elevator) located in the centre of the building (Figure 5-2b). The vertical load-resisting system is made of flat slabs supported by gravity columns and the shear walls. The compressive strength of the concrete is $f_c' = 30$ MPa, with an elastic modulus $E_c = 24{,}650$ MPa. The yielding strength of the steel reinforcement is $f_y = 400$ MPa, with an elastic modulus $E_s = 200{,}000$ MPa. The building consists of one basement (labelled B1), one ground storey (labelled G1), and 8 additional storeys (labelled sequentially from L1 to L8) (Figure 5-2c). The storey heights and typical wall cross sections are shown in Figures. 5-2c and e, respectively. Details of the wall cross sections and vertical and horizontal reinforcements of the existing building are provided in Tables 5-2, 5-3, and 5-4, respectively. Figure 5-2f illustrates the mean acceleration response spectrum of the selected ground motions versus the NBCC 2010 design spectrum for site class C.

Two other designs are implemented in the plan view of this building following the design approaches of NBCC 2010 and NBCC 2010+ for MD RC shear walls. The analysis indicates that it is impossible to meet the NBCC 2010 requirements for drift (2.5%) and shear force with the two existing cores, mainly because of the large irregular torsional effect in the existing building that was originally designed using two-dimensional models without considering the rotational mass. Therefore, four additional shear walls are added to the current plan view, and the thickness of the two cores is increased to 300 mm in two new designs according to NBCC 2010 and NBCC 2010+ (Figure 5-2d). A ductility-related force reduction factor R_d=2.0 and overstrength-related force modification factor R_0=1.4 for MD shear walls are used.

Details of shear wall cross sections with vertical and horizontal reinforcement of two new designs are provided in Tables 5-2, 5-3, and 5-4, respectively. The NBCC 2010+ design generally calls for more reinforcement than the NBCC 2010 design. However, the designs of shear wall 2 are identical for the two new approaches because both are controlled by the minimum steel requirement in CSA 23.3-04.

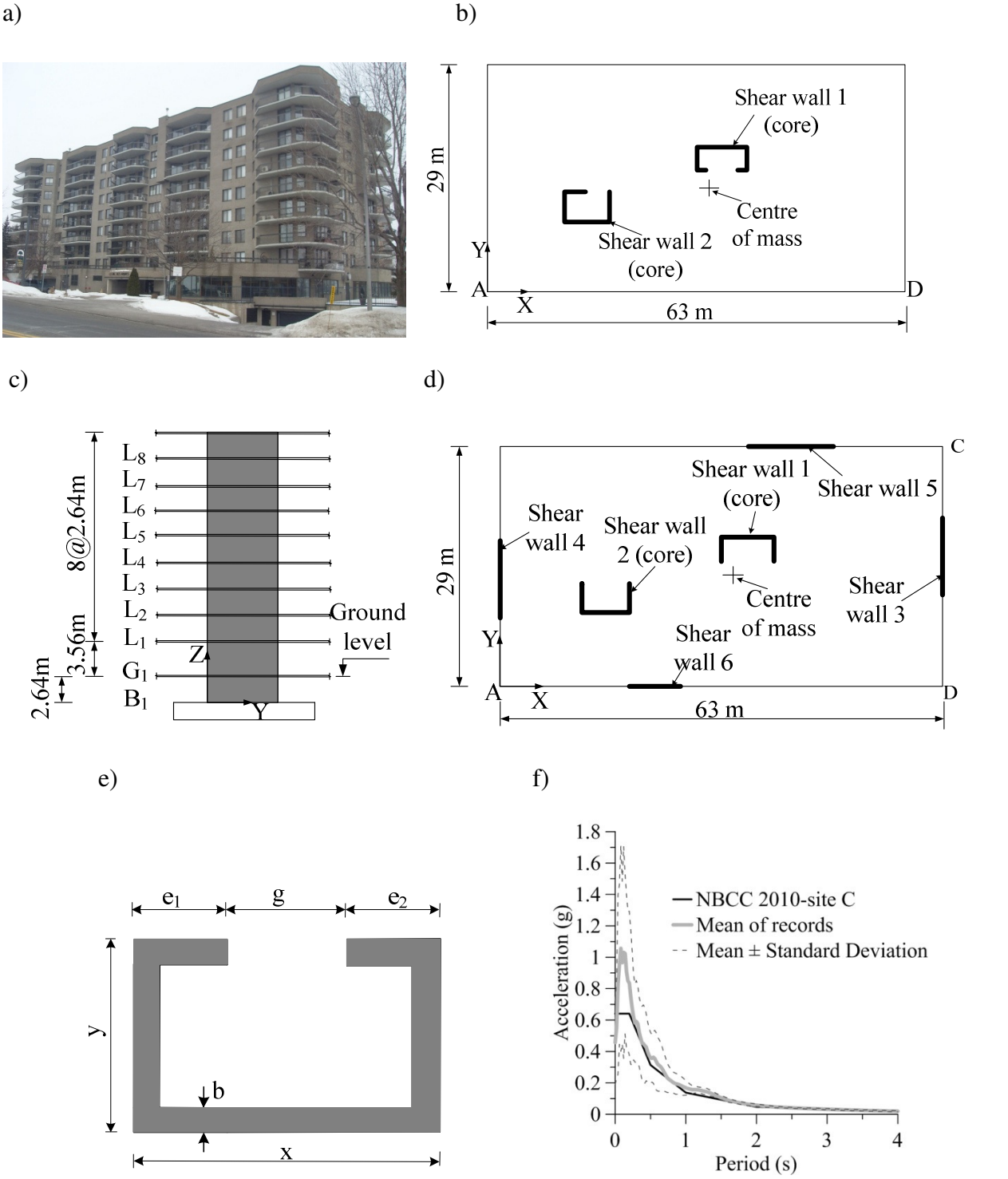

Figure 5-2: Building studied: (a) 10-storey RC building; (b) typical plan view; (c) typical vertical cross section; (d) typical plan view with added shear walls; (e) typical shear wall cross section; (f) mean response spectrum of the selected ground motion records versus NBCC 2010 design spectrum for site class C.

Table 5-2: Shear wall (SW) cross-sectional dimensions (see Figure 5-2e)

	NBC1977		NBCC 2010						NBCC 2010+					
SW[1]	1	2	1	2	3	4	5	6	1	2	3	4	5	6
b	0.25	0.20	0.30	0.30	0.40	0.40	0.40	0.40	0.30	0.30	0.40	0.40	0.40	0.40
x	5.45	4.54	5.45	4.54	-	-	6.0	4.24	5.45	4.54	-	-	6.0	4.24
y	2.55	3.00	2.55	3.0	6.94	6.94	-	-	2.55	3.0	6.94	6.94	-	-
e_1	1.25	0.40	0	0	-	-	-	-	0	0	-	-	-	-
e_2	1.25	3.12	0	0	-	-	-	-	0	0	-	-	-	-
g	3.15	1.02	5.45	4.54	-	-	-	-	5.45	4.54	-	-	-	-

Note: [1]: SW=shear wall N°;Unit is in metres (m).

Table 5-3: Percentage (%) of vertical reinforcement for the three design alternatives

	NBC1977		NBCC 2010						NBCC 2010+					
SW[1] Storey	1	2	1	2	3	4	5	6	1	2	3	4	5	6
B1	3.67	2.39	0.50	0.35	1.14	0.89	0.45	0.26	0.50	0.35	1.14	0.89	0.45	0.26
G	3.67	2.39	0.50	0.35	1.14	0.89	0.45	0.26	0.50	0.35	1.14	0.89	0.45	0.26
L1	2.52	2.39	0.50	0.35	1.14	0.89	0.45	0.26	0.50	0.35	1.14	0.89	0.45	0.26
L2	2.52	1.56	0.46	0.35	0.71	0.57	0.28	0.22	0.51	0.35	1.14	0.71	0.36	0.22
L3	1.96	1.56	0.46	0.35	0.71	0.57	0.28	0.22	0.51	0.35	1.14	0.71	0.36	0.22
L4	2.13	2.16	0.46	0.35	0.71	0.57	0.28	0.22	0.51	0.35	1.14	0.71	0.36	0.22
L5	1.33	1.36	0.46	0.35	0.43	0.35	0.43	0.22	0.50	0.35	0.79	0.57	0.28	0.22
L6	0.73	0.91	0.46	0.35	0.43	0.35	0.43	0.22	0.50	0.35	0.79	0.57	0.28	0.22
L7	0.33	0.55	0.46	0.35	0.43	0.35	0.43	0.22	0.50	0.35	0.60	0.57	0.28	0.22
L8	0.33	0.53	0.46	0.35	0.43	0.35	0.43	0.22	0.50	0.35	0.60	0.57	0.28	0.22

Note: [1]: SW=shear wall N°

Table 5-4: Percentage (%) of horizontal reinforcement at the base of the shear walls (SWs) using three design alternatives.

	NBC1975		NBCC 2010						NBCC 2010+					
SW[1] Storey	1	2	1	2	3	4	5	6	1	2	3	4	5	6
B1-X	0.40	0.33	0.33	0.33	-	-	0.25	0.25	0.33	0.33	-	-	0.41	0.25
B1-Y	0.40	0.33	0.33	0.33	0.36	0.25	-	-	0.33	0.33	0.71	0.56	-	-

Note: [1]: SW=shear wall No

5.4 Structural models of the studied RC shear wall buildings for EQ response analysis

5.4.1 Linear model using ETABS and building dynamic characteristics

Elastic models using ETABS are used to determine the modal properties of the buildings, to conduct linear analyses for the NBCC 2010 and NBCC 2010+ designs, and to evaluate the performances of the three designs (NBCC 1977, NBCC 2010, and NBCC 2010+). The models are developed according to the guidelines provided in NBCC 2010 for the two new designs and ASCE/SEI 41-13 for the evaluation of the three alternative design approaches. In ETABS models, the wall/slab elements, which are shell-type elements with a membrane and bending component, are used for walls and floor slabs. Rigid diaphragm constraints are used. The SFRSs are assumed to be decoupled from the slab for the storey under the ground level. Therefore, the seismic mass of the slab at ground level is not considered in the model. P-delta effects due to the axial compression load in the gravity columns are included by introducing a fictitious column located at the building's centre of mass.

That column carried a total gravity load acting on the gravity columns. However, the rotational degrees of freedom at the slab-column intersections of the fictitious column are released, so the columns do not participate in the building SFRS. The impact of the foundation is not accounted for in this study; instead, a fixed base is used. The analysis model is shown in Figure 5-3a. The main dynamic characteristics of the buildings are shown in Table 5-4.

a) b)

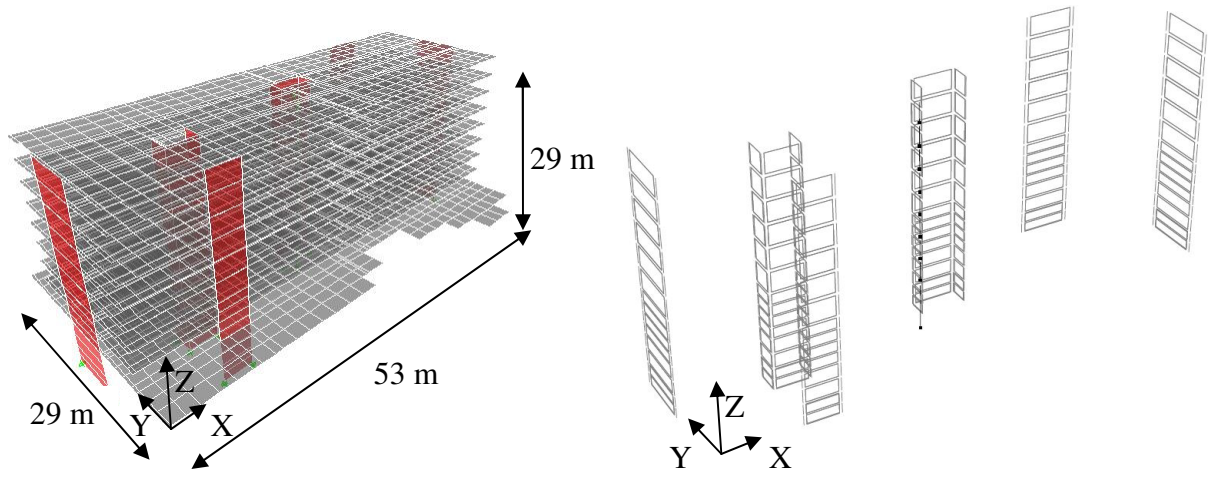

Figure 5-3: Finite element model: (a) linear model using ETABS and (b) nonlinear model using PERFORM 3D.

Table 5-5: Main characteristics of the studied buildings

Parameters		NBCC 1977	NBCC 2010	NBCC 2010+
Modes (using a cracked section I_{cr}=0.7Ig)	Mode 1	4.2* (Torsion)	1.5 (U_Y)	1.5 (U_Y)
	Mode 2	2.0 (U_Y)	1.4 (U_X)	1.4 (U_X)
	Mode 3	1.4 (U_X)	0.9 (Tors.)	0.9 (Torsion)
Plan area (m^2)		29×63	29×63	29×63
Wall area (m^2) (X/Y)		3.50/2.37	8.61/7.16	8.61/7.16
Wall inertia (m^4) (X/Y)		4.77/1.36	12.72/20.24	12.72/20.24

Note: X and Y denote the X and Y directions, respectively; * period (s)

5.4.2 Nonlinear flexural model using PERFORM 3D

In addition to the linear modelling, a nonlinear model of the studied building is built using the PERFORM 3D software (CSI, 2006) (Figure 5-3b). The model uses vertical fibre elements to explicitly model the nonlinear properties of the wall cross section. A complementary study indicated that considering the slab-bending component produced an insignificant effect on building behaviour; thus, the slab-bending component was not considered to contribute to the lateral strength of the building. However, the diaphragm effects are included. The model is fixed at the basement, and the P-delta effects are explicitly included by using the procedure described previously in the ETABS model.

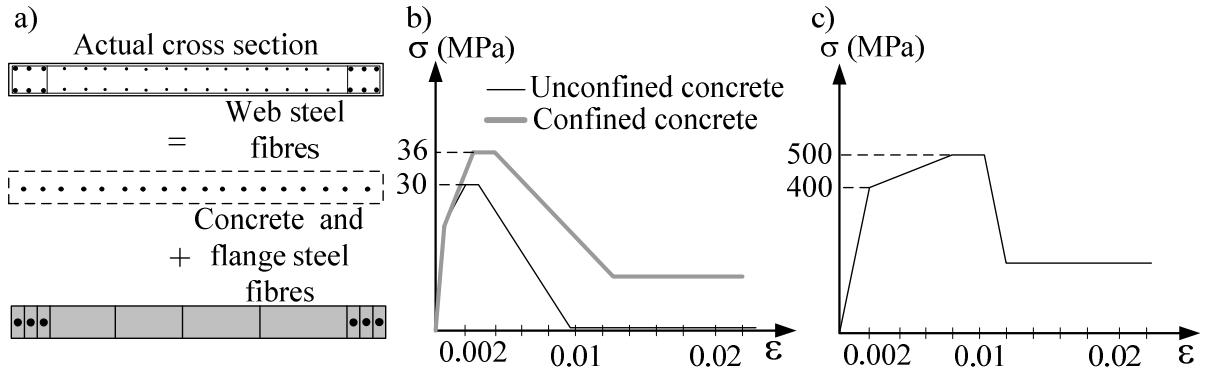

Figure 5-4: Flexural model of the wall: (a) fibre model; (b) uniaxial constitutive model of concrete; and (c) uniaxial constitutive model of steel.

For the modal and dynamic analyses, the masses are concentrated, following a lumped-mass approach at the centroid of every floor. The rotational inertias are also considered. The values of mass, rotational inertia, and location of the centroid of every floor are imported from ETABS models.

The walls are modelled with the PERFORM 3D shear wall compound elements and include inelastic sections over the height of the building. The flexural behaviour of the walls is described by a fibre model, as shown in Figure 5-4a. The behaviour of the concrete is represented by the concrete stress–strain uniaxial constitutive model shown in Figure 5-4b. As suggested by Luu et al. (2013), the tension stiffening effect is excluded in the model by simply neglecting the tensile strength of the concrete. The behaviour of the reinforcement steel is described by the uniaxial trilinear law as shown in Figure 5-4c.

In modelling the wall, one shear wall compound element is used over the storey height, except in the design plastic hinge regions, where two elements are used (Figure 5-3b) to better model the plastic hinge, which is expected to extend approximately one half the length of the wall.

The accuracy of this model for the cores (U-shaped) is verified by comparisons with quasi static cyclic tests of the U-shaped shear walls (Beyer et al., 2008) (Figures. 5-5a and 5-5b). Figures. 5-5b and c indicate the good agreement between the calculated and experimentally obtained hysteresis loops. Regarding the exterior shear walls with rectangular cross sections, the constitutive model is validated by comparison with the shaking table test results of Ghobanirerani et al. (2012) (Figure 5-6a). The results indicate good agreement between the time history top displacements calculated with PERFORM 3D and obtained experimentally (Figure 5-6b).

a)

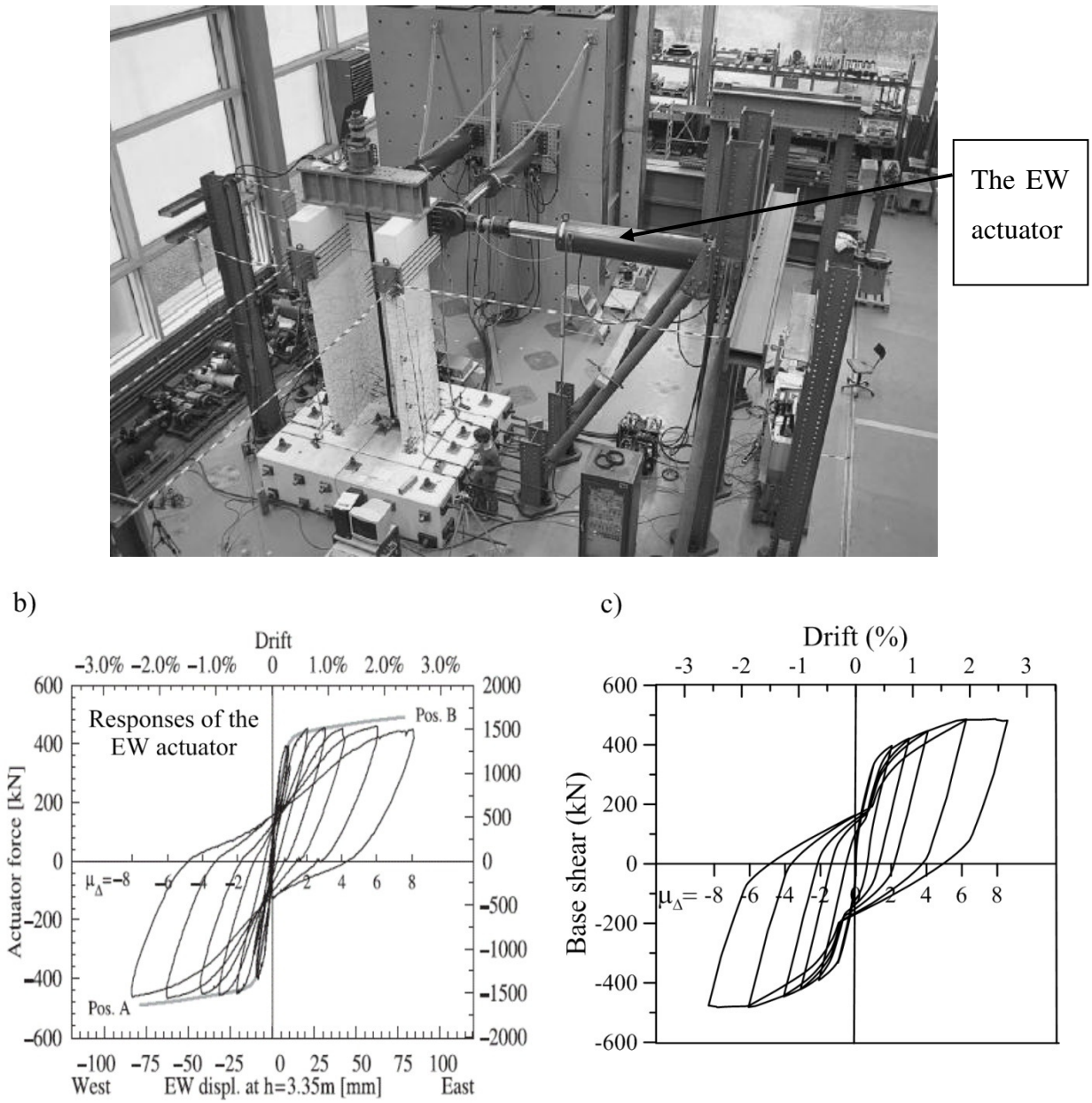

Figure 5-5: Comparison of the experimental and numerical responses of the U-shaped shear wall: a) test set-up of U-shaped shear wall; b) test results (Beyer el al., 2008) reprinted by permission of the publisher (Taylor & Francis Ltd, http://www.tandf.co.uk/journals), and c) PERFORM 3D predictions.

5.4.3 Nonlinear shear model

The shear behaviour of the walls is described by a composite steel–concrete model. Figure 5-7 presents the nonlinear backbone RC shear constitutive envelop and the simple effective elastic shear

models. This nonlinear shear envelop is proposed in ASCE/SEI 41-13 (ASCE 2013), which is used to assess seismic performance of the studied building in section 5.5. In the nonlinear backbone shear curve, the shear stress is elastic until 0.6 of the nominal shear strength is reached, and the deformations at the initiation of yielding and of lateral strength degradation are at shear strains of 0.004 and 0.0075, respectively (Figure 5-7).

Figure 5-6c compares the prediction of PERFORM 3D using this nonlinear shear envelop model with the shaking table test results of Ghobanirenani et al. (2012). When following the ASCE/SEI proposal for shear, PERFORM 3D underestimates the maximum base shear force prediction by approximately 30% because the shear stiffness after concrete cracking is underestimated (Figure 5-7). The use of ASCE/SEI recommendations might yield an unsafe base shear force prediction. Thus, the nonlinear shear backbone curve is applied only in section 5.5 for comparative analyses, which are performed to assess the seismic performance of existing buildings.

Figure 5-7 also provides a simple effective elastic shear model. The effective elastic shear model is used in the method proposed by Luu et al. (2014) for the fibre element program OpenSees (OS) (Mazzoni et al., 2006) as follows:

(a) Run the nonlinear finite element model using Vector (VT) 2 (Wong & Vecchio, 2002) to obtain the maximum shear force envelop.

(b) Calibrate the effective elastic shear in the fibre model until the shear force magnitude and distribution envelop along the building height are close to the corresponding shear force envelop predicted by VT2.

a)

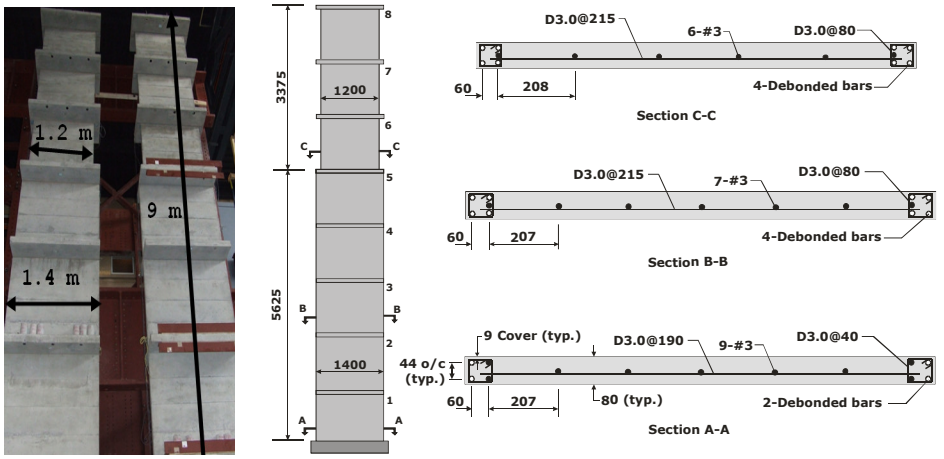

b)

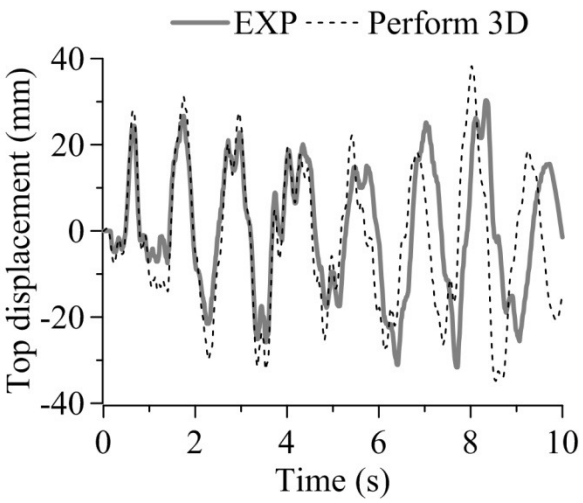

c)

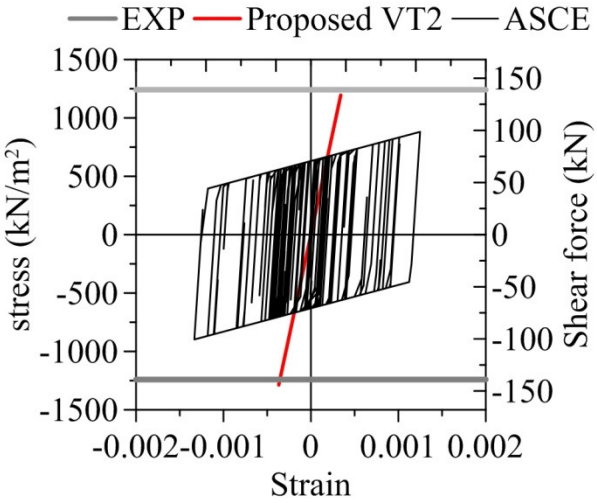

Figure 5-6: Comparison of the experimental and numerical responses of the rectangular-shaped shear wall: a) Shaking table tested wall; Comparisons between the experiments and PERFORM 3D for b) time history top displacement and c) base shear.

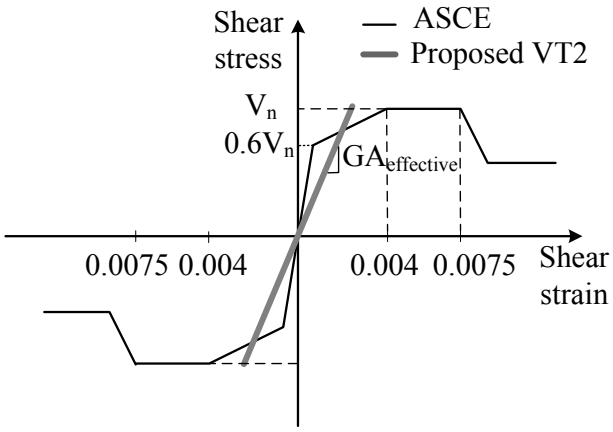

Figure 5-7: RC stress-strain shear model of the walls.

The method suggested by Luu et al. (2014) for the PERFORM 3D model is validated in Figure 5-6c by comparison with the shaking table test data of Ghobanirenani et al. (2012). The maximum base shear of the PERFORM 3D prediction is close to the experimental data (146 kN vs. 140 kN). In this PERFORM 3D model, the effective elastic shear stiffness was selected as 25% for the 1st storey and 5% for the 5th, 6th, and 7th storeys as suggested for OS models in Luu et al. (2013). Therefore, the proposed effective shear stiffness for the OS models for a set of full-scale buildings with the number of storeys ranging from 5 to 15 located in ENA on site classes C, D, and E in Luu et al. (2014) can thus be analysed using PERFORM 3D in this study. This application is expected to yield a more realistic maximum base shear prediction than the ASCE/SEI 41- 13 proposal. For 10-storey MD shear walls located in class C soil subjected to ENA EQ, as in this case study, Luu et al. (2014) suggested using an effective shear stiffness of 60% gross value for the first storey and a 30% gross value for the 5th, 6th, and 7th storeys. These values are selected in this study for the PERFORM 3D model to assess the performance of the NBCC 2010+ design approach in section 5.6.

5.5 Seismic performance assessment of the building

5.5.1 Overview of ASCE/41-13 guidelines

The building was assessed according to the following guidelines provided in ASCE/SEI 41-13 (ASCE 2013), a standard published by the American Society of Civil Engineers to provide guidance for design professionals to determine whether an existing building can adequately resist seismic forces. The standard provides three performance levels to identify potential deficiencies in seismic designs:

(a) Immediate Occupancy (IO): the building remains safe to occupy, and any repair is minor.

(b) Life Safety (LS): the building may experience extensive damage to structural and nonstructural components. Repairs may be required before the building can be reoccupied, and repair may be deemed economically impractical. The risk of the building to life safety by meeting this target building performance level is low.

(c) Collapse Prevention (CP): the building may pose a significant hazard to life safety due to failure of a nonstructural component. However, the building itself does not collapse. Loss of life may be avoided (ASCE, 2013).

In Canada, buildings are designed according to the Canadian building codes subjected to an earthquake that has a 2% probability of exceedance over 50 years. The target performance level of the building is LS. In this study, the building is adequate and safe if the design procedure provides a LS seismic performance.

To assess a shear wall according to ASCE/SEI 41-13, we must first determine whether the inelastic deformation of walls is governed by flexure or shear under lateral loading. The identification of each category depends on the relative strength of the wall resisting mechanisms (flexural and shear strengths). Therefore, one normally identifies whether the wall is controlled by flexure or shear by applying a uniform or inverted triangular lateral load distribution to a wall. Next, the internal shear force at the nominal flexural strength is calculated. The wall is considered to be controlled by shear if this value is greater than the shear strength of the component and controlled by flexure if the shear at nominal flexural strength is less than the shear strength of the component.

However, other studies (Luu et al., 2013; Ghobanirerani et al., 2012; Boivin & Paultre, 2012; Ruttenberg & Nsieri, 2006) have found that the seismically induced load distribution in a shear wall under EQ loading can vary significantly. A higher ratio between shear and flexural demands may occur at the base than for the ESFP with an inverted triangle or uniform load pattern, and thus, the shear wall could fail in shear prior to flexure. This consideration is particularly important when there is an irregularity in the torsion, as in the NBCC 1977 design. Therefore, an additional check is added to evaluate whether the response of the individual wall is controlled by shear or flexure. The linear time history dynamic analysis using PERFORM 3D is conducted instead of using a uniform lateral load distribution in this study. This analysis indicates that the two cores designed according to NBCC

1977 are controlled by shear instead of by flexure, as occurs when using uniform or triangular load patterns.

In addition, the studies of Ghobanirenani et al. (2012) & Pugh (2012) indicate that shear wall failure is not observed until 1.1 V_n, where V_n is calculated based on ACI 318-12 (ACI, 2012). Thus, the shear at nominal moment strength is calculated & then compared to 1.1 V_n in this study. The wall is controlled by flexure if the shear at nominal strength is less than 1.1 of the component's shear strength.

After identifying that the inelastic response of the shear wall is controlled by shear or flexure, we shall decide whether the considered action (shear or moment) is controlled by deformation or force. ASCE/SEI 41-13 specifies that moment and shear are normally controlled by deformation. However, the guidelines also prescribe that shear action shall be considered as force-controlled if the shear wall behaviour is controlled by shear and the axial load ratio at the base is equal to or more than 15% (Table 10-20 in ASCE (2013)), the case of the design according to NBCC 1977 in this study.

ASCE/SEI 41-13 provides different analysis procedures for assessing an existing building. The assessment can be performed using one or more of the following analysis types: i) linear static procedure (LSP), ii) linear dynamic procedure (LDP), iii) nonlinear static procedure (NSP), or iv) nonlinear dynamic procedure (NDP). All of the above analyses were considered in this study.

For linear analysis, the assessment is conducted by comparing demand-to-capacity ratios (DCRs) of the considered action in the component, called "m-factors", for deformation-controlled actions and "J-factors" for force-controlled actions. In this study, the two considered actions for a shear wall are moment and shear. The factor m is dependent on the axial load ratio and average shear stress and is provided in ASCE/SEI 41-13 for a shear wall controlled by either shear or flexure. The factor J is intended to account for the contribution of additional components (gravity columns) and is dependent on the level of seismicity, the target performance level, and whether actions introduced by adjacent components are expected to remain elastic. In this study, J is equal to 1.0 for the IO performance level and 2.0 for all other performance levels.

For nonlinear analysis, according to ASCE/SEI 41-13, the rotation (θ) over the plastic hinge region at the base of the member is used for a wall with an inelastic response governed by flexure. The acceptable deformation limits for shear walls deforming inelastically under a lateral load and

controlled by shear are presented in terms of the lateral drift ratios. The drift for multi-storey shear walls is the storey drift.

Component strengths are classified as nominal strength, Q_{CL}, for force-controlled actions and expected strength, Q_{CE}, for deformation-controlled actions (ASCE, 2013). In this study, the expected strength for RC components is equal to 1.25 times the nominal strength.

5.5.2 Seismic assessment of the studied building: results

This section presents the results of the seismic assessment of buildings designed according to NBCC 1977, NBCC 2010, and NBCC 2010+. The knowledge factor, which accounts for the uncertainty of the build data for the existing building, is set to 0.7 (ASCE 2013). The results for the linear analysis are expressed in terms of the DCR (m for deformation-controlled actions and J for force-controlled actions). In the nonlinear analysis, for deformation-controlled actions to be consistent with linear analysis results, the plastic rotations (rotation demand subtracted from yielding rotation determined according to ASCE/SEI 41-13) are normalised and presented by the Γ_θ factor (Eq. (5.16)), and IO becomes the reference performance level for comparison purposes.

$$\Gamma_\theta = m_{IO} \frac{\theta_d - \theta_y}{\theta_{IO}} \tag{5.16}$$

where θ_d is the rotational demand from the nonlinear analysis, θ_y is a yielding rotation determined according to ASCE/SEI 41-13, θ_{IO} is the acceptable plastic hinge rotation at the IO performance level, and m_{IO} is acceptable DCR at the IO performance level from linear analysis and is equal to 2.0 in this study (ASCE, 2013).

The rotational demand is determined as the equivalent plastic hinge rotations and thus necessitates the use of curvatures from multiple integration points along the fibre element. The plastic hinge length of one half the wall length is used herein, as prescribed in ASCE/SEI 41-13.

For force-controlled actions, a procedure similar to that used for deformation-controlled actions is applied to the normalised demand drift as follows:

$$\Gamma_\delta = m_{IO} \frac{\delta_d}{\delta_{IO}} \tag{5.17}$$

where δ_d is the drift demand from nonlinear analysis and δ_{IO} is the acceptable drift at the IO performance level.

5.5.3 Linear static procedure (LSP ETABS)

Figure 5-8 presents the DCR for both shear and moment from the LSP analyses using ETABS. Details of the ETABS model are provided in section 5.4.1. The analysis is conducted with only the NBCC 2010 and NBCC 2010+ designs. The design according to NBCC 1977 is not considered with this analysis type because the building is highly irregular in torsion and thus cannot be assessed using static analysis (ASCE, 2013).

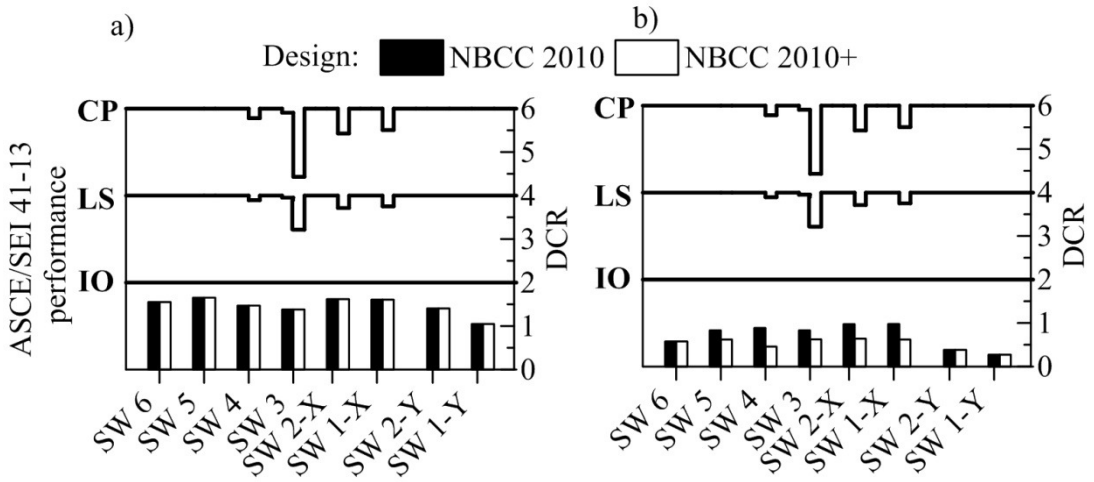

Note: Performance limits depend on axial load ratio and maximum average shear stress in the member, and thus vary with different SW and designs.

Figure 5-8: Linear static pushover analysis: a) moment and b) shear.

The input lateral load is determined using the fundamental period obtained from modal analysis using the ETABS model with effective wall stiffness suggested by ASCE/SEI 41-13. The torsional effect is considered by amplifying the force and displacement with the maximum displacement multiplier η of the building, which is equal to 1.26 and 1.05 for the Y and X directions, respectively.

The results indicate that the wall performance of the two designs is similar in flexure (Figure 5-8a) and different in shear (Figure 5-8b) demands because for the base, NBCC 2010+ requires only base shear forces to be amplified by the factor Ω_v. Therefore, the seismic performance of NBCC 2010+ is superior to NBCC 2010 for shear but similar for moment. However, both design approaches provide

seismic performance within the IO criterion under the considered NBCC 2010 earthquake UHS intensity.

5.5.4 Linear dynamic procedure (LDP ETABS)

Figure 5-9 presents the DCRs for both shear and moment from the LDP using ETABS. The linear dynamic analyses are conducted using MRSM for a 5% modal damping with the NBCC 2010 design spectra for site class C, as shown in Figure 2f. The ETABS model is the same as the model used in the LSP. The concurrent multidirectional seismic effect was considered by applying an additional 30% EQ loading perpendicular to the considered direction, as prescribed in ASCE/SEI 41-13.

For moment, the results indicate that the three design alternatives provide wall seismic performance within the IO and LS performance levels. There is no difference between NBCC 2010 and NBCC 2010+. NBCC 1977 exhibits the best performance among the three design procedures because of a significantly larger amount of vertical reinforcement at the base of the wall in the NBCC 1977 design compared to the NBCC 2010 and NBCC 2010+ designs (Table 5-3).

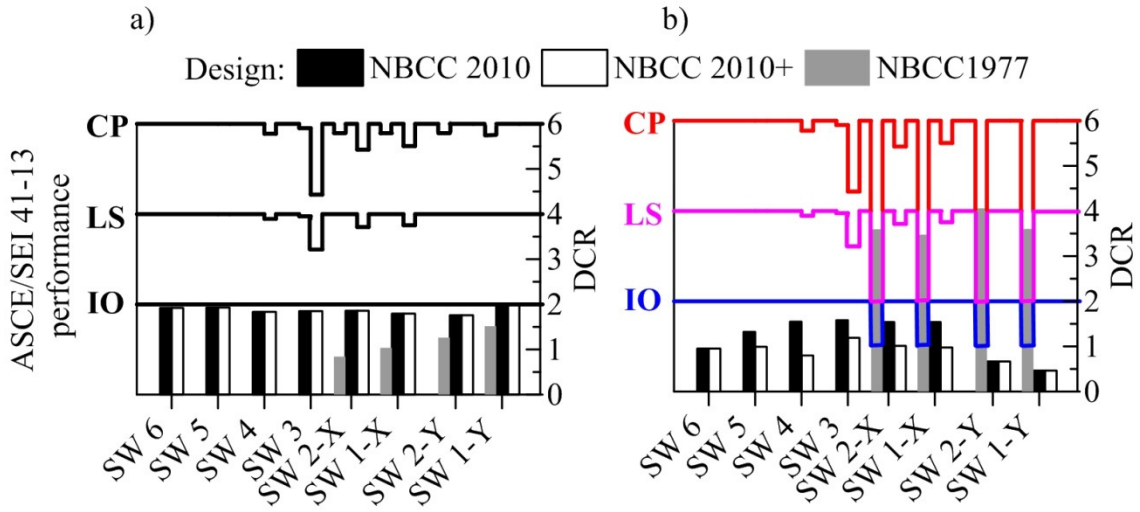

Note: Performance limits depend on axial load ratio and maximum average shear stress in the member, and thus vary with different SW and designs.

Figure 5-9: Linear dynamic analysis: a) moment and b) shear.

Similar to NSP, the seismic performance of the shear response of NBCC 2010+ is better than NBCC 2010, and both designs provide performance of the walls within the IO level. However, the walls designed according to NBCC 1977 are predicted to collapse in shear, and the existing as-built building is seismically unsafe.

5.5.5 Nonlinear static procedure (NSP PERFORM 3D)

Figure 5-10a presents the seismic performance assessment from NSP using PERFORM 3D. The PERFORM 3D model is described in section 5.4.2. Similar to LSP, the NSP is only conducted with the designs NBCC 2010 and NBCC 2010+.

NSP is conducted using the lateral load pattern from the first mode shape. The ASCE/SEI 41-13 ‘‘Coefficient Method’’ was used to determine the Target Drift (TD) ratio, then the TD was amplified by the maximum displacement multiplier η of the building to consider torsion as in LSP. TD ratios along the Y and X directions are 0.37% and 0.31%, respectively. The low TD ratios that have been obtained are due to the high-frequency content ground motions in the ENA region, which result in a low spectrum acceleration S_a corresponding to effective fundamental periods (T=1.4 s and 1.5 s for the X and Y directions, respectively) of the building.

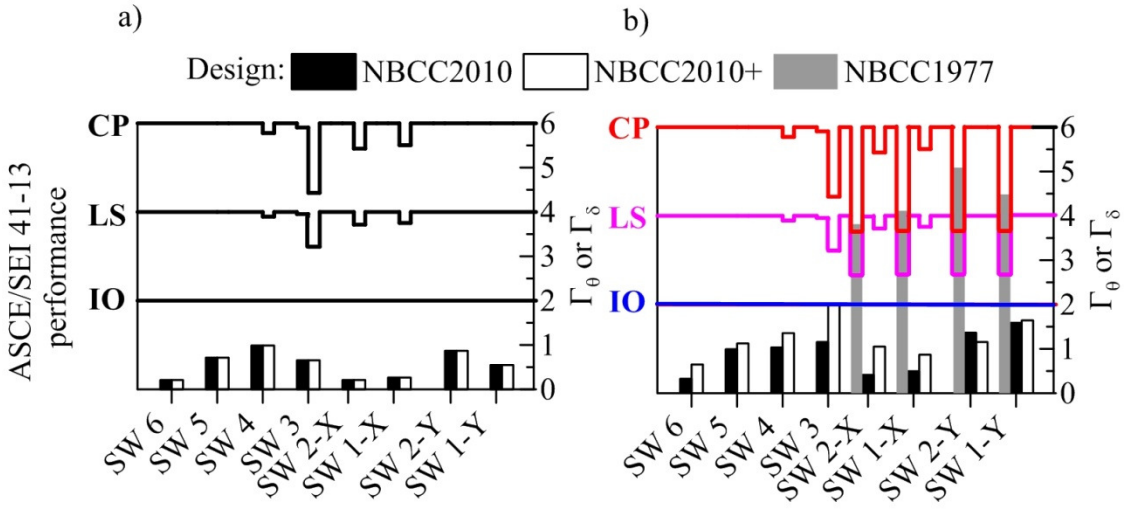

Note: Performance limits depend on axial load ratio and maximum average shear stress in the member, and thus vary with different SW and designs.

Figure 5-10: Nonlinear analyses: a) static pushover and b) dynamic.

For the PERFORM 3D NSP, the results for the overall shear wall performances are within the IO performance range. The performance objectives of building design LS for both NBCC 2010 and NBCC 2010+ are satisfied.

The difference between the performance of the NBCC 2010 and NBCC 2010+ designs is negligible because both designs have similar vertical reinforcement details at the base of the shear walls and because the HMEs are not captured in the NSP.

5.5.6 Nonlinear dynamic procedure (NDP PERFORM 3D)

The final assessment is the NDP using PERFORM 3D. The modelling parameters are the same as for the NSP. The damping is represented by a Rayleigh model, and the assumed damping ratio is 2.0%, assigned in modes 1 and 2. A set of 12 ground motions corresponding to the building site is used, consistent with those used for the previous studies (Luu et al., 2014). The 12 ground motions were selected and scaled according to the recommendations from Atkinson (2009). The mean acceleration response spectrum of the scaled ground motions is presented in Figure 5-2f. The mean spectrum is in good agreement with the design spectrum prescribed in NBCC 2010 used for the LSP, LDP, and NSP (Figure 5-2f). The mean results for each offset of 12 ground motions are used to evaluate the seismic performance of the three alternative designs.

For the walls designed according to NBCC 1977, which have inelastic responses controlled by shear, the factor Γ_δ presented in Figure 5-10b is the product of δ_d/δ_{IO} with m_{IO}. This adjustment is made to obtain more accurate comparisons between walls that have inelastic response controlled by flexure and shear in Figure 5-10b. The concurrent multidirectional seismic effects are considered by a similar method as in the LDP.

The results of the NDP indicate that the building designed according to NBCC 2010 is within the IO performance level. NBCC 2010+ provides a worse seismic performance than NBCC 2010 because the inelastic behaviour is constrained in the plastic hinge regions at the base for NBCC 2010+. However, inelastic behaviour could occur in the upper part of the wall in addition to the plastic hinge at the base, as for NBCC 2010 (NRCC 2010). The plastic hinge occurring in the upper part reduces the inelastic demand at the base of the wall (Panagiotou & Restrepo, 2009).

According to the acceptance criteria prescribed in ASCE/SEI 41-13, the NBCC 1977 design, which contains only two cores, exhibits unsafe performance. Both cores are predicted to collapse by shear failure. The performance of the building designed according to NBCC 2010+ and NBCC 2010 are generally within the IO level and slightly meet the LS level (SW3 for NBCC 2010+).

However, the acceptance criteria of ASCE/SEI 41-13 for shear walls were defined using experimental data from test specimens designed with heavily detailed reinforcement (Wallace, 2006)These acceptance criteria might be unsafe for the walls located in ENA; this region is moderately seismic, and thus, walls located in this region are typically designed with light detail reinforcement. Some recent studies have proposed considerably lower acceptance criteria for shear

walls (Kazaz et al., 2012; Gonzales & López-Almansa, 2012). Using the values proposed in Kazaz et al. (2012) and Gonzales & López-Almansa (2012) would yield different conclusions for the seismic performance level achieved by the building design under consideration.

5.6 Comparisons of different assessment procedures and recommendations

The static procedures (LSP and NSP) produced seismic DCRs larger than the seismic DCRs computed from the dynamic procedures (LDP and NDP) (Table 5-6). This result is not consistent with the expectations from the previous studies (Gonzales & López-Almansa, 2012; Hagen, 2012). in which the static procedure was more conservative than the dynamic procedure. In those studies, the static procedure was more conservative because of the high-predominant-frequency ground motions (on the order of 10 Hz), which are typical in the ENA region of this building. The HMEs on walls located in ENA are more important than the consideration in ASCE/SEI 41-13. In this building, in the Y direction of the NBCC 2010 design, the contribution to the base shear force demand from the LDP of the second mode is 1.13 times the LDP of the first mode. Thus, the static procedure (LSP or NSP) should be used with caution for buildings in which HMEs are expected to be important. We therefore recommend the use of linear dynamic analysis (LDP or NDP) for building shear walls located in ENA.

Table 5-6: Ratios of seismic performance between static and dynamic procedures

Design		SW	1	2	3	4	5	6
NBCC 2010	Linear	X	1.6[1]/1.8[2]	1.6/1.9	-	-	1.7/1.9	1.6/1.9
		Y	1.0/2.0	1.4/1.8	1.4/1.9	1.5/1.8	-	-
	Nonlinear	X	0.3/0.5	0.2/0.4	-	-	0.7/1.0	0.2/0.3
		Y	0.6/1.6	0.9/1.4	0.7/1.2	1.0/1.0	-	-
NBCC 2010+	Linear	X	1.6/1.8	1.6/1.9	-	-	1.7/1.9	1.6/1.9
		Y	1.0/2.0	1.4/1.8	1.4/1.9	1.5/1.8	-	-
	Nonlinear	X	0.3/0.9	0.2/1.1	-	-	0.7/1.1	0.2/0.7
		Y	0.6/1.6	0.9/1.2	0.7/2.0	1.0/1.4	-	-

Note: The ratio between Γ_θ, Γ_δ, or m obtained from static[1] and dynamic[2] analyses; for linear analyses, the maximum m value between shear and moment actions is selected.

Significantly better performance is obtained for the nonlinear procedures than for the linear procedures. The comparisons between the Γ_θ or Γ_δ results obtained from linear (LSP and LDP) and nonlinear (NSP and NDP) analyses are shown in Table 5-7. The difference is more considerable for static analyses than dynamic analyses. The average of the ratios between the results obtained using the linear and nonlinear analyses for the static and dynamic procedures are 3.6 and 2.1, respectively. However, use of both analysis types provides a similar seismic performance level according to the ASCE/SEI 41-13 acceptance criteria.

Table 5-7: Ratios of seismic performance between the linear and nonlinear procedures

Design		SW	1	2	3	4	5	6
NBCC 2010	Static	X	1.6[1]/0.3[2]	1.6/0.2	-	-	1.7/0.7	1.6/0.2
		Y	1.0/0.6	1.4/0.9	1.4/0.7	1.5/1.0	-	-
	Dynamic	X	1.8/0.5	1.9/0.4	-	-	1.9/1.0	1.9/0.3
		Y	2.0/1.6	1.8/1.4	1.9/1.2	1.8/1.0	-	-
NBCC 2010+	Static	X	1.6/0.3	1.6/0.2	-	-	1.7/0.7	1.6/0.2
		Y	1.0/0.6	1.4/0.9	1.4/0.7	1.5/1.0	-	-
	Dynamic	X	1.8/0.9	1.9/1.1	-	-	1.9/1.1	1.9/0.7
		Y	2.0/1.6	1.8/1.2	1.9/2.0	1.8/1.4	-	-
NBCC 1977	Dynamic	X	3.4/2.0	3.6/1.9	-	-	-	-
		Y	3.6/2.2	4.0/2.5	-	-	-	-

Note: The ratio between Γ_θ, Γ_δ, and m obtained from linear[1] and nonlinear[2] analyses; for linear analysis, the maximum m value between shear and moment actions is selected.

5.7 Comparisons between different design approaches and recommendations

Comparisons between the seismic performances of the buildings designed according to the three approaches (NBCC 1977, NBCC 2010, and NBCC 2010+ using ASCE/SEI 41-13) were provided in section 5.5. However, some recent studies (Luu et al., 2014; Ghobarirerani et al., 2012; Boivin and Paultre, 2012a; Rutenberg and Nsieri, 2006) found that current code requirements may underestimate the seismic shear at the base and flexural strength demands in the middle height and may thus lead to shear failure at the wall base and unintended plastic hinge formation in the upper part of the wall.

These deficiencies of the code are not addressed in the evaluation based on the ASCE/SEI 41-13 guidelines. These guidelines assume that shear walls follow well-established capacity design principles, which do not, consider nonlinear HMEs on structural wall responses correctly in their code implementation (Luu et al., 2014; Ghobarirerani et al., 2012; Boivin and Paultre, 2012a; Rutenberg and Nsieri, 2006). Thus, additional analyses must be conducted to evaluate the seismic performance of different design procedures.

The PERFORM 3D model used in ASCE/SEI 41-13 seismic performance assessment in section 5.5 was employed. However, as noted in section 5.4.3, using the nonlinear backbone hysteresis shear envelop suggested by ASCE/SEI 41-13 underestimated the seismic shear force demand at base of the shear wall by 30% compared to the shaking table tests (Ghobanirerani et al., 2012). Therefore, the simple effective shear stiffness suggested by Luu et al. (2014) was selected for the PERFORM 3D model in this section.

Tables 5-8 and 5-9 present the seismic performances of the three design approaches in both shear and flexure predictions. The base shear ratio, ψ_v, was obtained from the analyses of the three design alternatives subjected to the 100% EQ in the weak Y direction and 30% EQ in the X direction. The parameter ψ_v is defined as the ratio V_{NL}/V_d of the base shear forces from NTHA, V_{NL}, to the design base shear, V_d. In NBCC 2010, V_d is the product of the base shear obtained from MRSA calibrated using the ESFP and the overstrength factor, γ_w. For NBCC 2010+, V_d is the product of the base shear obtained from MRSA calibrated using the ESFP and the base shear factor Ω_v (Eq. (5.14)). Except for NBCC 1977, there is no information on shear force design values; thus, ψ_v is defined as the ratio of the base shear forces from NTHA, V_{NL}, to the design base shear resistance, V_r. The rotational ductility, μ_θ, in Table 5-9 is defined as the ratio of the rotational demand, θ_{max}, and the yielding rotation, θ_y, at the storey considered. The yield rotation, θ_y, was evaluated using the method presented by Paulay and Priestly (1992) and used in previous studies by Ghorbanirenani et al. (2012), Luu et al. (2013), and Luu et al. (2014).

Regarding the two rectangular cross sections for SW3 and SW4, the results indicate that there are deficiencies in the shear (at base) (Table 5-8) and moment (in the upper part) (Table 5-9) design resistances for NBCC 2010. NBCC 2010 underestimates these resistances because the nonlinear HMEs are not considered accurately (Luu et al., 2014). NBCC 2010+ provides a slight overestimate

(15%) of the seismic base shear force demand (Table 5-8) and eliminates the possibility of nonlinearity in the upper part of the walls (Table 5-9).

For SW1 and SW2, which have complex U-shaped cross sections, NBCC 1977 results in significant deficiencies for both the shear and moment responses. NBCC 1977 underestimates these responses because the rotational seismic mass is not considered in the two-dimensional models used for the design. For these shear walls, if the two-dimensional wall behaviour is considered (no cross-sectional torsional effect), NBCC 2010 and NBCC 2010+ could eliminate the possibility of a nonlinear response in the upper part of the wall but overestimate the base shear force designs. These methods overestimate the base shear force due to the extremely high overstrength factor in these U-shaped shear walls ($\gamma_{w=}$3.5 and 2.8 for SW1 and SW2, respectively). Therefore, the walls still behave in the elastic regime.

Table 5-8 also presents the base shear ratio, ψ_v, for the U-shaped sections while considering the cross-sectional torsional effect (3D shear wall section) of the shear wall for NBCC 2010+. These ψ_v values illustrate significant deficiencies of approximately 20% and 70% in shear force designs at the base for SW1 and SW2, respectively, because the nonlinearity in torsion is not accurately considered by R_dR_0 in the MRSA.

Table 5-8: Base shear ratio, ψ_v, for three alternative designs

Shear wall	NBCC 1977	NBCC 2010	NBCC 2010+	Eq. (5.14)	γ_w
SW1	2.611				-
SW2	3.021				-
SW1-Y w/o torsion	-	0.65	0.84	3.55	3.5
SW1-Y with torsion	-	-	1.20		
SW2-Y w/o torsion	-	0.84	0.88	2.85	2.5
SW2-Y with torsion	-	-	1.72		
SW3-Y	-	1.42	1.15	1.91	1.2
SW4-Y	-	1.51	1.15	1.91	1.2

Note: [1]In these cases, the value ψ_v is the ratio between V_{NL} and V_r.

Table 5-9: Storey rotational ductility, μ_θ, of different design approaches

Shear wall		NBCC 1977	NBCC 2010	NBCC 2010+
SW1-Y	B1	1.67	1.10	1.07
	L5	1.12	0.98	0.41
	L6	-	0.62	0.38
SW2-Y	B1	2.41	1.36	1.22
	L5	1.67	0.97	0.59
	L6	-	0.68	0.48
SW3-Y	B1		2.12	2.12
	L5		1.66	0.59
	L6		0.92	0.32
SW4-Y	B1		2.01	2.16
	L5		1.41	0.55
	L6		0.89	0.36

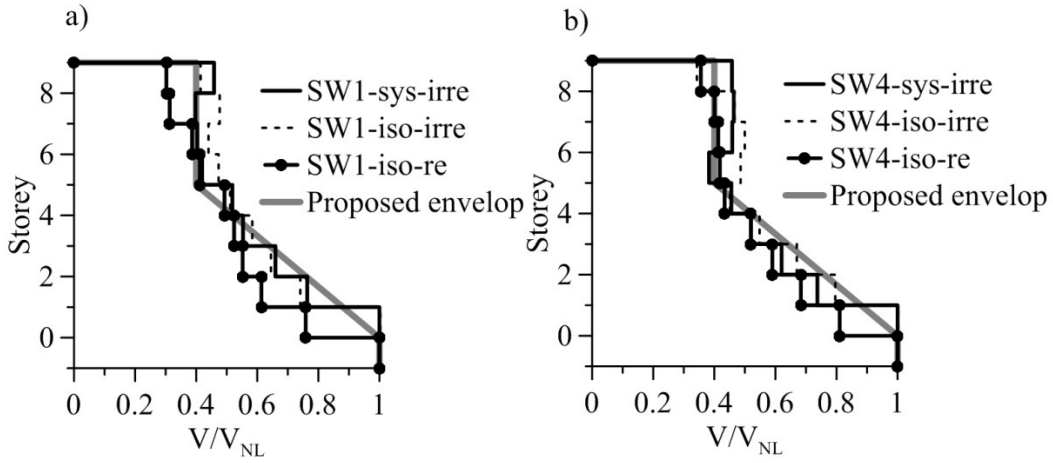

Figure 5-11: Shear envelops of: a) SW1 without considering cross-sectional torsion and b) SW4.

Figure 5-11 presents the shear force envelop for the U-shaped wall cross section for SW1 and the rectangular wall cross section SW4 in the Y direction, considering that all walls behave in an interacting structural system (SW1-sys and SW4-sys) compared to the shear force envelop proposed in (Luu et al., 2014) (Eq. 5-15). The storey shear force demands V along the wall height were normalised relative to the base shear from NTHA, V_{NL}. Figure 5-11 illustrates that the model proposed by Luu et al. (2014) underestimates the shear force demands at the ground level and in the upper part (level 8 for SW1 and levels 6-8 for SW4). The maximum underestimation is approximately 20% for level 7 of SW4.

However, Eq. (5.15) was based on a parametric investigation of isolated walls with regularly distributed mass along the wall height (Luu et al., 2014). The shear envelop of the wall in this study is different, as it has an irregular mass distribution (no consideration of seismic mass at the ground level) and considers the interactions between different walls (Ruttenberg and Nsieri, 2006). Therefore, two more models were developed and analysed. Both are isolated shear wall models, as developed in Luu et al. (2014), but one has a regular mass distribution (SW-iso-re) and the other has an irregular mass distribution (SW-iso-irre).

Figure 5-11 presents the results of the two additional analyses. The proposed design according to Eq. (5.15) still underestimates the shear force design in the upper part and at the ground level for the case of isolated shear walls with an irregular mass distribution for both the rectangular (SW4-iso-irre) and U-shaped cross sections (SW1-isi-irre). The underestimation is most critical at level 6 of SW4, at which the proposed design is approximately 30% less than the NTHA prediction. However, the proposed design using Eq. (5.15) can adequately reproduce the analysis results of the SW-iso-re case (Figure5-11). The maximum underestimation proposed by Eq. (5.15) compared with the analysis of SW-iso-re is at level 6 of SW4 at approximately 5%, illustrating that the underestimation of Eq. (5.15) for NTHA of the complete building design according to NBCC 2010+ in this study arises mainly from the irregular mass distribution at the ground level.

5.8 Summary and conclusions

This paper presented three alternative design approaches (NBCC 1977, NBCC 2010, and NBCC 2010+) to consider HMEs for MD RC ENA. Two approaches are based on previous and current versions of the NBCC (NBCC 1977 and NBCC 2010); the third approach is a proposed design based on NTHA using an experimentally validated constitutive shear wall model (NBCC 2010+). An existing building designed according to NBCC 1977 was selected and redesigned according to NBCC 2010 and NBCC 2010+. The seismic performance of the shear walls designed according to these three design approaches was assessed in the context of a real building. The assessment followed the acceptance criteria prescribed in ASEC/SEI 41-13 (ASCE, 2013). All procedures prescribed in ASCE/SEI 41-13, including the LSP, LDP, NSP, and NDP, were used to assess the building. The NDP was also conducted on a two-dimensional experimentally validated concrete shear wall constitutive model with a linear effective shear stiffness in addition to the constitutive model with the nonlinear backbone shear hysteresis envelop proposed by ASCE/SEI 41-13. Recommendations for

the appropriate analysis procedure (for assessment) and design approach for MD RC shear wall buildings located in ENA were made. The following conclusions and recommendations can be drawn from this study:

1) Using the acceptance criteria of ASCE/SEI 41-13, the designs according to NBCC 2010 and NBCC 2010 + achieve both the IO and LS performance levels, whereas the design according to NBCC 1977 is unsafe because of shear failure.

2) The results indicated that static procedures provided different conclusions related to building performances compared to dynamic procedures because of the significant HMEs in the ENA region.

3) Using the proposed effective shear stiffness based on finite element analysis to calibrate the fibre element model for two-dimensional shear walls more accurately predicts the base shear force than using the nonlinear shear hysteresis envelop of ASCE/SEI 41-13, which underestimated the shear force demand prediction by 30% compared to the experimental data obtained from shaking table tests of the shear wall specimens with a rectangular cross section.

4) In the context of a real building and considering the interaction between shear walls, an irregular mass distribution, and different shear wall section types, the NBCC 2010+ approach proposed by Luu et al. (2014) for the MD RC shear wall constrains the plastic deformation at the base of the wall.

5) The NBCC 2010+ design underestimated the base shear force demands computed from nonlinear dynamic analysis for U-shaped shear walls by approximately 70%. This underestimation occurs because the nonlinear cross-sectional torsional behaviour of the U-shaped shear wall design is not accurately modelled using the linear modal response spectrum analysis.

6) The shear force envelop in the upper part was affected by the irregular mass distribution but not by the interactions with other walls in a building system.

Additional studies are needed to determine appropriate acceptance criteria for walls located in ENA. The influence of wall cross section type, cross-sectional torsion, and irregular mass distribution must also be investigated further in future work.

References

ACI (2012). Building Code Requirements for Structural Concrete and Commentary. American Concrete Institute. ACI 318-08 .Farmington Hills, Mississippi. 2009. Print.

ASCE 41-13 (2007). Seismic rehabilitation of existing buildings. ASCE/SEI 41-06, American Society of Civil Engineers, Reston, VA, 2007.

Atkinson, G.M. (2009). EQ time histories compatible with the 2005 NBCC uniform hazard spectrum. Can. J. Civ. Eng., 36(6), 991-1000.

Beyer, K., Dazio, A., & Priestley, M. J. N. (2008). Quasi-static cyclic tests of two U-shaped reinforced concrete walls, in Journal of Earthquake Engineering, 12(7),1023-1053.

Boivin, Y. & Paultre, P. (2012a). Seismic force demand on ductile RC shear walls subjected to western North American ground motions: Part 2 - New capacity design methods. Can. J. of Civ. Eng., 39(7), 1157–1170, doi:10.1139/L2012-044

Boivin, Y. & Paultre, P. (2012b). Seismic force demand on ductile RC shear walls subjected to western North American ground motions: Part 1 - Parametric study. Can. J. of Civ. Eng., 39(7), 1157–1170, doi:10.1139/L2012-043

CEN. (2004). Eurocode (EC) 8 - Design of structures for earthquake resistance Part 1: General rules, seismic actions and rules for buildings, EN 1998-1. European Committee for Standardization (CEN), Brussels, Belgium.

CSI (2010). ETABS 3D: Structural Analysis Program,V 9.7.2 Computer and Structures, Inc., Berkeley, CA

CSI (2012). PERFORM-3D. Nonlinear Analysis and Performance Assessment for 3D Structures, V.5.0.1. Computers and Structures, Inc., Berkeley, CA, 2007.

CSA (2004). Design of concrete structures. CSA standard A23.3-04 (Update No. 3, August 2009), Canadian Standards Association, Toronto, Ont.

Kazaz, I., Gülkan, P. , & Yakut, A. (2012). Performance limits for structural walls: An analytical perspective. Engineering structure. 43, 105–119

Ghorbanirenani, I., Tremblay, R., Léger P., & Leclerc M. (2012). Shake table testing of slender RC shear walls subjected to Eastern North America seismic ground motions. ASCE J. Struct. Eng., 138(12):1515-1529.

Gonzales , H., & López-Almansa, F. (2012). Seismic performance of buildings with thin RC bearing walls. Engineering Structures. 34 (2012) 244–258

Humar, J. & Mahgoub, M. (2003). Determination of seismic design forces by equivalent static load method. Canadian Journal of Civil Engineering. 30:287-307.

Luu, H., Léger, P. & Tremblay, R. (2014). Seismic demand of moderately ductile reinforced concrete shear walls subjected to high-frequency ground motions. Can. J. Civ. Eng., 41(2) 125-135.

Luu, H., Ghorbanirenani, I., Léger, P. &Tremblay, R. (2013). Numerical modelling of slender reinforced concrete shear wall shaking table tests under high-frequency ground motions. Journal of Earthquake Eng., 17, (4), 517-542.

Mazzoni, S., McKenna, F., Scott, M.H., & Fenves, G.L. 2006. OpenSees Command Language Manual. Open System for Earthquake Engineering Simulation (OpenSees), Pacific Earthquake Engineering Research (PEER) Center, University of California, Berkeley, California, USA.

Mitchell D et al. Evolution of seismic design provisions in the National Building code of Canada. Can J of Civ Eng 2010; 37:1157-1170.

NRCC. (2010). National Building Code of Canada; Part 4: Structural Design. Canadian Commission on Building and Fire Codes, National Research Council of Canada (NRCC), Ottawa, Ont.

NZS. (2006). NZS 3101 Concrete structures standard, Part 1: The design of concrete structures; Part 2: Commentary on the design of concrete structures. Standards New Zealand, Wellington, New Zealand.

Ruttenberg, A. & Nsieri, E. (2006). The seismic shear demand in ductile cantilever wall systems and the EC8 provisions. Bull Earthquake Eng., **4**, 10.1007/s10518-005-5407-9. 1-21.

Panagiotou, M. & Restrepo, J. I. (2009). Dual-plastic hinge design concept for reducing higher mode effects on high-rise cantilever wall buildings, Earthquake Engineering & Structural Dynamics 38(12), 1359–1380.

Paulay, T., & Priestley, M.J.N. (1992). Seismic design of reinforced concrete and masonry buildings. John Wiley & Sons Inc., New York, United States of America.

Priestley, M.J.N., Calvi, G.M., & Kowalsky, M.J. (2007). Displacement-Based Seismic Design of Structures. Institute Universitariodi Studi Superiori (IUSS) Press, Pavia, Italy.

Pugh. J. (2012). Numerical Simulation of Walls and Capacity Design Recommendations for Walled Buildings. PhD thesis, University of Washington.

Wallace J.W., Massone L.M., & Orakcal K. (2006). St. Joseph's Healthcare Orange, California, SPC-2 Upgrade: E/W Wing Component Test Program – Final Report. Report No. UCLA SEERL 2006/1, University of California, Los Angeles, California, U.S.A.

Wong, P.S., & Vecchio, F.J. (2002). VecTor2 and Formworks User's Manual. Civil Engineering, University of Toronto, Toronto, Ont.

CHAPTER 6 GENERAL DISCUSSIONS

Recent numerical studies (Boivin & Paultre, 2012a; Rejec et al., 2012; Panagiotou & Restrepo, 2009; Velev, 2007; Panneton et al., 2006; Rutenberg & Nsieri, 2006; Priestley & Amaris, 2002) have investigated seismic responses of RC shear walls. These studies demonstrated that current code requirements may underestimate the seismic shear at the base and the flexural strength demands along the height, which may lead to shear failure at base of walls and unintended plastic hinge formation in the upper part of walls.

The underestimation of the demand in codes is attributed to inaccuracies in considering higher mode effects (HMEs) when structural walls behave in the nonlinear range. Researchers (Boivin and Paultre, 2012a; Rejec et al., 2012; Panagiotou & Restrepo, 2009; Velev, 2007; Rutenberg & Nsieri, 2006; Priestley & Amaris, 2002) have proposed methods to consider HMEs. However, most of the proposed methods were based on numerical studies using simple finite element structural analysis program with lumped plasticity beam elements or finite element models with assumptions that have not been validated using dynamic tests. Therefore, an investigation of HMEs using experimentally verified constitutive shear wall models is necessary.

Because of low and moderate seismic demand in eastern North America (ENA), moderately ductile (MD) RC shear wall designed with a ductility-related force modification R_d = 2.0 is the typical design technique for the seismic force resisting system of mid-rise buildings from 5 to 25 storeys. This type of structure is expected to sustain reduced inelastic demand compared to the other, ductile RC shear wall category (R_d = 3.5), described in the National Building Code of Canada (NRCC 2010). Therefore, the seismic responses of type MD shear walls can be significantly different from that of ductile shear wall, especially when the walls are subjected to ground motions exhibiting high predominant frequencies (approximately 10 Hz), typical in ENA. Consequently, there is a need to study this category of RC shear walls subjected to ENA earthquakes.

A shear wall research project is being conducted on this topic at Polytechnique Montreal, Canada to propose a practicable method for designs of RC shear walls located in ENA considering HMEs. In the first stage of the project, Ghorbanirenani et al. (2012) performed shake table tests on two 9 m high scale specimens of slender 8-storey moderately ductile RC shear walls. The walls had been designed in accordance with the 2005 National Building Code of Canada (NRCC, 2005) and the CSA A23.3-04 standard (CSA, 2004) and were subjected to ENA earthquake ground motions in the tests.

The test results indicated that shear and flexural demands from the code were underestimated. Inelastic behaviour was observed at the base and in the sixth storey of the specimens.

This thesis is the second stage of the shear wall project, and it focuses on numerical investigations of HMEs on structural wall responses. The thesis consists of three main phases, and each phases corresponds to one (available online or submitted) journal paper (Figure 6-1). The first two phases were restricted to isolated and two-dimensional RC shear wall models without considering cross-sectional torsional effect and interactions with other shear walls. On the other hand, the last phase investigated three-dimensional RC shear walls in the context of a real building.

The phase was to develop new constitutive shear wall models using both fibre (OpenSees-OS) (Mazzoni et al., 2006) and finite (Vector 2-VT2) (Wong & Vecchio, 2002) element programs. VT2 is based on 2D plane stress finite element theory and includes most of the phenomenological features present in RC members. OS is a multi-fibre beam element program based on the Euler-Bernoulli theory. OS represents an attractive alternative to finite element modelling (VT2), because it can reproduce the dominant inelastic flexural response anticipated in shear walls. The models were validated by large specimen shaking table test of Ghorbanirenani et al. (2012).

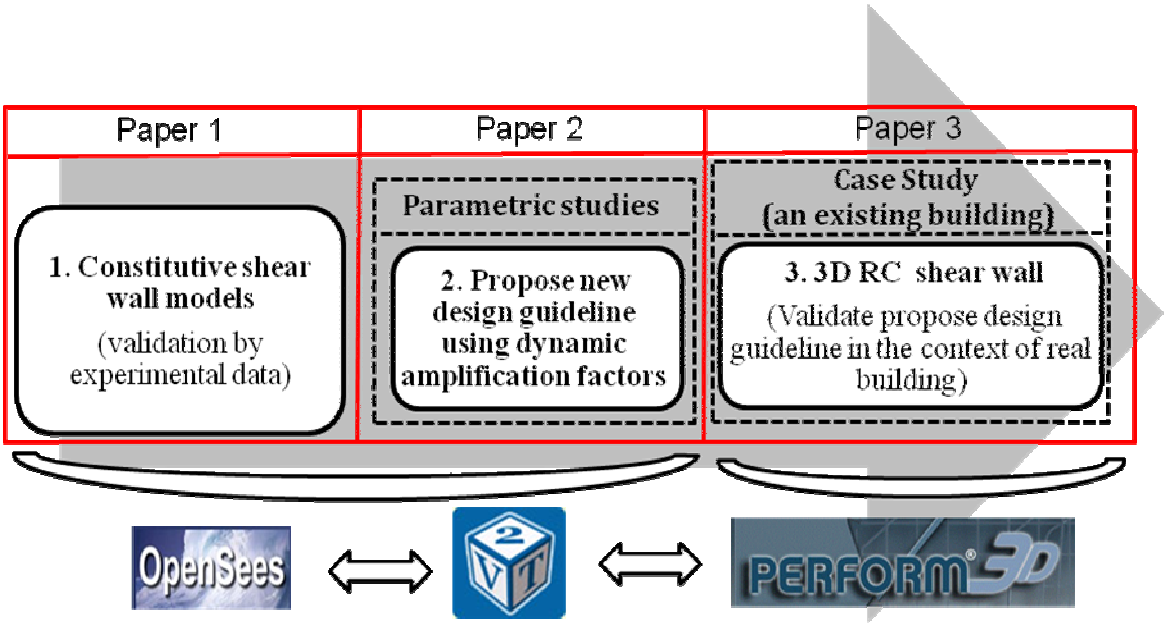

Figure 6-1: Overview of the thesis

In the second step, the proposed OS and VT2 modelling procedures in phase 1 were used as representative constitutive shear wall models to investigate HMEs. Parametric studies involving

nonlinear time history analyses (NTHA) using OS and VT2 were performed to investigate the influence of design parameters on the higher mode amplification effects and related seismic force demand. This research focused on type MD RC shear walls. The results were used to propose a new capacity design method considering higher mode amplification effects for type MD RC shear wall located in ENA. The method determined capacity design envelops for flexural and shear strength demands to achieve a single plastic hinge response at the wall base.

The last phase of this thesis was to validate the proposed design approach in phase 2 in the context of three-dimensional building with irregular structural properties, cross-sectional torsional effect, and considering interaction with the other shear walls. The validation was implemented by assessing the expected performance of RC shear wall configurations designed by proposed approach in phase 2 for a real building located in ENA. The results showed that the proposed design procedure in phase 2 could constrain plastic deformation at the base of the walls and predict accurately base shear force demand for plane (rectangular cross section shear walls). However, the related prediction underestimated approximately by 70% base shear force demand for U shape shear walls. Moreover, shear force envelop in the upper part of the wall was significantly affected by irregular mass distribution, but not by the effect of interactions with other walls.

There are limits in the capacity design method proposed for moderately ductile reinforced concrete shear walls in this thesis. First, the method was developed using the predictions of numerical studies of RC shear walls. The procedure to develop the shear wall constitutive shear wall models was validated by large scale specimen shaking table tests. However, the tests were isolated scaled planar cantilever shear walls with limitations because of laboratory conditions. The real responses of full scale shear walls with the presence of significant axial loads at wall bases and other structural elements such as slabs, beams, and columns are expected to be modified. In addition, there are significant uncertainties in numerical modelling predictions coming from the characteristics of input ground motions and the viscous damping ratio selected and their modelling. Changes in these parameters could affect the efficiency of proposed capacity design method if it is applied outside of the basic assumptions implemented during its development.

The capacity design proposed herein was based on studies of moderately ductile reinforced concrete shear walls (R_dR_0=2.8) located in eastern North America (ENA). The behaviour of ductile RC shear walls (R_dR_0=5.6) expected to sustain increased inelastic demand compared to moderately ductile shear walls might be different and should be investigated. Because high-frequency motions excite

further higher mode responses, the shear walls subjected to low frequency content western North America (WNA) with dominant frequency around 2Hz might expect smaller higher mode effects than the shear walls subjected to high frequency content ENA with dominant frequency around10Hz. However, the earthquake intensity in WNA that is significantly higher than in ENA could alter the seismic contribution of some higher modes (Priestly et al. 2007). Consequently, shear walls located in WNA also need future investigations on the higher mode effects on structural wall responses.

The seismic performance assessment of the building in the phase 3 of this thesis was conducted according to ASCE/SEI 41-13 guidelines ("Seismic Evaluation and Retrofit of Existing Buildings") (ASCE 2013). According to criteria prescribed in ASCE/SEI 41-13, the shear wall building designed according to the procedure presented in phase 2 (NBCC2010+) is safe, while the shear wall building design according to NBCC 1977 is not adequate. However, the conclusions are based on performance limit criteria from ASCE/SEI 41-13. These limits were proposed using tests with heavily detailed reinforced shear walls subjected to high earthquake intensity typical of western North America. These limits might not be entirely applicable for wall designed under low and moderate ENA earthquakes. These aspects need future investigation to propose adapted performance limit criteria for shear walls located in ENA.

The study of higher mode effects on 3D reinforced concrete shear walls in phase 3 was based on the numerical modelling validated by the cyclic tests of a U shape reinforced concrete shear wall subjected to bi-directional quasi-static cyclic loading available from Beyer et al. (2008). However, the validation did not address the torsional response specifically. Large scale multidirectional tests for U shape shear walls are in need in the future study to calibrate and validate the constitutive models of the U shape reinforced concrete shear walls.

Although there are some limits, this research project has been presented in a logical and consistent manner. It followed an appropriate methodology and series of simple to more complex examples for validation. Major existing problems identified in the literature review of RC shear walls design located in ENA considering higher modes effects were addressed. Possible solutions to resolve the existing problems were proposed. Moreover, the proposed solutions were implemented in a real building project for validation. The limitations of this project presented above are also suggestions for future study of RC shear wall design considering higher mode effects on structural wall responses.

CONCLUSIONS AND RECOMMENDATIONS

This Chapter is to complement, not to repeat, the conclusions in the three papers presented in the thesis (chapters 3, 4, and 5). It therefore focuses on the recommendations for future study on the topic of reinforced concrete shear wall design considering higher mode effects. Readers are invited to first read the conclusions in chapters 3, 4 and 5.

This research project proposed, for NBCC 2010 and CSA 23.3-04, a new capacity design method, considering higher mode effects for regular moderately ductile reinforced shear wall buildings located in eastern North America. The method is to determine capacity design envelops for flexural and shear strength demands to achieve a single base wall plastic hinge response.

The method was proposed using the results of nonlinear time history analysis parametric studies using an experimental validated constitutive shear wall models. The method was also implemented in a real building to validate its feasibility in the context of three-dimensional reinforced concrete shear walls considering cross sectional torsion, irregular mass distribution, and interactions between different shear walls while acting together as the seismic resistant lateral force system. More details of the developments and the applications of the proposed design method were presented in the three journal papers.

This research project has highlighted some issues that need to be investigated in future research projects as follows:

i) This study is restricted to shear walls located in eastern North America region. The extension of proposed design methodology for western North America should be implemented.

ii) This study is restricted to moderately ductile reinforced concrete shear walls (R_dR_0=2.8). The behaviour of ductile reinforced concrete shear walls (R_dR_0=5.6) expected to sustain increased inelastic demand compared to moderately ductile shear walls should be investigated.

iii) The effects of wall cross section type, cross sectional torsion, and irregular mass distribution are significant and need future investigations.

iv) Large scale experimental tests of U shape (and typical 3D cores) reinforced concrete shear walls subjected to multi-directional loadings are in need for future study.

iv) This research assumed that the wall foundations are adequate for transmission of base shears and moments and that they are fixed at their base using NBCC 2010 site foundation factors to represent

soil flexibility. However specific foundation geometry, stiffness, and boundary conditions as well as rigorous soil-structure interactions could affect the formation of the wall plastic hinges. Therefore, the more detailed effects of foundations should be considered in future studies.

REFERENCES

ACI . (2010). ACI-318-08, Building Code Requirements for Structural Concrete (ACI 318-08) and Commentary. American Concrete Institute, Farmington Hills, MI, USA.

ASCE. (2013). Seismic rehabilitation of existing buildings. American Society of Civil Engineers. Ed. Reston, VA: ASCE/SEI 41-13.

ASCE. (2010). Minimum Design Loads for Buildings and Other Structures. American Society of Civil Engineers. Ed. Reston,VA: ASCE/SEI 7-10.

Atkinson, G.M. (2009). Earthquake time histories compatible with the 2005 NBCC uniform hazard spectrum. Can. J. Civ. Eng., 36(6): 991-1000.

Beyer, K., Dazio, A., & Priestley, M. J. N. (2008). Quasi-static cyclic tests of two U-shaped reinforced concrete walls. Journal of Earthquake Eng., 12(7):1023-1053.

Bentz, E. C. (1999). Sectional Analysis of Reinforced Concrete Members. Ph.D. thesis, Department of Civil Engineering, University of Toronto.

Boivin, Y., & Paultre, P. (2012a). Seismic force demand on ductile RC shear walls subjected to western North American ground motions: Part 2 - New capacity design methods. Can. J. of Civ. Eng., 39(7), 1157–1170, doi:10.1139/L2012-044

Boivin, Y., & Paultre, P. (2012b). Seismic force demand on ductile RC shear walls subjected to western North American ground motions: Part 1 - Parametric study. Can. J. of Civ. Eng., 39(7), 1157–1170, doi:10.1139/L2012-043

CEN. (2004). Eurocode 8: Design of structure of earthquake resistance. Part 1 General rules, seismic action and rules for buildings (EN 1998-1*)*. Brussels.

Cheng, F. Y., Mertz, G. E., Sheu, M. S., & Ger, J. F. (1993). Computed versus observed inelastic seismic low-rise RC shear walls. ASCE J. Struct. Eng., 119(11), 3352-3275.

Clough, R. W., & Johnston, S. B. (1966). Effect of stiffness degradation on earthquake ductility requirements. Proceedings of the Japan Earthquake Engineering Symposium, Tokyo, Japan, 195-198.

Coleman, J., & Spacone, E. (2001). Localization issued in force-based frame elements. ASCE J. Struct. Eng., 127(11), 1257–1265.

CSA. (2004). CSA A23.3-04, Design of concrete structures. Canadian Standards Association, Mississauga, ON, Canada.

CSI. (2006). Perform 3D: Nonlinear Analysis and Performance Assessment for 3D Structures. Computer and Structures, Inc., Berkeley, CA

CSI. (2010). ETABS 3D: Structural Analysis Program,V 9.7.2. Computer and Structures, Inc., Berkeley, CA

CSI. (2010). SAP 2000: Structural Analysis Program,V15.1.0/1. Computer and Structures, Inc., Berkeley, CA

Mitchell, D., Paultre, P., Tinawi, R., Saatcioglu, M., Tremblay, R., Elwood, K., Adams, J., & DeVall, R. (2010). Evolution of seismic design provisions in the National building code of Canada. Can. J. Civ. Eng. 37: 1157–1170.

Filiatrault, A., D'Aronco, D., & Tinawi, R. (1994). Seismic shear demand of ductile cantilever walls: a Canadian perspective. Can. J. Civ. Eng., 21(3), 363-376.

Gilles, D. 2011. In situ dynamic properties of building in Montréal determined from ambient vibration records. PhD. Thesis. Department of Civil Engineering and Applied Mechanics, McGill University, Montréal, Que.

Ghorbanirenani, I., Tremblay, R., Léger, P., & Leclerc, M. (2012). Shake Table Testing of Slender RC Shear Walls Subjected to Eastern North America Seismic Ground Motions. ASCE J. Struct. Eng., 138(12), 1515–1529. DOI: 10.1061/(ASCE)ST.1943-541X.0000581

Ghorbanirenani, I., Rallu, A., Tremblay, R., & Léger, P. (2009a). Distribution of Inelastic Demand in Slender R/C Shear Walls Subjected to Eastern North America Ground Motions. ATC-SEI Conference on Improving the Seismic Performance of Existing Buildings and Other Structures, San Francisco, CA, pp. 1-13.

Ghorbanirenani, I., Velev, N., Tremblay, R., Palermo, D., Massicotte, B., & Léger, P. (2009b). Modelling and Testing Influence of Scaling Effects on Inelastic Response of Shear Walls. ACI Structural Journal, 106(3), 358-367.

Gonzales , H., & López-Almansa, F.(2012). Seismic performance of buildings with thin RC bearing walls. Eng. Struct., 34 (2012) 244–258.

Grange, S., Kotronis, P., & Mazars, J. (2009). Numerical modelling of the seismic behaviour of 7-story building: NEES benchmark. Materials and Structure, 42, 10.1617/s11527-008-9462-y. 1433-1442.

Humar, J. & Mahgoub, M. (2003). Determination of seismic design forces by equivalent static load method. Canadian Journal of Civil Engineering. 30:287-307.

Kazaz, I., Gülkan, P., & Yakut, A. (2012). Performance limits for structural walls: An analytical perspective. . Eng. Struct., 43 (2012) 105–119

Kazaz, I., Ahmet, Y., & Polat, G. (2006). Numerical simulation of dynamic shear wall tests: A benchmark study. Computer and Structures, 84(8-9), 10.1016/j.compstruc.

Kent, D., & Park, R. (1971). Flexural member with confined concrete. Journal of Structural Division, Proceedings of the American Society of Civil Engineers, 97(ST7), 1969–1990.

Kim, Y., Kabeyasawa, T., Matsumori, T., & Kabeyasawa, T. (2011). Numerical study of a full-scale six-storey reinforced concrete wall-frame structure tested at E-Defense. Earthquake Engng Struct. Dyn., DOI: 10.1002/eqe.1179.

Krawinkler, H. (2006). Importance of good nonlinear analysis. Struct. Design Tall Spec. Build., 15, 10.1002/tal.379. 515-531.

Loh, C.-H., Wan, S., & Liao, W.-I. (2002). Effects of hysteretic model on seismic demands consideration of near-fault ground motions. Struct. Design Tall Spec. Build., 11, 10.1002/tal.182. 155-169.

Lu, X., & Wu, X. (2000). Study on a new shear wall system with shaking table test and finite element analysis. Earthquake Engng Struct. Dyn., 29(10), 1425-1440.

Luu, H., Léger, P., & Tremblay, R. (2014). Seismic demand of moderately ductile reinforced concrete shear walls subjected to high-frequency ground motions. Can. J. Civ. Eng. 4, 41: 125–135 dx.doi.org/10.1139/cjce-2013-0073.

Luu, H., Ghorbanirenani, I., Léger, P., & Tremblay, R. (2013). Numerical modelling of slender reinforced concrete shear wall shaking table tests under high-frequency ground motions. Journal of Earthquake Eng., 17, (4), 517–542.

Martinelli, P., & Filippou, P. C. (2009). Simulation of the shaking table test of a seven-story shear wall building. Earthquake Engng Struct. Dyn., 38(5), 587-607.

Mazzoni, S., McKenna, F., Scott, M. H., & Fenves, G. L. (2006). OpenSees Command Language, Manual, Open System for Earthquake Engineering Simulation (OpenSees). Pacific Earthquake Engineering Research Center, University of California Berkeley, CA.

Munir, A., & Warnitchai, P. (2012). The cause of unproportionately large higher mode contributions in the inelastic seismic responses of high-rise core-wall buildings. Earthquake Engng Struct. Dyn. DOI: 10.1002/eqe.2182.

NRCC. (2005). National Building Code of Canada, 12th ed. National Research Council of Canada, Ottawa, ON, Canada.

NZS. (2006). NZS 3101.1&2:2006, Concrete Structures Standard: Part 1 – The Design of Concrete Structures Standards New Zealand. Wellington, New Zealand.

Rad, B. R. (2009). Seismic shear demand in high-rise concrete walls. Ph.D. thesis Civil Engineering, The University of British Columbia.

Rejec, K., Isaković, T., & Fischinger, M. (2012). Seismic shear force magnification in RC cantilever structural walls, designed according to Eurocode 8. Bull Earthquake Eng, 10.1007/s10518-011-9294-y. 1-20.

Ruttenberg, A., & Nsieri, E. (2006). The seismic shear demand in ductile cantilever wall systems and the EC8 provisions. Bull Earthquake Eng., 4, 10.1007/s10518-005-5407-9. 1-21.

Orakcal, K., & Wallace, W. (2006). Flexural modelling of reinforced concrete walls experimental verification. ACI Structural Journal, 103(2), 196-206.

Palermo, D., & Vecchio, F. J. (2002). Behavior of three-dimensional reinforced concrete shear walls. ACI Structural Journal, 99(1), 81-89.

Palermo, D., & Vecchio, F. J. (2007). Simulation of Cyclically Loaded Concrete Structures Based on the Finite-Element Method. ASCE J. Struct. Eng., 133(5), 728-738.

Panagiotou, M., & Restrepo, J. I. (2009). Dual-plastic hinge design concept for reducing higher-mode effects on high-rise cantilever wall buildings. Earthquake Engng Struct. Dyn., 38(12), 1359-1380.

Panagiotou, M., Restrepo, J. I. & Conte, J. P. (2007). Shake table test of a 7-story full scale reinforced concrete structural wall building slice phase II: T-wall. SSRP 07-08 Report Dept. of Struct. Eng., Univ. of California at San Diego,CA.

Panagiotou, M., Restrepo, J. I. & J.P., C. (2011). Shake table test of a 7-story full scale reinforced concrete structural wall building slice phase I: rectangular wall. ASCE J. Struct. Eng., 137(6), 691-701.

Panneton, M., Léger, P. &Tremblay, R. (2006). Inelastic analysis of a reinforced concrete shear wall building according to the NBCC 2005. Can. J. Civ. Eng., 33(7), 854-871.

Park, R., Priestley, M. J. N. & Gill, W. (1982). Ductility of square-confined concrete columns. ASCE J. Struct. Eng., 108(4), 929–950.

Paulay, T., & Priestley, M. N. J. (1992). *Seismic Design of Reinforced Concrete and Masonry Buildings*. John Wiley & Sons, Inc., New York.

Priestley, M.J.N., Calvi, G.M., & Kowalsky, M.J. (2007). *Displacement based design of structure*. IUSS Press: Pavia, Italy.

Priestley, M. J., & Amaris, A. D. (2002). Dynamic amplification of seismic moments and shear forces in cantilever walls. Research Report ROSE No. 01 Rose School, University of Pavia, Pavia, Italy.

Powell, G. (2010). *Modelling for structural analysis, behaviour and basics*. Computers & Structures, Inc. Berkeley, California 94704 USA. 365p.

Pugh. J.(2012). Numerical Simulation of Walls and Capacity Design Recommendations for Walled Buildings. PhD thesis, University of Washington.

S-Frame software inc. (2012). S-concrete: Concrete Section Design, version 10.00.40. Maycrest WayRichmond, B.C., Canada.

Schotanus, M. I., & Maffei, J. R. (2008). Computer modelling and effective stiffness of concrete wall buildings. Tailor Made Concrete Structures – Walraven & Stoelhorst (eds). Taylor & Francis Group, London, ISBN 978-0-415-47535-8.

Seckin, M. (1981). Hysteretic Behaviour of Cast-in-Place Exterior Beam-Column-Slab Subassemblies. Department of Civil Engineering, University of Toronto, Ph.D, 266.

Seismosoft. (2011). SeismoStruct: Software applications for analysis of structures subjected to seismic actions. Pavia, Italy

Schotanus, M. I., & Maffei, J. R. (2008). Computer modelling and effective stiffness of concrete wall buildings. Tailor Made Concrete Structures – Walraven & Stoelhorst (eds). Taylor & Francis Group, London, ISBN 978-0-415-47535-8.

Sullivan, T. J., Priestley, M. J. N., & Calvi, G. M. (2008). Estimating the higher-mode response of ductile structures. Journal of Earthquake Eng., 12(3), 456–472.

Velev , N. (2007). Influences of higher modes of vibration on the behaviour of reinforced concrete shear walls structures. Master thesis, École Polytechnique de Montréal, Département des génies civil, géologique et des mines, Montréal, Que.

Takeda, T., Sozen, M. A., & Nielsen, N. N. (1970). Reinforced concrete response to simulated earthquakes. ASCE J. Struct. Eng., 96(12), 2557-2573.

Thomsen IV, J. H., & Wallace, J. W. (2004). Displacement-based design of slender reinforced concrete structural walls - experimental verification. ASCE J. Struct. Eng., 130(4), 618-630.

Tremblay, R., Ghorbanirenani, I., Velev, N., Léger, P., Leclerc, M., Koboevic, S., Bouaanani, N., Galal, K., & Palermo, D. (2008). Seismic response of multi-storey reinforced concrete walls subjected to Eastern North America high frequency ground motions. Proc. 14WCEE., Beijing, China, Paper no. 05-01-0526.

Tremblay, R., Léger, P., & Tu, J. (2001). Inelastic Seismic Response of Concrete Shear Walls Considering P-Delta Effects. Can. J. Civ. Eng., 28(4), 640-655.

Vecchio, F. J. (2000) . Disturbed Stress Field Model for Reinforced Concrete: Formulation. ASCE J. Struct. Eng., 126(9), 1070-1077.

Vecchio, F. J., & Collins, M. P. (1986). The modified compression-field theory for reinforced concrete elements subjected to shear. ACI Structural Journal, 83(2), 219-231.

Vecchio, F. J., & Lai, D. (2004). Crack shear-slip in reinforced concrete elements. Journal of Advanced Concrete Technology, 2(3), 289-300.

Wallace, J. W. (2007). Modelling issues for tall reinforced concrete core wall building. Struct. Design Tall Spec. Build. 16, 615–632. DOI: 10.1002/tal.440.

Wallace J.W., Massone L.M., & Orakcal K. (2006). St. Joseph's Healthcare Orange, California, SPC-2 Upgrade: E/W Wing Component Test Program – Final Report. Report No. UCLA SEERL 2006/1, University of California, Los Angeles, California, U.S.A

Wiebe L., Christopoulos C., Tremblay R., & Leclerc M.(2013). Mechanisms to Limit Higher Mode Effects in a Controlled Rocking Steel Frame. 1: Concept, Modelling, and Low-Amplitude Shake Table Testing. Earthq Eng Struct Dyn 2013; 42(7): 1053-1068.

Wong, P. S., & Vecchio, F. J. (2002).VecTor2 & Formworks user's manuals. Department of Civil Engineering, University of Toronto, pp.213.